INSA National Report on Seismological Research in India: 2019 – 2022

Ajay Manglik[1]

[1]CSIR-National Geophysical Research Institute, Uppal Road, Hyderabad 500007, India

March 29, 2023

IASPEI National Correspondent, INSA IUGG-IGU National Committee

(e-mail: ajay@ngri.res.in)

Summary

The Indian National Science Academy (INSA), the National Adhering body representing India in the International Union of Geodesy and Geophysics (IUGG), submits a National Report to the IUGG during its General Assembly, held every four years. The present chapter is a compilation for the International Association of Seismology and Physics of the Earth's Interior (IASPEI), one of the eight Associations of the IUGG, encompassing the scientific activities carried out in the country during 2019-2022, in the field of seismology. The chapter is arranged to categorize the contributions under internal structure of the Indian lithosphere and sub-lithospheric mantle, crust and upper mantle deformation, seismic attenuation, seismic hazards, triggered seismicity, environmental seismology, paleoseismology and seismological networks. In addition, the chapter includes activities related to societal projects and outreach programs. It is not an exhaustive review of the entire Indian contribution to seismology and allied fields during this period but a window to the topics covered within the framework of IASPEI.

During the reporting period, researchers from several Indian R&D and Academic Institutions continued adding new results on the crustal and upper mantle structure of the Indian shield, both at regional and geological province scale. The Himalaya has been a major focus of seismological research for many Institutes who operated broadband seismological networks from Kashmir to Arunachal along the Himalayan arc. The data from these networks have facilitated in enhancing our understanding of the structure of the Main Himalayan Thrust, crustal and upper mantle structure as well as the dip of the underthrusting Indian plate, seismicity monitoring, and estimation of attenuation. Some of these networks also include accelerographs for strong ground motion studies. A few studies also focused on mapping of the mantle transition zone beneath the Indian Ocean Geoid Low. The studies on anthropogenic seismicity added near-field investigations in the Koyna - Warna region through borehole seismology. Organization of the Joint Scientific Assembly of IAGA and IASPEI during 21-27 August 2021 (JSA-2021) was a major event during this period related to the IUGG activities. Originally, the event was planned to be hosted at Hyderabad, India, but due to the COVID-19 pandemic it was organized in virtual mode. Initiatives have been taken to nucleate the field of environmental seismology in the country.

Keywords: IUGG, IASPEI, INSA, National Report, Seismology

1. Introduction

The International Association of Seismology and Physics of the Earth's Interior (IASPEI) is one of the eight Associations of the International Union of Geodesy and Geophysics (IUGG), dedicated to promotion of international cooperation and coordination of scientific studies in the field of seismology, Earth's internal structure and Tectonophysics. The Indian National Science Academy (INSA) is the National Adhering body representing India in the IUGG. INSA submits a National Report to the IUGG during its General Assembly, held every four years. The report consists of major scientific studies related to the eight Associations of the IUGG, carried out in the country during the preceding four years. The present chapter is a compilation for the IASPEI based on the scientific activities carried out in the country during 2019-2022, in the field of seismology.

The present chapter briefly lists major contributions from India during the reporting period in the realm of IASPEI. Many R&D Institutes and Academic Departments in the country pursue seismological research. The National Center for Seismology under the Ministry of Earth Sciences (MoES), Government of India, is the nodal agency for monitoring and reporting earthquake activity in the country. It has got a network of more than 150 broadband seismological stations spread across the country. In addition to this, several seismological networks are operated by R&D Institutes under CSIR, DST, MoES and State Government of Gujarat, and Academic departments under IITs and IISERs, mainly for region-specific seismological research. These are briefly covered in Section 10.

The chapter has been prepared based on the inputs received from many researchers belonging to these Institutes/Departments. However, it is not an exhaustive review of all the Indian contribution to seismology and allied fields during this period. The chapter is arranged to categorize the contributions under internal structure of the Indian lithosphere and sub-lithospheric mantle, crust and upper mantle deformation, seismic attenuation, seismic hazards, triggered seismicity, environmental seismology, paleoseismology and seismological networks. In addition, the chapter includes activities related to societal projects and outreach programs.

2. Seismological Imaging of the Indian Lithosphere and Mantle

2.1 Indian Shield Region

Inversion of receiver functions (RF) revealed that the Deccan Volcanic Province (DVP) and the Eastern Dharwar Craton (EDC) have distinct crustal structure in terms of crustal thickness, average composition, shear wave velocity variation and nature of the crust-mantle boundary (Kumar S., et al., 2020). Using a similar methodology, Gupta and Kumar (2022) estimated the thickness of the lithosphere beneath EDC and DVP and found it to be $\sim$50–60 km thinner in the DVP compared to that in the EDC. Arjun et al. (2022) carried out a joint modelling of teleseismic travel-time residuals, Bouguer gravity anomaly and surface topographic data to delineate the nature of the continental lithosphere beneath the Archaean Dharwar craton along an ENE-WSW traverse and reported an estimate of the Te and its role in supporting the topographic loads imposed by the Western Ghats, located near the western margin of the Southern Indian shield.

Rao and Ravi Kumar (2022a) studied the crustal and uppermost mantle structure of the Western Ghats (WG) by slant stacking, common conversion point imaging and harmonic decomposition of RFs. Their results reveal a large crustal thickness of $\sim$ 45 km in the central part of the WG, which decreases to $\sim$ 39 km in the southern and $\sim$ 37 km in the northern parts. The RFs also reveal a strong sub-Moho low velocity layer. By jointly inverting receiver function and surface wave group velocity dispersion, Mandal et al. (2022a) found that the Moho depth ranges from 39.5 to 42 km, while the lithospheric thickness varies from 108 to 120 km across 6 stations beneath the Palghar region in Maharashtra. Inversion of receiver functions from a network of 10 stations in the vicinity of Hyderabad revealed a 4-layered crust with a 16-km-thick high-velocity lowermost crustal layer, a 9-km-thick upper crustal layer with a Vp of 6.27 km/s, a middle and upper lower crust between 9–22 km depth (Mandal et al., 2022c). The modelled Moho depths vary from 35.4 to 37.6 km across the region.

During 2013-2017, CSIR-NGRI maintained a seismic network of 15 three-component broadband stations in the Eastern Indian Craton (EIC). Results from joint inversion of receiver functions and surface wave group dispersion show a marked crustal thinning of 5–10 km and a 90 km thick lithosphere below the Singhbhum-Odisha-Craton (SOC), with a flat crust having a thickness of 42 km below the Chotanagpur Granitic Gneissic Terrain (CGGT) (Mandal, 2019a). A marked crustal and lithospheric thinning beneath SOC is also seen (Mandal et al., 2021). In addition, this study showed a relatively smaller degree of crustal (2–4 km) and lithospheric thinning (4–10 km) beneath the Eastern Ghat Mobile Belt, south of the SOC. Despite a thick crust, they note a 15–20 km lithospheric thinning associated with the CGGT. Based on results from H-K stacking and CCP imaging, a secular variation of the Archean crust formation is inferred in the Eastern Indian Shield (Mandal, 2022a). They observed a correlation between crustal age and composition within the ellipsoidal Paleoarchaean cratonic domain in the SOC. In analogy with the Paleoarchaean and Mesoarchaean granite-greenstone terrains such as the eastern Pilbara, Barbeton, and Kappvaal cratons, Mandal et al. (2021) suggested that crust formation during the Paleoarchaean SOC may have involved a thick oceanic mafic plateau followed by polybaric melting resulting in pulses of felsic magmatism with concurrent gravitational reorganization via Rayleigh Taylor Instabilities.

A similar study indicated crustal and lithospheric thinning beneath Kachchh, along with a 2-6% reduction of Vs across the Lithosphere-Asthenosphere-Boundary (Mandal, 2019b). Local earthquake tomography of the Kachchh rift zone (Mandal, 2020a, 2022b) showed two prominent high-velocity anomalies within the crust which were attributed to mafic plutons. Paul H., et al. (2021) estimated the crustal thickness and uppermost mantle velocity beneath the Gujarat region using Moho-reflected phases and found that the Kachchh region has a thicker crust (43 km) owing to a root and high uppermost mantle velocity.

Pn (Illa et al., 2021a) and Sn tomography (Illa et al., 2021b) of the Indian Shield and adjacent regions reveals that the upper mantle of the Indian shield is characterized by a Pn velocity of 8.12–8.42 km/s, while a large part of the central Indian shield has a higher mantle-lid velocity of $\sim$ 8.42 km/s with a dominant anisotropic value of $\sim$ 7.5% amounting to a variation of 0.2–0.3 km/s (Fig.1).

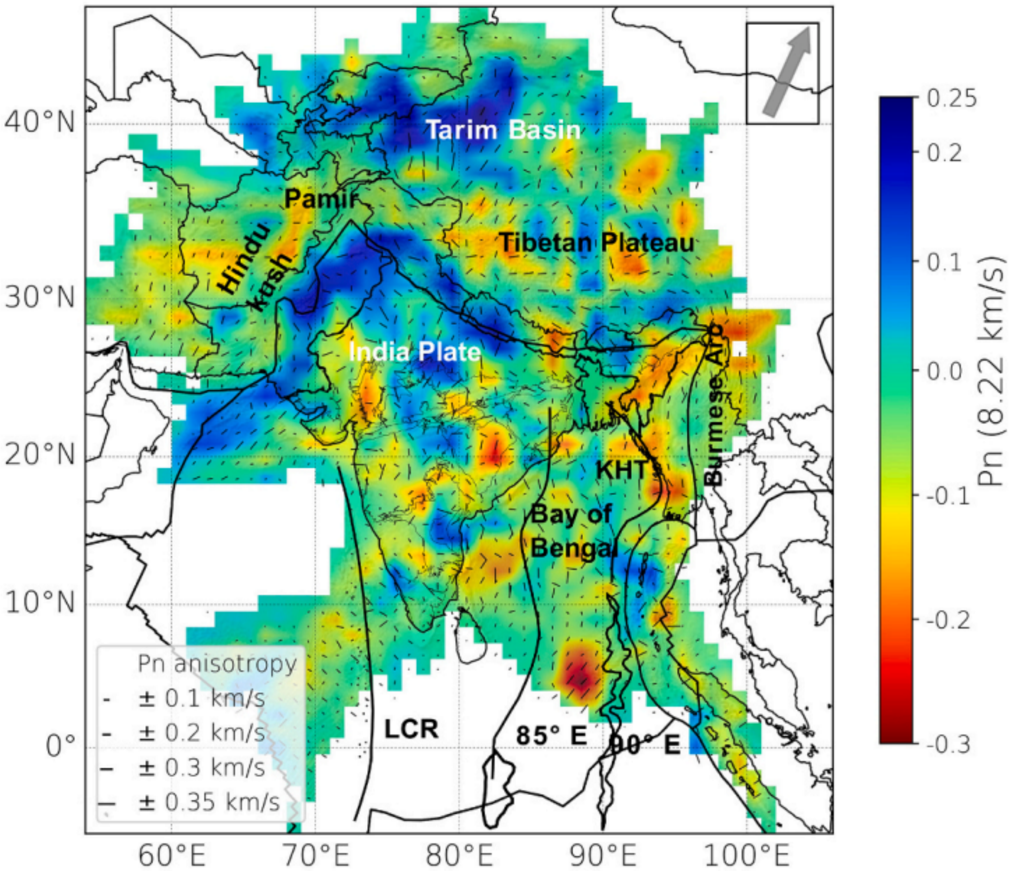

Figure 1. Pn velocity of the upper mantle of the Indian shield and adjoining regions obtained on a grid of 1°×1° size. Pn anisotropy results with magnitudes are also superimposed to illustrate the correspondence between anisotropy patterns and the major velocity anomalies. KHT- Kerguelen hotspot track. The gray arrow in the top right corner indicates the present-day Indian plate motion direction. (From Illa et al., 2021a) (*Reprinted from Tectonophysics, Vol 813, Bhaskar Illa, K.S. Reshma, Prakash Kumar, D. Srinagesh, C. Haldar, Sanjay Kumar, Prantik Mandal, Pn tomography and anisotropic study of the Indian shield and the adjacent regions, 228932, Copyright (2021), with permission from Elsevier.*)

Srinu et al. (2021) investigated the X-discontinuity beneath India, using P-RFs at seismological stations deployed on the Indian shield and the Himalaya. They detect the X-discontinuity as a sporadic and thin feature in the depth range of 246–335 km, with a sharp shear velocity jump of 2.5-3.6%.

The DVP is considered to have its genesis in the interaction of the Indian plate with the Réunion mantle plume. Sharma J., et al. (2021) investigated the group velocity dispersion data in the period range of 6-100 s derived from waveforms of 77 regional earthquakes recorded at 38 broadband stations and performed surface wave tomography. The results revealed signatures of magmatic underplating and a thick crust beneath the Kachchh seismic zone and Western Ghats. A predominant low-velocity zone beneath the Cambay, Saurashtra, and adjoining regions was interpreted as a residual thermal anomaly and thin lithosphere as a result of weakening due to plume-lithosphere interaction.

Singh and Singh (2019) presented a high-resolution seismic image of the hitherto-elusive crustal architecture of the Eastern Ghat Mobile Belt (EGMB) and its contact with Archaean cratons using teleseismic receiver functions. The results reveal a thick crust (40 km) with oppositely dipping Moho below the contact between the EGMB and the Bastar craton. The crust of Bastar craton extends ($\sim$ 75 km) eastward beneath the EGMB-Bastar surficial contact. Jana et al. (2022) constrained the velocity model by jointly inverting the surface wave dispersion data with receiver function data (Fig.2). The lithospheric and asthenospheric velocity model excludes the possibility of southward accretionary growth of Singhbhum craton to form Rengali province. Also, a metasomatically altered zone has been reported in some areas. The signature of removal of lithospheric root beneath the investigating region indicates the thermo-mechanical destruction caused by plume hotspots during the northward drift of proto-India.

Mullick et al. (2022) obtained a 3-D shear velocity model of South Indian Precambrian terrains at a lateral resolution of 55 km down to 250 km depth by inversion of fundamental mode Rayleigh wave phase velocity dispersion data in the period range of 30-140s, which shows a 150-200 km thick lithosphere beneath most of the Archaean Dharwar craton. An extraordinary high shear velocity (up to 4.8 km/s) and thick lithosphere (150 km) are observed beneath the Proterozoic Carbonatite complex, located at the south-eastern edge of the Dharwar craton. They inferred a compositional modification of the lower lithosphere at the south-western margin of the Dharwar craton and lithospheric erosion in the Granulite terrain both possibly due to interaction with the Marion mantle plume at $\sim$ 90 Ma.

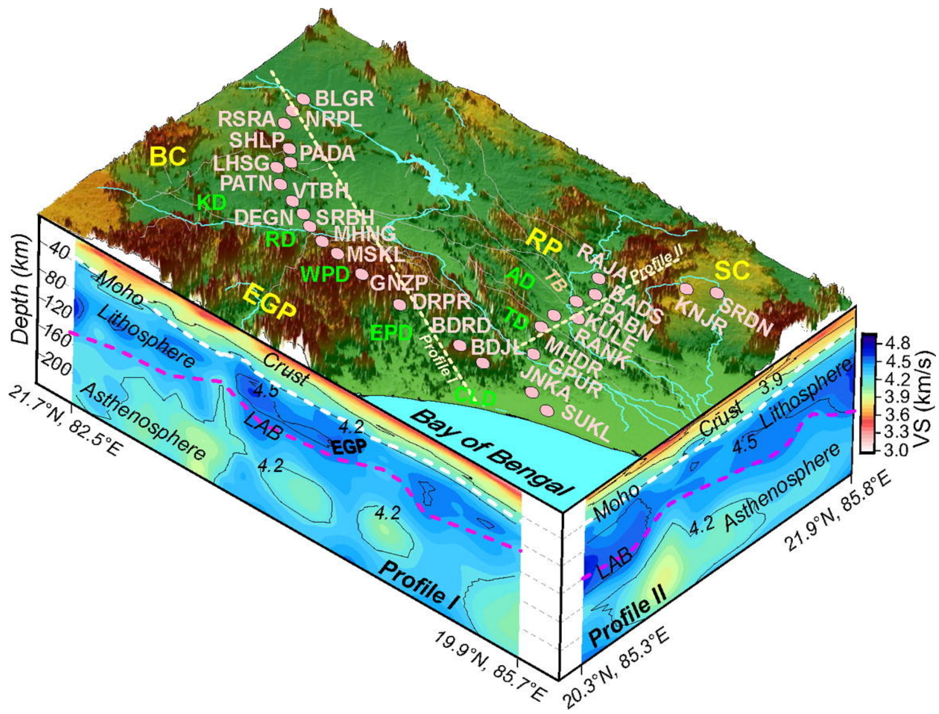

Figure 2. Shear velocity structure of the upper mantle along two profiles, obtained from joint inversion of the surface wave dispersion data and receiver functions. (From Jana et al., 2022) (*Reprinted from Gondwana Research, 111, Niptika Jana, Chandrani Singh, Arun Singh, Tuna Eken, Arun Kumar Dubey, Abhisek Dutta, Arun Kumar Gupta, Lithospheric architecture below the Eastern Ghats Mobile Belt and adjoining Archean cratons: Imprints of India-Antarctica collision tectonics, 209-222, Copyright (2022), with permission from Elsevier.*)

Das and Rai (2019) generated a 3-D shear velocity image of the crust through joint inversion of the P- RFs and Rayleigh wave group velocity dispersions, derived from cross correlation of ambient noise, to study the linkage and the boundary between the Dharwar craton and the Southern Granulite Terrain (SGT). The study delineated a 10–15 km thick high shear velocity layer in the lowermost crust of the southern part of the WDC continuing into the SGT up to 40 km beyond the E-W trending southern limb of the Palghat-Cauvery shear zone, suggesting that the Dharwar craton continues further south of the mapped orthopyroxene boundary to the Palghat shear zone.

Vashishtha et al. (2022) used surface wave data from the April 25, 2015, Nepal earthquake (Mw 7.8) and its aftershocks, recorded at eleven stations in India to estimate group velocities of both Love and Rayleigh waves. All stations are at regional distances from the earthquake sources. It is observed that the group velocities for both Love and Rayleigh waves obtained from the mainshock data are lower than those obtained from aftershock data for stations located towards W and SW of the earthquake source region. Such a variation of group velocity obtained from mainshock and aftershock data for different stations may be due to source directivity for the mainshock affecting the source group time, which in turn affects the travel time of surface waves at different periods.

2.2 Himalaya

Kanna and Gupta (2020) studied the crustal structure of the Garhwal Himalaya along a linear profile, using regional travel times and receiver function analysis. Their receiver function modeling showed a prominent intra-crustal low velocity layer with a flat–ramp–flat geometry beneath the Main Central Thrust zone and a variation in the Moho depth from $\sim$ 45 km beneath the Sub Himalaya to $\sim$ 58 km to the south of the Tethys Himalaya. A similar study in the NW Himalaya and Ladakh-Karakoram indicates that the Moho depth increases from $\sim$ 46 km below the Gangetic Plain to $\sim$ 78 km at the southern flank of the Karakoram Fault. Several intra-crustal low-velocity layers were seen and the MHT is mapped as an LVL (Kanna and Gupta, 2021).

Gupta S., et al. (2022) examined the P-wave velocity (Vp) and Vp/Vs variations using local earthquake arrival time measurements recorded over 41 seismic stations operated during November 2006 to June 2008 in the Kumaun–Garhwal Himalaya. In the 0–25 km depth range, the Vp and Vp/Vs varies between 4.8–6.8 km/s and 1.55–1.85, respectively and show a heterogeneous structure in the upper-mid crust. The seismic images exhibit signatures of unconsolidated sediments, close to the Main Frontal Thrust, and Klippes (Lansdowne and Almora) in the uppermost crust. In the upper-mid crust, the observed low Vp and high Vp/Vs (1.82–1.85) along with available conductivity values indicate saline-rich aqueous fluid and partial melt. Using the inferred crustal composition and constraints from earlier information, they proposed the bottom of these fluid zones as the top of the underthrusting India Plate, which shows a flat-ramp-flat geometry at 16–21 km depth. The earthquakes of moderate and smaller magnitude mostly occur in the fluid-rich zone above the mid-crustal ramp in the underthrusting Indian Plate. Madhusudhan et al. (2022) calculated the uppermost mantle seismic (Pn and Sn) velocities using 12 regional earthquakes recorded by 33 digital broadband seismological stations from the Gangetic plain to the Tethys Himalaya along a $\sim$ 160 km profile and showed that the Moho dips in the north direction with an overall dip angle of 3.43°- 4.2° in the Eastern Kumaun Himalaya.

Mandal et al. (2021c) imaged the lateral variations in the Moho depths and average crustal composition across the Kumaun–Garhwal Himalaya, through H-K stacking of 1400 radial P-RFs from 42 broadband stations. The modeled Moho depth and average crustal Vp/Vs values vary from 28.3 to 52.9 km and 1.59 to 2.13, respectively. They also mapped three NNE-SSW trending transverse crustal blocks in Uttarakhand Himalaya that extend down to the lithosphere-asthenosphere boundary. Local earthquake tomography of the Kumaun-Garhwal Himalaya (Mandal et al., 2022b; Gupta S., et al., 2022) shows a low velocity (Vp, Vs), high Vp/Vs mid-crustal layer, which was identified as the Main Himalayan Thrust associated with metamorphic fluid/partial melt.

The Himalaya-Karakoram-Tibet region characterizes a unique setup of crustal and upper mantle structure related to present-day geodynamics. Kumar N., et al. (2019) performed surface wave tomography studies that reveal highly variable shear wave velocity structure indicating signatures of underthrusting of the Indian plate beneath Eurasia. The study reveals a NE-dipping Moho with its depth increasing from $\sim$ 40 km beneath the frontal Himalaya to 70-80 km below the collision zone. Low near-surface seismic velocities indicate thick sediments (5-6 km) in the Indo-Gangetic plains. Broader low-velocity zone at mid-crustal depth beneath the southern parts of Tibet and Karakoram fault is due to the presence of partial melting and/or aqueous fluids.

Kumar V., et al. (2022) used ambient noise cross-correlations from 530 seismological stations along with surface wave observations from 1,261 earthquakes to image the crust beneath the western Himalaya-Asia convergence zone encompassing western Himalaya-western Tibet-Ladakh-Karakoram-Pamir-Hindu Kush. The seismological data from the PASSCAL experiments, the Global Seismograph Network, experiments in Kyrgyzstan, Kazakhstan, Tajikistan, China, Nepal and western Tibet, French deployments in western Kunlun and Kazakhstan and Indian deployments in the western Himalaya were used in this study that resulted in 22,726 inter-station Rayleigh wave dispersion measurements in the period band of 5 to 60 s at a horizontal resolution of less than $0.5°\times0.5°$. The 3-D shear wave velocity image revealed that the northern limit of the Indian crust extends beyond the Qiangtang block in western Tibet (77°- 82°E) and till the central Pamir farther west. The study suggests a continuation of LVZs across the Karakoram Fault at a depth below 20 km, indicating the fault's upper crustal depth extent.

The seismicity in the Kumaun Himalaya is concentrated in the Chiplakot Crystalline Belt (CCB). WIHG conducted a passive seismological study using receiver functions (RFs) along a profile (see Fig.1 of Hazarika et al., 2021). The H-K stacking analysis of RFs of teleseismic earthquakes reveals a significantly high value of the Poisson's ratio ($\sim$ 0.28) in the Dharchula region of the CCB which is coincident with the earthquake cluster (Hajra et al., 2019). The RF inversion and Common Conversion Point (CCP) stacking imaging reveals a variation of crustal thickness from $\sim$38 km in the Indo-Gangetic Plain to $\sim$ 42 km near the Vaikrita Thrust (see Fig.6 of Hazarika et al., 2021). A ramp ($\sim$ 20°) structure on the MHT is revealed beneath the CCB. The spatial and depth distribution of seismicity pattern beneath the CCB and presence of steep dipping imbricate faults inferred from focal mechanism solutions suggest a Lesser Himalayan Duplex structure in the CCB above the MHT ramp (Hazarika et al., 2021; Hajra et al., 2021).

Medved et al. (2022) obtained 3D models of the crust and uppermost mantle beneath the NW Himalaya down to a depth of 120 km by local earthquake seismic tomography using data of India Meteorological Department (IMD) complemented by the Global International Seismological Centre (ISC) Catalogue. Their results suggest that the Indian Plate not only underthrusts northwards below the Himalaya but also bends westwards as it gets closer to the Hindukush Region. A peculiar feature of the model is a high-velocity anomaly in the Kaurik Chango Rift, interpreted as a remnant of the oceanic crust, left after the closure of the Indo-Tethys Ocean. In the seismically active Delhi-Haridwar Ridge, a low-velocity upper crustal layer is possibly associated with sediments of the Indo-Gangetic Plain and with a large number of fault structures.

Mir et al. (2021) estimated the shear wave velocity structure, together with Moho depths for the NW Himalaya, Hindu Kush and the Pamirs at a potential resolution of $0.5°\times0.5°$ and at $1°\times1°$ in the surrounding area (Fig.3), by inverting fundamental mode Rayleigh wave group velocities calculated from regional earthquake ($\Delta \leq 2500$ km) data, and also from their joint inversion with teleseismic receiver functions at 38 out of the 59 broadband stations in the region. The results illuminate a) the deeper root zone structures of the main geomorphic features, b) a pervasive low velocity layer (Vs $\sim$ 3.1 km/s) at $\sim$ 30 km depth beneath the NW Himalaya. Another notable result is the distinctly shallower Moho beneath the Kashmir Himalaya apparently segmented by arc-normal shear zones that cross the rupture zones of the 1905 Kangra and the 2005 Kashmir earthquakes, in turn, marked by the current epoch seismicity.

A high-resolution seismic image of the crust beneath the Arunachal Himalaya is documented by Singh A., et al. (2021), using RF analysis of data from 32 broadband seismic stations deployed in the Arunachal Himalaya during 2010-2016, along with data from the HIMNT, SIKKIM, Hi-CLIMB, and GANSSER networks. Their results reveal lateral variations in the crustal structure with the Moho depth varying from 40-60 km. They also observe a comparatively less complex crust, absence of a prominent mid-crustal ramp, a highly deformed layer running parallel to the Main Himalayan Thrust, and an intermittent anisotropic low velocity layer in the middle crust.

In a recent study (Ravi Kumar et al., 2022), receiver function images of the detachment, mid-crustal ramp and the Moho of the underthrusting Indian plate along four profiles in the Arunachal Himalaya are documented (Fig.4). The results reveal a clear Moho signature in the depth range of 40 to 65 km, with the detachment mapped in the depth range of $\sim$ 10 to 20 km. A mid-crustal ramp can be traced in the higher Himalaya especially along one profile. Singh A., et al. (2021) imaged the crust beneath the Arunachal Himalaya using teleseismic receiver functions. A mechanically weak middle crust beneath Arunachal Himalaya, highly deformed layer parallel to MHT, and comparatively less complex crust beneath Arunachal than Nepal and Sikkim are some important observations that have been reported in this study.

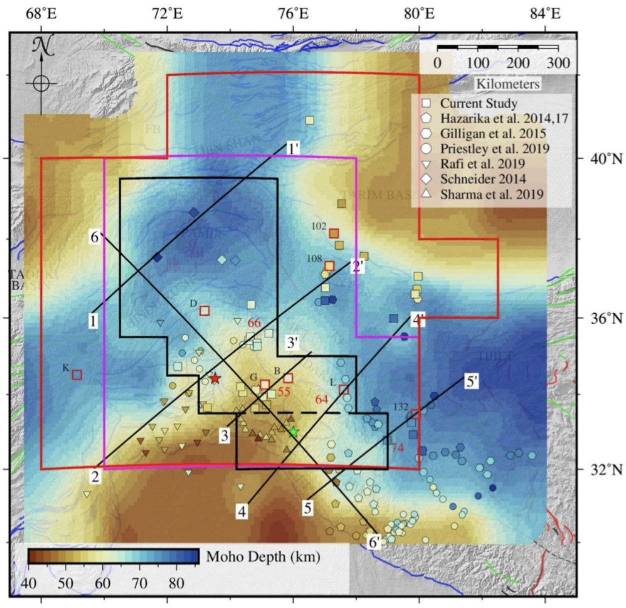

Figure 3. Posterior Moho depth estimates for the Kashmir Himalaya region. The average Moho depth in the region is found to be ~ 70 km, with higher depths beneath Tibet and the Pamir and shallower ones beneath the Tarim, Tadjik and Fergana basins, as well as the Himalayan foreland basin. (From Mir et al., 2021) (*Courtesy CSIR-4PI*)

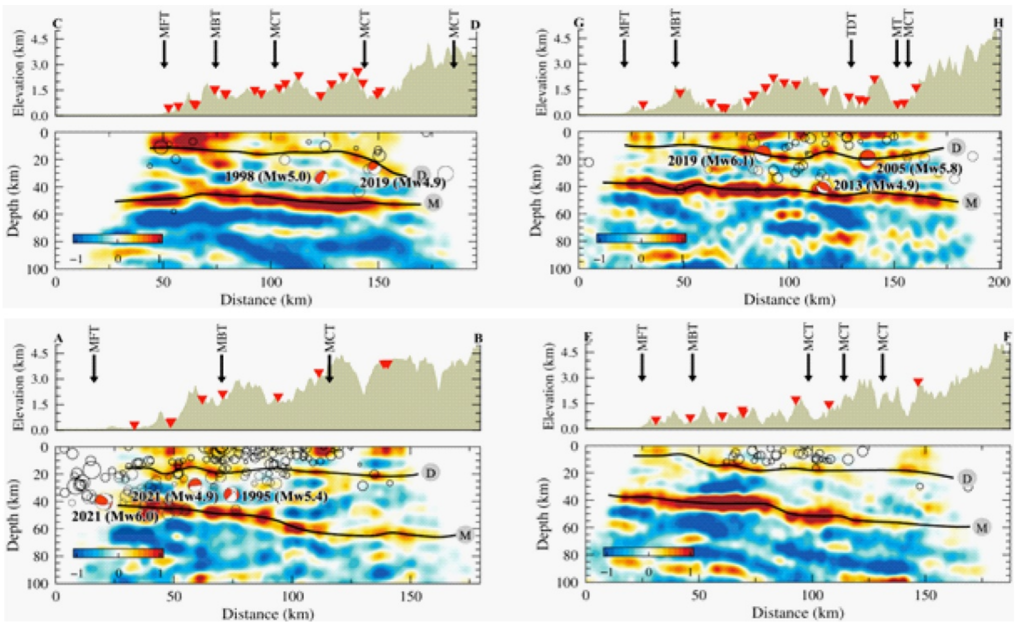

Figure 4. 3D migrated P-RF images along the Arunachal Himalaya profiles along with the elevation within ±50 km. Focal mechanisms of moderate magnitude earthquakes and local seismicity are superimposed on the 3D migrated images (circles). D: Detachment and M: Moho are marked based on P-RF images. (From Ravi Kumar et al., 2022) (*Reprinted from Journal of Asian Earth Sciences, 236, Ravi Kumar Mangalampalli, Padma Rao Bommoju, Mahesh Perugu, Vempati Venkatesh, Scattered wave imaging of the Main Himalayan Thrust and mid-crustal ramp beneath the Arunachal Himalaya and its relation to seismicity, 105335, Copyright (2022), with permission from Elsevier.*)

Crustal thickness in the NE India including the eastern Himalaya is investigated using surface wave tomography and the RF studies (Kundu et al., 2020; Kumar A., et al., 2021). The results reveal that the Bengal Basin comprises thick sediments (up to $\sim$ 20 km) with thickness increasing from west to east. The Moho depth increases from $\sim$ 40 km in the Shillong plateau and Brahmaputra valley to $\sim$ 70 km beneath the Higher Himalaya and southern Tibet. The crustal thickness and Poisson's ratios reveal thickening of the crust from $\sim$ 46 km beneath the Brahmaputra valley in the west to $\sim$ 55 km in the western part of the Lohit Plutonic Complex (LPC). Similar analysis carried out in the Siang Window of the NE Himalaya reveals a variation of crustal thickness from $\sim$ 38 km in the Brahmaputra valley (Pasighat) to $\sim$ 53 km at the northern boundary of the window (Gelling area). The estimated Poisson's ratio in the Brahmaputra valley is low (0.23), suggesting a felsic composition of the crust. It is intermediate in the Mishmi Thrust zone (0.249–0.261) and in some parts of the LPC. A high Poisson's ratio (0.277–0.293) is obtained for the Tidding Tuting Suture Zone (TTSZ) and western part of the LPC, indicating the presence of aqueous fluid/partial melt in the crust (Kundu et al., 2020).

Shukla et al. (2022) investigated the crustal configuration beneath northeast India based on receiver function analysis of teleseismic earthquakes recorded by 19 broadband seismological stations using H-k stacking method. The study reveals a large variation in crustal thickness and Poisson's ratio which are correlated with the complex geology and tectonics of the region. The crust is observed to be thinner (36.5–41.6 km) beneath Bengal Basin, Shillong Plateau, and the Brahmaputra valley compared to the Indo-Burma Ranges (IBR) ($\sim$ 40–54 km) and Arunachal Higher Himalaya (TAWA station, $\sim$ 45 km) and Sikkim Himalaya (GTK station, $\sim$ 46.5 km). A large variation of Poisson's ratio is observed in the region ($\sim$ 0.230–0.306).

On the occasion of the Diamond Jubilee Year of CSIR-NGRI in 2021, Manglik et al. (2021) reviewed the geophysical studies carried out by the Institute since 1961 for the crustal and upper mantle structure of the Himalaya.

2.3 Indo-Burmese Arc

Saikia et al. (2020) investigated the mantle transition zone (MTZ) structure beneath the eastern Himalaya, southern Tibet, Assam valley, Burmese arc and Bengal basin regions using receiver functions of 327 stations. A depression in the 410 and 660 km discontinuities is observed beneath the Bengal basin and to the east of the eastern Himalayan syntaxis. The 410 is elevated by 10 km along the Himalayan collision front, while it deviates in the range of $\pm$5 km beneath most parts of Tibet and the Himalayan Foredeep. The 410 and 660 km discontinuities are uplifted by nearly 10 km beneath the Arunachal Himalaya. They observe a thick (>20 km) transition zone beneath the Burmese Arc and close to the Tengchong volcano.

Dubey et al. (2022) presented 3-D P- and S-wave velocity perturbation maps of the upper-mantle beneath eastern Himalaya and Burmese subduction zones. Tomograms revealed that the subducting Indian lithospheric plate extends up to Bangong-Nujiang Suture Zone, overturns and descends steeply beyond 200 km below the Himalayan arc. A southward plunging detached slab can be traced beyond 600 km. Results reveal no evidence for the detachment of a S-E deflecting Indian lithospheric slab below the Burmese arc.

Surface wave tomography reveals thick sediments represented by low shear wave velocity down to $\sim$ 21 km depth in the eastern Bengal Basin beneath the southern Indo-Burma Range (IBR) (Kumar A., et al., 2021; Chanu et al., 2022). Tomography images also report subduction of Indian plate beneath the Burmese arc with signatures of a medium of high shear wave velocity below $\sim$ 50 km to $\sim$ 75 km depth.

2.4 Indian Ocean and Bay of Bengal

Rao et al. (2020) investigated the mantle transition zone (MTZ) structure beneath the Indian Ocean Geoid Low (IOGL) region using P-RFs. 3-D time-to-depth migration of P-RFs reveals a thin MTZ primarily due to an elevation of the 660 km discontinuity. This is suggestive of anomalously hot temperatures in the mid-mantle beneath the IOGL region, possibly sourced from the African Large Low Shear Velocity Province (LLSVP). The seismic structure of the D'' layer beneath the Indian Ocean is investigated by modeling the ScS-S and PcP-P differential travel time residuals (Rao and Ravi Kumar, 2022b). Modeling of the residuals using a grid search approach revealed velocity perturbations in the range of -3.06% to 5.72% for the shear and -4.81% to 5.47% for compressional waves in the D'', which were positive below the Indian Ocean Geoid Low (IOGL) and negative below the adjoining region (Fig.5). The results reveal presence of high velocity material atop the Core Mantle Boundary (CMB) beneath the IOGL.

Paul and Ravi Kumar (2022) identified salient features of the mantle beneath the Indian Ocean and Ross Sea, by analyzing 8 global tomographic models. Their study indicates low velocity anomalies of dVs $\sim$ 1.1% in the $\sim$ 400–680 km depth range and inconsistent high velocity anomalies of dVs $\geq$ 1% at depths below 1600 km beneath both Indian Ocean and Ross Sea. A consistent low velocity structure throughout the mantle beneath the southwestern Indian Ocean and east Africa is associated with a plume from the African LLSVP. Forward modeling of the Geoid indicated that the E-W extent of the IOGL, influenced by upper mantle anomalies, could be precisely predicted, however, the N-S extent is underestimated since the lower mantle anomalies are inconsistent.

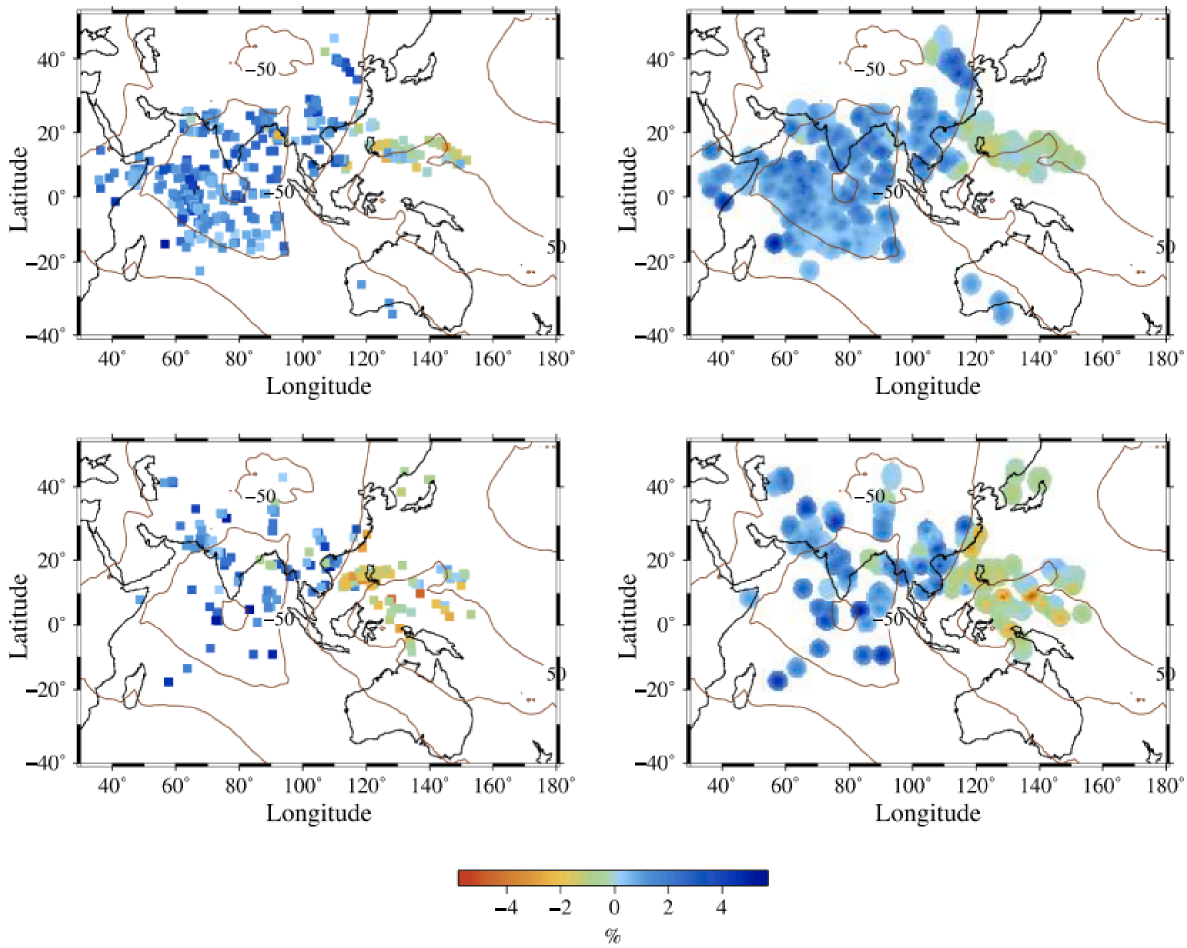

Figure 5. Percentage of shear (top left panel) and compressional wave velocity perturbations (bottom left panel) required to explain the observed differential travel time residuals in a 220 km thick layer above the CMB. Averaged shear (top right panel) and compressional wave velocity perturbations (bottom right panel) in the bottom 220 km of the mantle are inferred from the corrected travel time residuals. (From Rao and Ravi Kumar, 2022b) (*Reprinted from Journal of Asian Earth Sciences, 225, Padma Rao B., Ravi Kumar M., Lowermost mantle (D" layer) structure beneath the Indian Ocean: Insights from modeling of ScS-S and PcP-P residuals, 105038, Copyright (2022), with permission from Elsevier.*)

Saha et al.(2021) mapped the 3-D shear wave velocity of the uppermost mantle beneath the Bay of Bengal using fundamental mode Rayleigh wave group velocities calculated along 21,600 crisscrossing paths from cross correlation of ambient noise as well earthquake seismograms. They obtained distinctly different lithospheres beneath the eastern and western Bay of Bengal, on either side of 86°E longitude. The western Bay of Bengal has $>$ 120 km thick layered lithosphere and shear wave velocity of 4.7 km/s beyond 90 km depth whereas the eastern

Bay of Bengal has thinner lithosphere (60–75 km) with minimum velocity of $\sim$ 4.2 km/s, which is anomalously low for an old ocean.

3. Seismic Anisotropy, Crust and Mantle Flow

3.1 Crustal Deformation

3.1.1 Doda - Kishtwar Region, NW Himalaya

Splitting analysis of local earthquake waveforms in the Doda-Kishtwar region, NW Himalaya results in 47 individual shear wave splitting measurements (Roy et al., 2021b). The fast polarization azimuths (FPAs) primarily show two distinct patterns oriented along ENE-WSW and NW-SE directions. Both the patterns are in the Chamba sequence suggesting two deformation patterns. For the first pattern, both stations and events are located in the proximity of the Chenab River whereas for the second pattern the FPAs are parallel to the structural trend of the Chamba sequence. The FPAs are either perpendicular or sub-parallel to the maximum horizontal stress (SHmax), suggesting structure-induced anisotropy. A possible reason for the observation of the first pattern is that the shear wave samples the fluid-filled fractures in the fault zones resulting in FPAs parallel to the Chenab River, with large delay times. The extensional tectonic structures of the NW Himalaya could explain the second pattern of anisotropy.

3.1.2 Arunachal Himalaya

Shear wave splitting analysis beneath Arunachal Himalaya using waveforms of 396 local earthquakes recorded at 32 stations resulted in 76 well constrained splitting measurements (Nanajee et al., 2022). The delay times vary from 0.02 to 0.30 s, and are clustered around 0.07 s. There is a significant variation in the orientation of FPAs. The western part of Arunachal Himalaya is associated with smaller delay times (mostly $<$ 0.10 s) and has large variation in the FPAs. The FPAs mostly vary from E-W to NNW-SSE along the westernmost profile. The observed anisotropy is associated with heterogeneities in the lithological properties, and the anisotropy is both stress-induced and structure-induced. There is a small crustal block in the central part of Arunachal, in which the FPAs are parallel to the strike of the Himalayan arc and are associated with structure-induced anisotropy. In the eastern part of the Arunachal Himalaya, a variation in the orientation of FPAs is observed from north to south. In the north, the FPAs are parallel to the strike of the Siang River in the eastern Himalaya syntaxis, suggesting structure-induced anisotropy. While in the south, the FPAs are mostly parallel to SHmax, suggesting stress-induced anisotropy.

3.1.3 Southeastern Tibet

Tiwari A.K., et al. (2022a) obtained a depth-dependent crustal anisotropic signature beneath SE Tibet using directional dependence of receiver functions. The obtained upper crustal (0-20 km) anisotropic orientations, which are orthogonal to major faults and suture zone, suggest structure induced anisotropy beneath the region. The anisotropic orientations of the middle (20-40 km) and lower (40-70 km) crust suggest ductile deformation due to crustal flow beneath the region. This study along with previous SK(K)S and direct-S splitting measurements suggests partial coupling between the crust and upper mantle beneath the region.

3.1.4 Shillong Plateau - Mikir Hill, NE India

Data from a 17-station broadband seismic network have been used to study correlation between polarization direction of crustal anisotropy with seismogenic stress field at different locations of the Shillong-Mikir Plateau and its vicinity in northeast India (Baruah et al., 2021). The stress field has been determined around the stations using focal mechanism solutions (FMS) by waveform inversion. It is observed that polarization direction of crustal anisotropy is consistent with that of the maximum horizontal stress as well as the minimum horizontal stress. In addition, two orthogonal fast polarizations are also noted in some locations. The bivariate nature of suggests that the major mechanisms of seismic crustal anisotropy are not only due to the regional stress, but active faults and other geological conditions play a significant role in contemporary orientation of seismic crustal anisotropy and seismogenic stress field.

Earthquake source mechanisms obtained through waveform inversion reveal that the closely spaced Mishmi, Tidding, and Lohit faults are steeply dipping thrust sheets (dip $\sim 50°$) that accommodate large crustal shortening, owing to the indentation process and clockwise rotation tectonics. The Walong fault is characterized by strike-slip motion which helps to facilitate the clock-wise rotation of crustal material around the syntaxis (Hazarika et al., 2022). Radial anisotropy interpreted within the Eastern Himalaya Syntaxis (EHS) and the Indo-Burmese Ranges based on surface wave dispersion reveals stronger anisotropy in the deeper part below ˜40 km depth (Chanu et al., 2022).

3.2 Upper Mantle Deformation

3.2.1 Ladakh - Karakoram zone (LKZ)

Seismic anisotropy of the upper mantle beneath the eastern LKZ and northwest Himalaya has been investigated based on splitting in SKS waveforms recorded at 28 broadband seismic stations (Fig.6). In the frontal part of the Himalaya, the Fast Polarization Directions (FPDs) are mostly parallel or sub-parallel to the strike of the Himalayan orogeny suggesting deformation in the shallow lithospheric mantle under compression owing to the India-Asia collision. On the other hand, FPDs observed in the Lesser, Higher, and Tethyan Himalaya largely follow the NE-oriented absolute plate motion (APM) of the Indian plate which can be attributed to basal shear as the Indian plate moves above the asthenospheric mantle, with a minor contribution from shallow lithospheric deformation. A complex anisotropy pattern is observed in the Indus Suture Zone. The FPDs near the Karakoram Fault Zone are parallel or sub-parallel to its strike. The study suggests that KF extends up to the lithospheric mantle accommodating the India-Asia collision and facilitating extrusion in the Tibetan Plateau (Paul A., et al., 2021).

3.2.2 Western Himalaya

Upper mantle anisotropy beneath the western Himalaya is investigated using data from 62 broadband seismic stations (Biswal et al., 2020; Kumar V.P., et al., 2022). Of these 62 stations, around 18 stations are located along a linear profile in the Kumaun-Garhwal Himalaya traversing the Himalaya from south to north. The study region mostly comprises of Himachal (Biswal et al., 2020) and Kumaun-Garhwal (Kumar V.P., et al., 2022) Himalaya. The FPAs are mainly oriented along the ENE-WSW and $\sim$ E-W directions, respectively, and a few in the NE direction (see Fig.4 of Kumar, V.P., et al., 2022). Also, very few observations in the Kumaun-Garhwal Himalaya are oriented along the $\sim$ SE-NW direction. The delay times mostly vary from 0.2 and 1.7 s, mostly between $\sim$ 0.4 to $\sim$ 1.0 s. In the Kumaun-Garhwal Himalaya, the average delay time gradually decreases from 0.9 to 0.7 s in the sub- and lesser Himalaya to 0.6 s in the MCT zone and the higher Himalaya. There is not much variation in the orientation of FPAs from south to north in the Himachal and Kumaun-Garhwal Himalaya.

Another study on shear wave splitting (Kumar N., et al., 2021) reveals that both stress and structure-induced anisotropy prevail in the Kumaun Himalaya. The anisotropy directions are mainly NE-SW, N-E and NW-SE, in agreement with the observed gravity lineaments (Hajra et al., 2022b).

3.2.3 Shillong Plateau

Mohanty and Singh (2022) investigated the shear wave splitting using SKS, SKKS, PKS phases for Shillong Plateau and have found that the deformation patterns beneath the northern and central Shillong Plateau are dominated by the asthenospheric forces controlling the absolute plate motion (APM) of the Indian plate in a no net rotation frame in a distinctive NE direction. Also, they have reported that at the southern proximity of the Shillong Plateau, the deformation pattern seems to be aligned parallel to the major regional geological structures. The coherent lithospheric deformation along with transpressional tectonics act as the major source of anisotropy at this southern end.

3.2.4 Rajasthan Craton

Shear wave splitting parameters are obtained at four broadband seismic stations in Rajasthan using core-refracted phases (Mandal, 2019c). The delay time was found to vary from 0.3 to 2.4 s and clustered around 1.6 and 1.7 s. The FPAs are found to vary from 8° to 175°. However, most of them are along the NE direction, parallel to the absolute plate motion (APM) direction of the Indian plate in the no-net-rotation frame. The basal drag could be the primary cause for the observed APM parallel anisotropy beneath the Rajasthan craton. It is inferred that the coherent lithospheric fabrics in the Rajasthan craton were formed during the Archaean and survived subsequent Paleoproterozoic tectonic events.

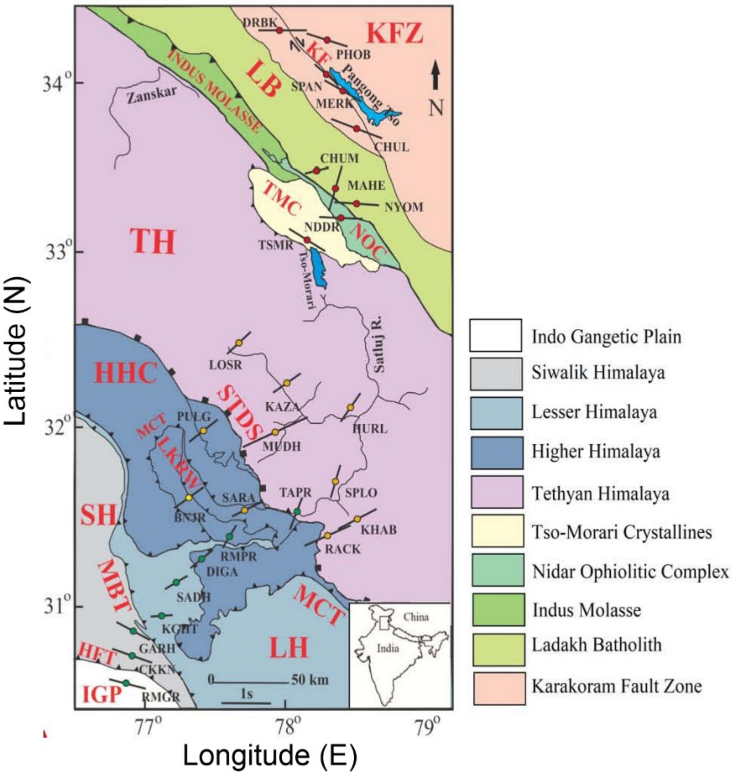

Figure 6. Simplified tectonic map of the Ladakh-Karakoram zone and northwest Himalaya. The orientation and length of the bar plotted with the red dots indicates predominant Fast Polarization Direction and splitting delay time (δt), respectively. (From Paul A., et al., 2021) (*Reprinted from Journal of Geodynamics, 144, Arpita Paul, Devajit Hazarika, Monika Wadhawan, Naresh Kumar, Upper mantle anisotropy in the northwest Himalaya and Ladakh-Karakoram zone based on SKS splitting analysis, 101817, Copyright (2021), with permission from Elsevier.*)

3.2.5 Kachchh rift zone

Shear wave splitting observations beneath twelve broadband seismic stations in the Kachchh rift zone (KRZ), Gujarat, are estimated using the core-refracted phases (Singh and Mandal, 2020; Mandal, 2021). In total, 443 new measurements are obtained. The mean value of FPAs varies from 49.41° to 103.78° at the stations, with an average value of 76.91°. Similarly, the delay times are found to cluster around 1.39 to 2.34 s at the stations. Most of the FPAs are clustered around 60°and 80°, suggesting an ENE-WSW direction, near parallel to the E-W trending Kachchh rift axis. It is suggested that the upper mantle anisotropy beneath the KRZ is parallel to the Kachchh rift axis. It is generally observed that rift zones are generally characterized by large delay times, which also suggests significant anisotropic contribution from the asthenospheric flow-induced anisotropy. Thus, the KRZ region is associated with a thick anisotropic layer, with mantle anisotropy parallel to the Kachchh rift axis direction caused by both frozen lithospheric anisotropy and asthenospheric flow-induced anisotropy.

3.2.6 Western Ghats

The mantle deformation pattern beneath the Western Ghats, India, is investigated using shear wave splitting of core-refracted phases at 17 broadband seismic stations (Sribin et al., 2021). In total, 193 measurements are obtained, comprising 52 splitting and 141 null measurements. The delay times are found to vary from 0.3 to 2.8

s, and the FPAs from N6° to N177°. The dominant direction is found to be NE, parallel to the APM direction of the Indian plate in a no-net-rotation frame. The dominant cause for the observed anisotropy is shear at the base of the lithosphere. The E-W orientation at stations close to the western coast, especially in the northern part of the Western Ghats can be associated with the lithospheric stretching along the west coast, associated with rifting process. Also, the coast parallel FPAs oriented along N-S and NNW-SSE direction with delay times varying from 0.6 to 1.2 s at stations away from the coast could be associated with the edge flow due to the transition from a thick to a thin lithosphere.

3.2.7 Profile across the Dharwar Craton and the Cuddapah Basin

Upper mantle anisotropy is investigated along a west-to-east profile having 38 broadband seismic stations covering mid-Archaean Western Dharwar Craton (WDC), late-Archaean Eastern Dharwar Craton (EDC), and Proterozoic Cuddapah Basin (CB) (Saikia et al., 2019). The orientation of FPAs varies from -50° to 5° in the WDC, -40° to 30° in the EDC and -5° to 85° in CB and further east. The delay times vary from 0.4 to 2.0 s, with the average being 1 s. In the WDC, the orientation of FPAs is found to align along the strike of shear zones and faults. This suggests frozen-in anisotropy in the lithosphere, possibly established during the lithospheric evolution in mid-late Archaean. In the EDC, the orientation of the FPAs deviates from the APM direction, suggesting anisotropy frozen-in from the episodes of late Archaean to Proterozoic period. The splitting trend beneath the CB and Eastern Ghats (EG) follows the strike of the rift along with plate motion direction, indicating that the anisotropy is influenced by a combination of frozen anisotropy due to continental rifting along the eastern margin of the Indian plate and active asthenospheric flow.

3.2.8 NW-SE Profile across the DVP and the EDC

The upper mantle anisotropy is investigated beneath the DVP and the EDC at fifteen broadband seismic stations located along a NW-SE profile (Sivaram et al., 2022). In total, 71 measurements are obtained by performing shear wave splitting analysis of core-refracted phases. The orientation of FPAs suggests variation in splitting parameters along the profile. In the DVP, the orientation of FPAs is along NE-SW with the delay times varying from 0.5 to 1.2s. In the EDC and EGMB (Eastern Ghat Mobile belt), the FPAs are along NW-SE in EDC and NE-SW in EGMB, and the delay times vary from 1 to 1.4 s. The non-APM orientation in EDC suggests frozen-in anisotropy in a thick lithosphere, associated with the late Archaean to Proterozoic events or the last major episode of tectonic and magmatic activity during 2.6 Ga. In the DVP, the deformation seems to represent the predominant APM-trending asthenospheric anisotropy beneath a thinned lithosphere. Possibly, the upper mantle is influenced by shear interactions from the geologically recent $\sim$ 65 Ma Deccan plume event. In the EGMB, the FPAs are sub-parallel to the APM direction, which suggests imprints of rifting.

3.2.9 Eastern Ghat Mobile Belt (EGMB)

Jana et al. (2019) carried out shear wave splitting analysis using core refracted PKS, SKS, SKKS phases to capture the collisional signature preserved beneath the EGMB. This is the first geophysical evidence deciphering the episodic collisional history of EGMB. The fast axis directions have shown absolute plate motion as the dominant cause. Though in Rengali province and Mahanadi rift zone, splitting shows signatures of previous collisions. Jana et al. (2021) evaluated the seismic anisotropic signatures and mantle deformation patterns using Reference Station Technique for the EGMB and its surroundings. This study found new evidence of frozen anisotropic signature demarcating eastern Phulbani domain from western Phulbani domain. The dominant effect of absolute plate motion has been observed beneath the Bastar craton. The distinct nature of Chilka lake from its surroundings suggests Chilka lake to be a separate block.

3.2.10 Synthesis of upper mantle anisotropy beneath India

Around $\sim$ 2500 published individual shear wave splitting measurements from more than 350 broadband seismic stations are synthesized to present the mantle deformation scenario beneath India (Roy et al., 2021a). On a continental scale, the delay times are found to cluster around 0.8 s, with the FPAs predominantly along the APM direction. This is attributed to basal shear due to the interaction between the lithosphere and asthenosphere. A significant deviation from the APM is observed from south to north. The deviation from APM is categorized into four sub-regions, namely northeastern (NE), north, central, and south India (Fig.7). For the NE and north India, it is attributed to the Indo-Eurasian collision tectonics. For NE India, it is found to be parallel to the strike of the orogens, suggesting coherent deformation in the upper mantle. For central India, the deviation is attributed to frozen anisotropy associated with widespread magmatism in the DVP, paleo-rifting and collisional events in the eastern Indian shield. The deviation is stronger in southern India than in central or northern India, primarily in the DVP, WDC and the northern part of Southern Granulite Terrain (SGT). This probably reflects the lithospheric evolution process in the mid-to-late-Archaean, continental rifting in the western and eastern margins, ocean closure and subduction in the northern part of SGT. Back azimuthal variation in the splitting measurements in southern India suggests layered anisotropy and/or variation among different blocks.

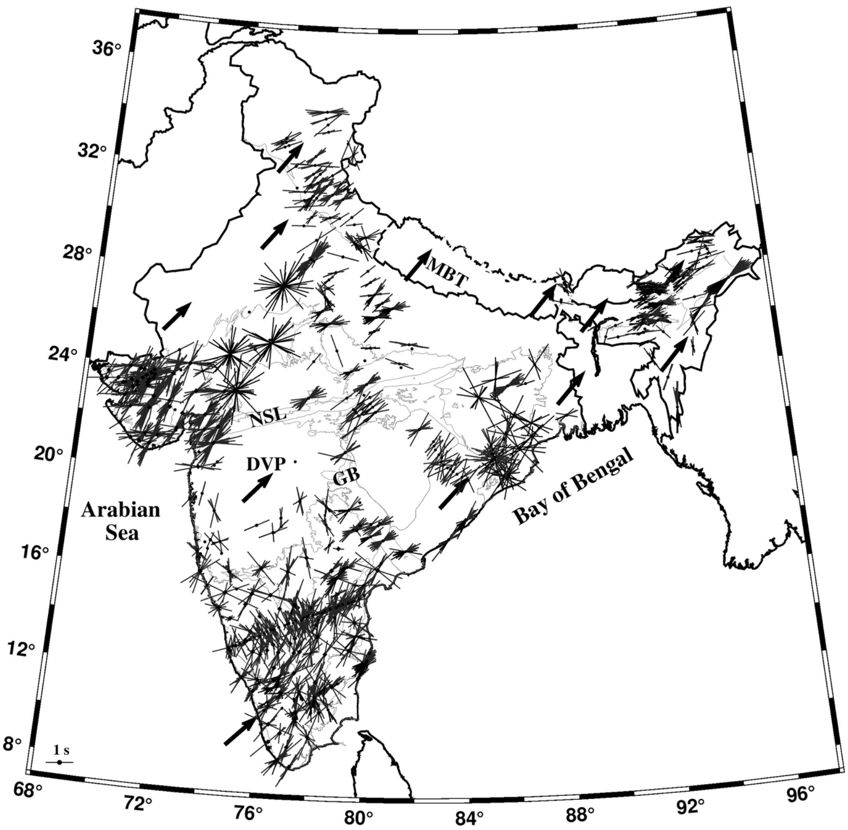

Figure 7. Map showing the individual splitting measurements at the station locations. The orientation and length of the blue lines correspond to the fast polarization azimuth (FPA) and delay time, respectively. Insets on the left (top & bottom) contain the histogram and rose diagram by considering all measurements for the delay time and fast polarization azimuth, respectively. Inset on the right represents the FPA and delay times along the AA' and BB' profiles. FPAs lies in the pink fill of the histogram and are considered to be along the APM direction. Black arrow represents the absolute plate motion direction in a no-net rotation frame (DeMets et al., 2010, Geophy. J. Int., v.181, pp.1-80). IYS - Indus-Yarlung Suture, MCT – Main Central Thrust, MBT – Main Boundary Thrust, NSL – Narmada Son Lineament, DVP – Deccan Volcanic Province, GB – Godavari Graben. (*Courtesy Dr. M. Ravi Kumar and Dr. Sunil K. Roy, CSIR-NGRI*)

3.2.11 Pn anisotropy of the Indian shield

High-resolution P-wave velocity and anisotropy structure of the hitherto elusive uppermost mantle beneath the Indian shield and its surrounding regions are obtained using 19,500 regional Pn phases from 172 broadband seismic stations (Illa et al., 2021a). The effect of continental rifting, collision and orogeny is reflected in the Pn velocity image. The cratons in the Indian shield have uppermost mantle velocities ranging from 8.02 to 8.42±0.05 km/s. Prominent highs and lows are observed in the shield region related to mantle deformation episodes, as the Indian plate has experienced major tectonic activity during and after the breakup from the Gondwanaland. The Pn and SKS anisotropic fast axis directions are consistent, except for the Indian shield, revealing that the Indian cratons are distinct with an altered uppermost mantle preserving the remnant anisotropy. The FPAs are consistent in the collision environments in the west, Himalaya, and Burmese arc region.

3.2.12 Anisotropy of NW DVP using Surface waves

The anisotropic and isotropic variations within the crust and upper mantle beneath the NW DVP are investigated using surface waves (Sharma J., et al., 2021). Results reveal different intra-crustal layers, lid, and a low-velocity zone (LVZ). The LVZ comprises a uniform asthenospheric low-velocity layer (LVL) of average V_{SV} 4.44 km/s and V_{SH} 4.47 km/s, and another LVL with an average V_{SV} 4.45 km/s and V_{SH} 4.41 km/s. A negative radial anisotropy is observed in the LVZ, indicating the dominance of vertical flow. This could be related to partial melts, volatile materials and/or a thermal anomaly.

4. Seismic Attenuation

Sivaram and Gupta (2022) investigated the frequency-dependent seismic attenuation characteristics of the crust beneath the Kumaun Himalaya using seismic coda waves (Qc-1) and high-frequency body waves (Qα-1 and Qβ-1). The results show that that the seismic attenuation is different for the Lesser Himalaya and the Higher Himalaya segments, which could possibly be due to the mechanism of underthrusting and deformation in the Lesser Himalaya segments, leading to a dominant scattering attenuation and the multitude of fractures and pores in the crust.

Seismic wave attenuation study has been performed for the Kinnaur and Garhwal-Kumaun regions of the NW Himalaya using data of low magnitude- and micro-earthquake events (Kumar and Yadav, 2019; Kumari et al., 2020, 2021; Monika et al., 2020; Kumar P., et al., 2021). Attenuation characteristic divide the Kinnaur Himalaya into three zones correlating with crustal/lithosphere structure and micro-earthquake activity. Decreasing attenuation with depth indicates more heterogeneities in the upper crust which can be explained by the effect of turbidity. The attenuation largely depends on the heterogeneities developed due to the collision of the Indian and the Eurasian plates. The attenuation is larger in the Tethys Himalaya than in the High Himalayan crystallines. Small value of the resonance frequency and comparatively high attenuation to the north of the South Tibetan Detachment Zone indicate presence of low-grade meta-sedimentary rocks in the upper crust of the Tethys Himalaya (Kumar P., et al., 2021).

A series of studies on coda, body wave, and surface wave attenuation have been carried out for the Tibet and Nepal Himalaya regions. These studies suggest dominance of intrinsic attenuation for the Nepal Himalaya and southern Tibet. The second region shows dominance of scattering attenuation at higher frequencies ($>$ 8 Hz) (Singh C., et al., 2019a; Biswas and Singh, 2019). Similar studies have been carried out for western Tibet and Karakoram fault region (Biswas and Singh, 2020a, 2020b, 2020c; Sarkar et al., 2021; Jaiswal et al., 2022), and southeastern Tibet (Tiwari A.K., et al., 2022b).

Singh C., et al. (2019a) investigated the spatial variations of coda wave attenuation structure using local events for Andaman-Nicobar Subduction Zone. The study shows high attenuation near Narcondum volcanic island, which also coincides with low-Vp zone, suggesting change in crustal properties. The results also reveal a good correlation between $Q_{\circ}$ and seismicity, suggesting the presence of a highly scattered medium.

Singh C., et al. (2019b) investigated the spatial variations of Pg attenuation structure in Nepal Himalaya by the "Two-Station method" applied to 2325 waveforms obtained from 435 events recorded at 151 stations deployed across Nepal Himalaya. Their results suggest that the areas around the existing faults and lineaments exhibit very low Q values. They inferred that intrinsic attenuation plays a major role in causing the high apparent Pg attenuation in the crust of Nepal Himalaya. This may be mainly caused by highly pressurized fluids trapped within a thin low-velocity layer (LVL) at shallow depths.

Das and Mukhopadhyay (2020) studied the spatial variation in attenuation characteristics in Northeast India using coda Q. The average frequency dependencies of coda wave attenuation for a 30 s window length are estimated as Qc(f) = 135 ± 7f0.99± 0.03, Qc(f) = 109 ± 7f1.10±0.03 and Qc(f) = 90 ± 2f1.04±0.02 for Shillong Plateau, Mikir hills and surrounding River valley, and Indo-Burma Ranges respectively. It is observed that Q0 is greater for the Shillong Plateau than the other sub-regions. For window lengths $\geq$ 55 s, the central part of the Indo-Burma Ranges has higher Qc values at 10 and 12 Hz compared to the Shillong plateau.

Lg-Q for the Indian Shield derived from tomographic inversion varies from 50 to 650, while the frequency-dependent parameter varies between 0.4 and 1.1 with an average value of 0.7. Structural features such as rifts, suture zones, sedimentary, and active regions are characterized by high attenuation ($Q_{\circ}$<200) (Reshma et al., 2022).

5. Crustal Structure of Seismically Active Regions by Non-seismic Methods

5.1 Himalaya

5.1.1 Seismotectonics of the Sikkim Himalaya

The occurrence of deep crustal strike-slip earthquakes in the Sikkim Himalaya is indicative of the ongoing transverse tectonic deformation of the Indian plate, in addition to the N-S convergence related deformation within the Himalayan wedge. The two dominant tectonic forces operating in this region could lead to a complex variable spatial deformation within the Indian lithosphere. Two-dimensional modeling of magnetotelluric data incorporating the NW-SE transverse tectonic trend within the Main Central Thrust zone (MCTZ) yields a lithospheric electrical resistivity structure of the region down to 100 km. By integration of these results with other geophysical information, seismological data and in conjunction with a kinematic wedge model, Pavankumar and Manglik (2021) proposed a comprehensive tectonic model for the Sikkim Himalaya that highlights the complex nature of the lithospheric structure (Fig.8). A major contact beneath the MCTZ separating two geologically and compositionally distinct blocks of the underthrusting Indian plate is suggested to be a NW-SE trending lithospheric-scale fault in this segment of the Himalaya. The tectonic model also demonstrates another crustal-scale tectonic feature beneath the Main Frontal Thrust that demarcates a transition zone of moderately conductive crust of the Ganga Foreland Basin and a resistive crustal block beneath the Sub-Himalaya.

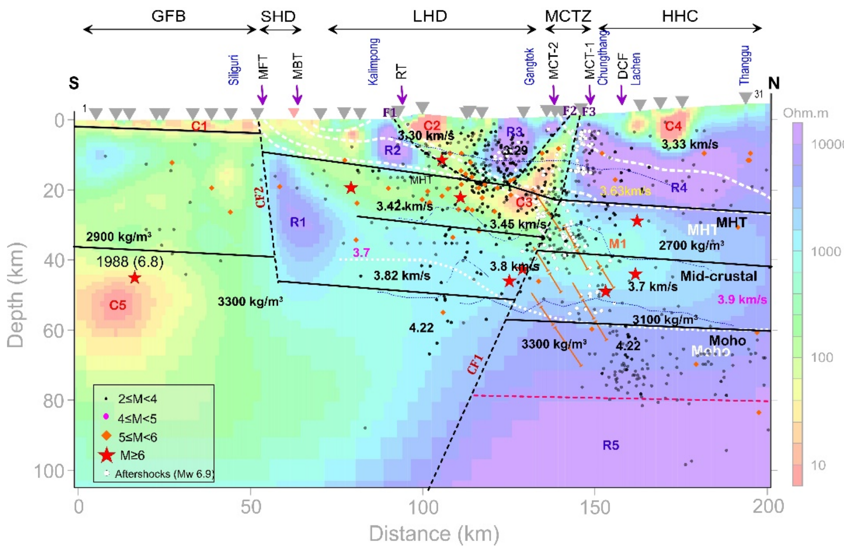

Figure 8. A tectonic model proposed for the Sikkim Himalaya based on the lithospheric geoelectric structure obtained by the present MT experiment and available seismic and density information as well as a kinematic model of the wedge structure. (From Pavankumar and Manglik, 2021) (*Reprinted from Physics and Chemistry of the Earth, Parts A/B/C, 124, G. Pavankumar, Ajay Manglik, Complex tectonic setting and deep crustal seismicity of the Sikkim Himalaya: An electrical resistivity perspective, 103077, Copyright (2021), with permission from Elsevier.*)

5.1.2 Gravity Modeling of the Kopili and Bomdila fault regions

An integrated approach based on seismotectonics, gravity and magnetic data is utilized to understand the tectonic activity of the Kopili and Bomdila Faults bounding the Mikir Hills (Sharma S., et al., 2018). The Kopili Fault dips

NE at 75° whereas the Bomdila Fault dips NNE at 50-55° angle. The bottom of seismogenic zones is inferred to be 45±2 km and 50±2 km for the Kopili Fault and the Bomdila Fault regions, respectively. The low gravity values over the Bomdila Fault area indicate presence of thick alluvial deposits while lesser sediment thickness is observed along the Kopili Fault.

5.2 Indian Shield Region

5.2.1 Magnetotelluric investigations in the vicinity of the Delhi Seismic Zone

The Delhi Seismic Zone (DSZ) in the northwest Indian shield is one of the seismically active intraplate regions with frequent occurrence of small-to-moderate magnitude earthquakes. These earthquakes occur mainly along the NE-SW oriented Proterozoic Aravalli-Delhi Fold Belt (ADFB) and NNW-to-NW trending Delhi-Sargodha Ridge (DSR). However, the detailed subsurface architecture of DSZ and its surrounding areas concealed by alluvial sediments is still unclear. Pavankumar et al. (2021) and Manglik et al. (2022) conducted magnetotelluric (MT) experiments across the DSR and the ADFB, respectively, to image this region in terms of electrical resistivity structure. The results yield a northward dipping electrical conductor ($<$ 10 m) down to 20-25 km for the DSR whereas the ADFB buried beneath the alluvial sediments of the western Ganga Basin consists of a collage of nearly vertical conductive and resistive blocks and a sharp resistive contrast. These blocks appear to continue beneath the Kumaun-Garhwal Himalaya. These results have significant implications for earthquake hazard potential of both the region, the DSZ and the Uttarakhand Himalaya.

5.2.2 Pre-eruptive crustal electrical structure and tectonics of the recent Palghar earthquake swarm activity region, Maharashtra

The DVP is a major geological domain of the Indian peninsular shield. Though the region is considered to be seismically stable, it has experienced some significant intraplate earthquakes, as well as swarm type earthquake activity at Bhatsa, Silvasa, Navsari, Nasik, Valsad and more recently at Palghar. Pavankumar et al. (2020) carried out MT studies along two profiles covering the Bhatsa and the Palghar earthquake swarm regions. Geoelectric models of these two regions depict strong resistivity contrast suggesting that the crust below the basalt cover is fragmented. The zones of fragmentation coincide with the major pre- and post-eruptive tectonic structures, e.g. the West Coast fault, the Panvel Flexure and the Kurudwadi rift.

5.2.3 Seismogenesis of intraplate Kachchh rift in western India by Magnetotellurics

The Kachchh basin comprises a set of E-W trending faults and fault bounded uplifts. Since historic past, the region is experiencing moderate to large magnitude earthquakes and is considered as one of the most active intraplate regions of the world. Magnetotelluric studies carried out in various segments of the region yield well resolved electrical images of the deep crust, enabling delineation of the broad geometry of various active faults (Nagar et al., 2021). The MT models in conjunction with 3-D relocated hypocenters provide better constraints on the geometry of the seismogenic segments of the faults at depth. Among the various intra- basin faults, the South Wagad Fault (SWF) has a downward lower crustal extension that possibly connects to a fluid reservoir in the upper mantle. However, the Kachchh Mainland, Katrol Hill, Gedi and Allahbund faults are limited to the upper crustal depths. The North Wagad Fault is inferred as an antithetic splay of the SWF.

6. Seismic Hazard, Risk and Strong Ground Motion Studies

6.1 Strong Ground Motion and Earthquake Hazard Assessment

6.1.1 Plate boundary regions

Mir and Parvez (2020) simulated bedrock level peak ground motion at 2346 sites on a regular grid of 0.2°x0.2° in NW Himalaya from 543 simulated sources, using the stochastic finite-fault, dynamic corner frequency method, with particular emphasis on Kashmir Himalaya. Acceleration time series generated are then integrated to obtain velocity and displacement time series, which are all used to construct a suite of hazard maps of the region. The expected PGA values for the Kashmir Himalaya and Muzaffarabad are found to be $\sim$ 0.3–0.5g and for the epicentral region of the 1905 Kangra event, to be 0.35g. The PGA values estimated in this study are in general found to be higher than those implied by the official seismic zoning map of India produced by the Bureau of Indian Standards. Major events in Kashmir Himalayas, such as those of 1555, 1885 and 2005, are simulated individually to allow comparison with available results. This study provides a first-order ground motion database for safe design of buildings and other infrastructure in the NW Himalayan region.

Kumar and Sharma (2019) performed a detailed study on the temporal evolution of seismicity in and around the seismic gaps in the Himalayan region. They segmented the region into four meridional regions (A) 80°E to 83.5°E, (B) 83.5°E to 87.5°E, (C) 87.5°E to 90°E, and (D) 90°E to 98°E along with a fixed latitude belt. A homogeneous catalogue with $3 \leq M_b \leq 6.5$ was used for the spatial and temporal analysis of seismicity in terms of b-value. It is found that pockets of lower b-values coincide over and around stress accumulated regions. The observed low b-value before the occurrence of the Nepal earthquake of 2015-04-25 supports the argument of impending occurrence of moderate to large magnitude earthquake in Sikkim and north-east Himalayan region in future.

Singh S.K., et al., (2020) documented the site amplification at 28 sites in the Indo-Gangetic Plains (IGP) using the RSS (ratio of the source spectrum) technique. The fundamental frequency (f_o) of the sites increases from 0.12 Hz near the foothills of Himalaya to 2.0 Hz at the southern edge of the basin and the amplification reaches about 10. At several sites, is difficult to select and an amplification of ~ 5 in broadband is in the range 0.12–0.7 Hz. Application of standard spectral ration (SSR) technique to teleseismic *S*-wave data recorded in the IGP reveals that this approach may be useful in the estimation of amplification at low frequencies (< 0.5 Hz).

Sharma N., et al. (2021) targeted two largest magnitude earthquakes (2017-02-06 M 5.1 and 2017-12-06 M 5.6) recorded by the CSIR-NGRI network in Uttarakhand. They estimated the peak ground acceleration (PGA), peak ground velocity (PGV) and peak ground displacement (PGD) from recorded waveforms and acceleration, velocity and displacement response spectra at different structural periods for districts like Haridwar, Rudraprayag, Almora, Tarikhet and Thakurdwar. Their simulation reveals that the displacement spectra for many Himalayan earthquakes obey a circular crack model with fall. The high stress drop (70 and 100 bars) estimations suggest high release of energy in the seismic zone V region which hosted the 1991 Uttarkashi (M 6.8) and 1999 Chamoli (M 6.3) earthquakes. The PGA values estimated at Rudraprayag district (168 cm/s^2) bring the district under moderate to severe intensity zone even for moderate size earthquakes.

Strong motion data from the network operated by WIHG in the Himalaya have been used to quantify seismic hazard assessment in the form of attenuation, site effects, and simulation of strong ground motion for different sectors of the Himalaya, e.g. Garhwal and Kumaun (Uttarakhand), Kinnaur (Himachal Pradesh), Nubra-Shyok (Ladakh), and NE India (Sandeep et al., 2019a, 2019b, 2019c, 2020, 2022; Kumar P., et al., 2019). This work provides great insight into exploring recent trends in seismology and earthquake engineering for seismic hazard evaluation.

In the Jammu & Kashmir sector of the Himalaya, the thrust faults are blind and large-scale folding is the only expression of active deformation at the surface, making it difficult to assess seismic hazard in this region. O'Kane et al. (2022) used field, satellite and seismological observations to determine the fault geometry for this region and modeled the potential hazard scenarios. Their results suggest that earthquakes that rupture the buried, shallow part of the locked Main Himalayan Thrust could generate PGVs that are >3 times larger than earthquakes of the same magnitude on its deeper portions.

Gogoi et al. (2023) estimated ground motion parameters (GMPs) by processing 125 accelerogram records of 26 earthquake events, with 375 components, that originated in NE India and its vicinity with special emphasis on the 2016-01-M6.7 Tamenglong earthquake. Moreover, Ground Motion Prediction Equations were developed through multiple regression analysis on observed data of 8 GMPs namely, PGA, PGV, Arias Intensity, Characteristics Intensity, Housner Intensity, Cumulative Absolute Velocity, Effective Design Acceleration and Acceleration Spectrum Intensity. The developed equations are representative of statistics on changes in amplitudes of parameters with varying distances and magnitude in connection to NE India. Besides, newly developed GMPEs can be applied to 4–6.8 magnitude earthquakes and valid up to 525 km of distance.

Boruah et al. (2022) attempted estimation of site amplification factors of different geomorphological units in Shillong city using the distribution of PGA due to maximum credible earthquakes that originated in nearby major faults and average shear wave velocity (Vs30) values for various geomorphological units. The amplification for the highly dissected land in the city is found to be maximum within a range of 2.77–2.92, while the high plateau segment is characterized by least values (2.01–2.16). Simultaneously, the effective ground motion mapped on the surface indicates a maximum value of 0.6–0.94g for a probable earthquake of Mw 8.1 on the Dauki fault. Similarly, Dhubri and Kopili faults might produce a ground motion of 0.05–0.08 and 0.22–0.33g for a maximum credible earthquake of Mw ~ 7.0, respectively.

The distribution and dissipation of post-seismic stress have been investigated for the Garhwal-Kumaun region based on spectral analysis of P-waveforms of local earthquakes (Hajra et al., 2022a). The study detects significantly lower stress drop compared to the overall values for the Central Seismic Gap region suggesting incomplete dissipation of the accumulated stress. The high-stress drop events are predominant along the MHT at mid-crustal depths, with the upper ~ 10 km of the brittle crust rarely hosting any strong earthquake. The b-value is estimated as 0.64 ± 0.08 for the Kumaun Himalaya, which is low compared to the Garhwal and the rest of the NW Himalaya.

The Ladakh-Karakoram zone (LKZ) is a unique testing ground for understanding the geodynamic evolution of the Himalaya-Karakoram orogeny. Despite the accumulation of a large amount of strain energy that originated due to the India-Asia collision along the Karakoram fault, earthquakes of $M\geq 7.0$ are considerably less in the Karakoram Fault Zone compared to the Himalayan seismic belt in the northwest Himalaya. Earthquake source parameter study in the LKZ through spectral analysis of P-waves of local earthquakes reveals low-stress drop earthquakes (~ 0.06-64.36 bar) caused by the possible presence of aseismic creeping patches in the Karakoram Fault. A partial stress drop mechanism is proposed for low-stress drop in the forearc region (Paul and Hazarika, 2022).

Although the 1950 Assam earthquake (Mw 8.7) endures as the largest continental earthquake ever recorded, its exact source and mechanism remain contentious. Coudurier-Curveur et al. (2020) analyzed the spatial distributions of reappraised aftershocks and landslides to estimate the hitherto unknown surface rupture extent along the Mishmi and Abor Hills. Their results from two key sites (Wakro and Pasighat) suggest over twice as large coseismic surface throw (7.6 ± 0.2 m vs. $> 2.6\pm0.1$ m) and average thrust dips (25–28° vs. 13–15°) on the Mishmi Thrust (MT) and Main Himalayan Frontal Thrust (MFT).

The Shillong Plateau is a peculiar geodynamic terrane hosting significant seismic activity outboard the Himalayan belt. This activity is often used as an argument to explain an apparent reduced seismicity in the Bhutan Himalayas. Although current geophysical and geodetic data indicate that the Bhutan Himalaya accommodates more deformation than the Shillong Plateau, it is aimed to quantify the extent to which the two geodynamic regimes are connected and potentially interact through stress transfer. Grujic et al. (2018) compiled a map of major faults and earthquakes in the two regions and computed co-seismic stress transfer amplitudes. Results indicate that the Bhutan Himalaya and the Shillong Plateau are less connected than previously suggested. The 1897 Assam earthquake (Mw 8.25) that affected the Shillong Plateau did not cause a stress shadow on the Main Himalayan Thrust in Bhutan as previously suggested. Similarly, the 1714 Bhutan earthquake (Mw 8 ± 0.5) had negligible impact on stress accumulation on thrust faults bounding the Shillong Plateau.

An earthquake of magnitude Mw 5.7 shook the northeastern region of India on 2017-01-03 at 14:39:0.5 local time. The duration of the tremor lasted for about 5–6 s and had its epicenter in Dhalai District, Tripura, India. Even though the earthquake was of moderate magnitude, it caused damage to several masonry dwellings in Tripura and triggered soil liquefaction, lateral spreading, and landslides near the epicentral area. Anbazhagan et al. (2019) reported field reconnaissance observations of geotechnical effects and damage to buildings following this earthquake. In addition, the distribution of surface PGAs caused by the earthquake was estimated from the empirical equations based on the available data.

6.1.2 Intraplate regions

Surve et al. (2021) performed seismic hazard studies for the Mumbai city (financial capital of India), having a population of over 18 million. Two seismicity models, linear and areal, were used to compute the seismic hazard of Mumbai with an updated earthquake catalogue and latest knowledge on seismotectonics of the region. The hazard values for Mumbai corresponding to 475-year and 2475-year return periods are computed. Hazard maps at bedrock level for 2% and 10% probability of exceedance in 50 years were prepared. The hazard levels obtained in the present study are lower than those reported for the same area by previous researchers. The lower seismic hazard can be attributed to the fact that in this study, the Koyna–Warna region is used as one of the five independent source regions and reservoir triggered seismicity at times might reduce the overall seismic hazard in nearby regions.

Mandal and Asano (2019) modeled the low-frequency (0.1–1 Hz) ground motions excited by the 2006-04-06 event, using the finite difference method assuming a point source, to assess the robustness of the constructed velocity structure model. At most of the stations, the observed and simulated velocity waveforms are found to be in good agreement in terms of both amplitude and ground motion duration. They also computed synthetic ground velocities at numerous locations within the basin, for both the 2001 Bhuj mainshock (finite-fault source) and the 2006 aftershock (point source) cases, using a 3-D velocity model. Their work revealed that the presence of low velocity sediments within the Kachchh rift basin plays a key role in modifying/amplifying the ground motions in 0.1–1.0 Hz range.

The study of two earthquakes (2006-03-07 and 2006-04-06, Mw 5.5) in the Kachchh seismic zone by Mandal (2020) revealed that the estimated normalized response spectra at strong motion accelerograph sites in the Tertiary formations or near a zone of geological contact between the Jurassic/Tertiary formations, exceeded the design response spectra in the period range of 0.07–0.2 s, correlating with the complete collapse of low-rise buildings, water tanks and dams during the 2001 Bhuj earthquake. On the other hand, the normalized acceleration spectrum of corresponding to hard sediments (rock site) is found to not exceed the design spectrum, correlating with the lack of damage in the Mesozoic hill zone. It is also noticed that the spectral acceleration values at a few sites lying on the Quaternary formations have exceeded the design spectra at 3–4 s, suggesting these sites to be hazardous for engineered reinforced structures like bridges.

A rare lower crustal earthquake occurred on 2021-07-25 near Hyderabad, India. Mandal et al. (2022) used waveforms from 9 broadband stations and computed the average corner frequency, seismic moment, moment magnitude, stress drop, and source radius as 3.87 Hz, 7.14E+14 N-m, 3.75, 3.92 MPa, and 229 m, respectively. The mean crustal Q for the region was modeled to be 2182+-1178, suggesting lower crustal attenuation below the Hyderabad region. However, the spatial distribution of the modeled crustal Q values revealed a high Q zone to the east of Hyderabad city, while a moderate Q zone was found west of the city. It is inferred that this lower crustal intraplate earthquake with a large stress drop of 3.9 MPa might have been generated due to the sudden movement on an almost vertical fault due to high pore-fluid pressure caused by the presence of CO_2-rich mantle fluids.

Srinagesh et al. (2021) analyzed a sequence of about 965 earthquakes in the magnitude range of 0.1–4.6. The main shock of moderate-sized earthquake (2020-01-26, $M_L \sim 4.6$) is located in the Palnadu sub-basin of the Cuddapah basin. It was felt both in the states of Telangana and Andhra Pradesh. The earthquakes prior and after the M_L 4.6 quake are located close to the thrust and along the periphery of the backwaters of the Pulichintala reservoir. The epicentral parameters obtained from double difference technique, using a minimum 1-D velocity model, illuminated a steep seismogenic structure extending down to 8 km depth,. The b-value estimate is 0.82 for a completeness magnitude of Mc 1.8 and could be associated with an intraplate event having a longer recurrence time. The focal mechanism solution obtained from waveform inversion reveals a pure double-couple mechanism of a strike-slip motion with a reverse component on a N–S trending focal plane.

Sharma A., et al. (2021) derived a new M_L scale, using the Grey Wolf Optimization, a swarm intelligence-based global optimization technique, for the first time, that is M_L=logA+1.2588logR+0.0002789R-2.2265, where A is the amplitude measured in millimeters, and R is the hypocentral distance in km. The new ML scale derived here is valid up to 400 km. The newly derived scale has a drop of 21.37% in the overall standard deviation of all magnitude residuals when station corrections are considered in comparison to the previously used scale.

Sivaram (2021) simulated high-frequency ground motions at five stations in the National Capital Region (NCR) of India for a large hypothetical Mw 8.5 earthquake and an intermediate Mw 6.8 earthquake in the Himalayan central seismic gap, at fault-distances of about 200–300 km, and indicated that the far-reaching and adverse ground-motion intensities might affect intermediate-high rise structures (period 0.4–0.8 s) in the NCR due to the predominance of fluvial deposits. Nagamani et al. (2020) identified different zones of seismic amplification in the Surat district of Gujarat, India, which are the hub of many mining and industrial projects like oil and natural gas.

Strong motion data from the network operated by ISR have been used in several engineering seismology applications, such as, estimation of source parameters, site characterization, development of ground motion prediction equation and ground motion modeling. The data recorded from the past decade have been used to characterize various sources in the Kachchh rift and other parts of Gujarat (Kamra et al., 2020). It is found from the study that stress drop of earthquakes (M 4.0-5.1) in the Kachchh rift are in the range 2.3-10.4 MPa with an average of 5.3 MPa. The estimated seismic moment and the source radius are in the range dyne-cm and 0.43-1.32 km, respectively. The same exercise was carried out for the Saurashtra region (Kamra et al., 2021). For this region, the stress drop varies in the range 0.9-6.9 MPa with an average of 3.3 MPa. A regression relationship between observed accelerations and accelerations estimated from broadband data has been developed exclusively for the Gujarat region (Chaudhary et al., 2022).

6.1.3 Study of Earthquake Swarms

Srinagesh et al. (2020) studied earthquake activity in the Palghar region, Maharashtra, India. Until 31 August 2019, a total of 4854 earthquakes have been located here, whose local magnitude (M_L) varies from 0.1 to 4.1. Majority of the earthquakes ($\sim 94\%$) were located in the depth range of 4–16 km. The precise earthquake relocations reveal two clusters. The N–S trending cluster north of 20.04°N extends to a depth of 10 km, whereas the NE–SW trending cluster to the south of 20.04°N extends to 16 km depth. The shallow northern cluster is noticed to be sandwiched between two mapped mafic intrusions, whereas the deeper southern segment shows earthquakes clustering around the mafic intrusion. The modeled composite focal mechanism solutions for both the north and south clusters suggest normal faulting with a minor strike–slip component as the dominant deformation mode for the Palghar region. From relocated seismicity, they detected a deeper seismically active zone (with M $>$ 3) at 4–16 km depth, occupying a crustal volume of 1440 km^3.

Mandal et. al. (2021b), conducted a comprehensive analysis of swarm activities in two regions of the Indian shield – (i) Palghar (Maharashtra) and (ii) Pulichintala (Andhra Pradesh). The 3-D mapping of b-value and fractal correlation dimension (D2) reveals that the Palghar sequence follows typical characteristics of swarm activity (the b and D2 values vary from 0.1 to 2.5, and 0.39 to 2.62, respectively). On the contrary, the Pulichintala sequence (with b and D2 values varying from 0.2 to 1.68, and 0.68 to 3.0, respectively) shows negative characteristics. The Palghar region is interpreted as a region of higher tectonic stresses.

Swarm activity similar to that at Palghar in Maharashtra (Mahesh et al., 2020), has been observed in Navsari and Jamnagar districts in South Gujarat and Saurashtra. At Navsari, a swarm activity was observed around the Keliya dam from Sep.2016 just after the Indian monsoon period that continued for about 4 months. Again, the swarm activity recurred in Aug.2017 and continued for about 5 months. A local network of four stations was installed by ISR to monitor the swarm activity, in addition to the Gujarat state seismic network (Sateesh, et al., 2019; Srijayanthi et al., 2022). A total of 1048 earthquakes were located around the Keliya dam and 229 events in the Dadra and Nagar Haveli (DNH) region from Sep.2016 to June 2018. The seismicity in both the regions followed a $\sim$ NW–SE trend. It was confined to an area of 13 km x 2 km with a depth extent of 3 km at Navsari and 15 km x 2 km with depth of 6 km in DNH. In the Jamnagar district, ISR observed post-monsoon swarm activity in Sep.2019 with 76 clustered earthquakes having NW-SE trend that are in line with the strike of local lineaments and dykes.

Parija (2021) critically examined the 2011-09-18 Sikkim earthquake of M 6.9 and found it to be associated with episodes of precursory swarms, quiescence, mainshock and aftershocks. The precursory swarm and quiescence period consist of four earthquake swarms and one foreshock event of magnitude (mb $\geq$4.5) in the epicenter preparatory zone of the 2011 Sikkim earthquake. The 2011 Sikkim earthquake had about five aftershocks of magnitude (mb) $\geq$ 4.5 between 2011 and 2014 for the same region.

Parvin et al. (2021) analyzed two swarm activities in the Hyderabad region and found small absolute stress drop values ($<$ 1 MPa) and a positive correlation between the static stress drop and the magnitude of the earthquake with seismic moment varying between $-0.09 < M_L < 1.52$. They observed a clear correlation of earthquakes associated with the fractures and faults in the vicinity of water bodies which are more sensitive to variations in hydrostatic pressures caused by vertical flow recharge from rainfall and deeper pore-fluid pressure diffusion.

Rekapalli and Gupta (2021) tried to understand the foreshock-aftershock patterns, main shock to the largest aftershock magnitude ratio, and difference in magnitude of two moderate injection-induced seismicity (IIS) earthquake sequences from Oklahoma, USA, namely, Prague (M 5.7, 2011) and Pawnee (M 5.8, 2016), and comprehend the shallow crustal heterogeneity. The analysis of temporal variation of “b” value from 2002 to 2018 suggests an increase in b-value after 2009. A reduction in b-value after 2016, in response to the reduced injection volumes is noted. A sharp fall in b-value usually precedes the main shocks of magnitude M $\geq$ 3.5. The foreshock b-values are lower than the regional b-value and aftershock b-values are higher than the regional b-value within the error limits. The investigated earthquake sequences fall under Type 2 of Mogi’s model. The characteristics of ISS observed at Oklahoma are similar to the observations for the reservoir-triggered seismicity (RTS). However, with multiple injection wells operating from time to time in the region with varying amount of fluids injected, the entire IIS at Oklahoma has an appearance of a swarm.

Wadhawan et. al. (2021) studied a highly clustered shallow (<0.4 km) earthquake activity of low magnitude with accompanying rumbling sound in Sadrabadi and Zilphi villages in Dharni Taluka of the Amravati district, Maharashtra during the monsoon period of 2018 and found it to have the characteristics of a swarm. They found a strong correlation between rainfall and swarm activity and categorized it as hydro-seismicity, resulting from hydro-fracturing of the soil/weathered basalt and collapsing and caving of the rocks. In the past, no such activity has been reported from the region during or after the monsoon, despite the fact that there was more rainfall in 2019. Therefore, they suggest that the low magnitude earthquake swarm at a very shallow depth might have been induced by the percolation of monsoonal rainwater through the weathered and fractured rock-mass associated with the fault system of the Narmada Son failed rift region.

6.1.4 Earth Observation for Crustal Tectonics and Earthquake Hazards

Elliott et al. (2020) illustrated the current methods for the exploitation of data from Earth Observing satellites to measure and understand earthquakes and shallow crustal tectonics. The aim of applying such methods to Earth Observation data is to improve our knowledge of the active fault sources that generate earthquake shaking hazards. Examples of the use of Earth Observation, including the measurement and modelling of earthquake deformation processes and the earthquake cycle using both radar and optical imagery are provided. They also highlighted the importance of combining these orbiting satellite datasets with airborne, in situ and ground-based geophysical measurements to fully characterize the spatial and timescale of temporal scales of the triggering of earthquakes from an example of surface water loading. Finally, they concluded with an outlook on the anticipated shift from the more established method of observing earthquakes to the systematic measurement of the longer-term accumulation of crustal strain.

6.1.5 Contributions of Space Missions to Better Tsunami Science: Observations, Models and Warnings

Global Navigation Satellite System (GNSS) data have a key role in better describing the ground deformation following a tsunamigenic earthquake close to the coast. The GNSS observations complement seismological data to constrain the rupture model rapidly and robustly. Interferometric Synthetic Aperture Radar (SAR) also contributes to this field, as well as optical imagery, relevant to monitoring elevation changes following subaerial landslides. The observation of the sea-level variations, in the near field and during the propagation across the ocean, can also increasingly benefit from GNSS data (from GNSS buoys) and from robust satellite communication: pressure gauges anchored on the seafloor in the deep ocean contribute to warning systems only by data continuously transmitted through satellites. The sounding of ionospheric Total Electron Content (TEC) variations through GNSS, altimetry, or a ground-based airglow camera, is a promising way to record tsunami initiation and propagation indirectly. Finally, GNSS, optical and SAR imagery are essential to map and quantify the damage following tsunami flooding. Satellite data are expected to contribute more to operational systems in the future provided they are reliably available and analyzed in real time (Hebert et al., 2020).

6.1.6 Aftershock Duration of Strong to Major Himalayan Earthquakes

Earthquakes of M$\geq$ 5 tend to be locally damaging, specifically when these are the aftershocks of larger earthquakes, as the main shock would have weakened the structures. For the rescue operations and general well-being of the residents, it is helpful if an estimate is available as to how long M $\geq$ 5 aftershocks would continue to occur. Earthquakes M $\geq$ 6.5 tend to be followed by aftershocks of M $\geq$ 5. In this study by Gupta and Rekhapalli (2022), aftershock sequences of seven earthquakes of magnitude M $\geq$ 6.5 were analyzed. Six among these are in the Himalayan region and the remaining one is in the near vicinity in China. The analysis suggests that the number of M $\geq$ 5 aftershocks and the duration of their occurrence decrease with the decrease of the mainshock magnitude. For the 2008 Sichuan earthquake of M 7.9 there were 136 M $\geq$ 5 aftershocks, while for 1975 Kinnaur earthquake of M 6.8 there were only 9. The aftershock duration of the Himalayan region earthquakes obeys the exponential law, where the A and c are constants associated with regional fault settings. This relation is helpful in providing an estimate of the time for which M $\geq$ 5 aftershock activity would continue after the occurrence of M $\geq$ 6.5 earthquakes.

6.2 Microzonation Studies

CSIR-NGRI prepared a first-cut Earthquake Disaster Risk Index (EDRI) map to capture the relative risk across Lucknow and Dehradun cities. These maps were handed over to the State Disaster Management Authority of respective States.

CSIR-4PI carried out microzonation of Srinagar region of the Kashmir Valley (Gupta S.V., et al., 2020, 2022). They conducted an extensive high-resolution microtremor ambient noise survey at 429 locations. The acquired dataset was processed using the Horizontal to Vertical Spectral Ratio (HVSR) technique to map the resonance frequency, the thickness of sedimentary cover and to identify areas prone to seismic amplification. The HVSR curves show the peaks in the range of 0.22 Hz to 9.96 Hz indicating heterogeneous and complex sedimentary cover in the region. Inversion of the HVSR curves gives the shear waves velocity distribution which highlights two distinct reflective surfaces in most of the areas. They also used the estimated fundamental frequency of various types of houses/buildings located in Srinagar city to assess the possibility of resonance in case of occurrence of any earthquake.

ISR has undertaken site-specific seismic hazard assessment and microzonation studies for areas of rapid growth, e.g. Special Investment Regions, Special Economic Zones, large and tall structures, and industrial hubs. These include Liquified Natural Gas / Liquid Petroleum Gas storage tanks at Mundra, Dhamra (Odisha), Dadra and Nagar Haveli, cable stayed bridge at Zuari River, Goa, and Indian Oil Corporation Ltd. Bongaigaon Refinery. The Institute has completed seismic microzonation of Bhuj city under a Ministry of Earth Sciences (MoES) sponsored project. In addition, it has undertaken seismic microzonation study of Amritsar, Meerut, Agra, Lucknow, Kanpur, Varanasi, Patna and Dhanbad towns under a project sponsored by MoES.

The concept of seismic vulnerability is a yard-stick of damage estimation from a probable earthquake, considering physical cum social dimension and enables a basis for decision-makers to develop preparedness and mitigation strategies. Baruah et al. (2020) used several parameters, e.g. shear wave velocity characteristics, geomorphology, slope angle, building typology, and the number of occupants, to estimate the dimension of vulnerability for the Shillong city. Based on this study, they inferred that more than 60% of Shillong city falls under moderate to high vulnerability and the rest is less vulnerable.

7. Triggered Seismicity and Borehole Seismology

Under certain suitable geological conditions, anthropogenic seismicity due to mining, geothermal and natural gas/oil production, filling of artificial water reservoirs, and high-pressure fluid injection has been reported globally. The reservoir-triggered seismicity (RTS) is most prominent, having been reported from hundreds of locations, with at least five sites where earthquakes exceeding M 6 occurred, claiming human lives and destruction of properties. The most important correlate for RTS to occur is the height of water column in the reservoir. Certain common characteristics of the RTS sequences have been identified, which discriminate them from normal earthquake sequences. During the reporting period, it was documented for the first time that the Injection Induced Seismicity (IIS) in Oklahoma, USA has characteristics like RTS (Rekhapalli and Gupta, 2021). An Editorial on Anthropogenic Seismicity (Gupta H.K., 2021a) and why Koyna is the most suitable site for near field investigations of earthquakes (Gupta H.K., 2021b, 2021c, 2021d, 2022b) were discussed in detail. It has been discovered that the DVP is hosting all the three types of earthquake sequences (Gupta H.K., 2022a).

Evidence for migration phenomenon:

An earthquake of Mw 4.0 occurred on 3 June 2017, south of Warna Dam, in the vicinity of the Western Ghat Escarpment (WGE), India. This earthquake is associated with a foreshock–aftershock sequence of 123 events of M_L 0.5–3.5, forming an intense cluster. This sequence occurred over a course of one month, beginning in the last week of May 2017, and seismicity continues. This earthquake sequence occurred at a new location compared with the past 50 years of seismicity of the region. Prior to the new earthquake sequence of 2017, the earthquakes were bounded between latitude 17.1°–17.4°N, which supports the southward migration of seismicity in the region and suggests that the cluster is a part of the continuing RTS seismicity over the last five decades (Shashidhar et al., 2019a, 2019b).

Automatic detection of microearthquakes in borehole records:

For the first time, an automatic detection workflow was successfully implemented to seismological data recorded in deep boreholes situated in the Koyna-Warna region. This workflow allowed identification of about twice as many events as compared to the time-consuming manual data processing. Also, a two-stage grid-search algorithm provided additionally better constraints on the absolute event locations. Further, a relative location process of these events using a waveform similarity approach was performed. These new events provided a tighter clustering than was obtained earlier. The seismicity trend correlates well with the anomalies obtained from airborne lidar studies. It is believed that the improvements achieved in detection and locations of microearthquakes using the borehole seismograms will provide better understanding of the RTS of the Koyna-Warna region (Shashidhar et al., 2020).

Stress drop variations of triggered earthquakes at Koyna-Warna:

The spectral ratio technique (SRT) is implemented for the estimation of source parameters of local earthquakes (M_L 0.5-4.0) of the Koyna–Warna region, western India. The SRT uses the concept of empirical Green's function and accounts for the path and site effects; thus, it contributes to the optimal estimates of the source parameters. Here, the corner frequencies and stress drops of a new earthquake sequence that occurred during 1 May - 25 June 2017 were calculated and compared with the stress drop behavior of the existing seismicity cluster in the region. The dependency of stress drop with increasing seismic moment of these earthquakes was also tested. A total of 689 P-wave spectra of earthquakes recorded by a short-period borehole and a broadband surface seismic network are utilized for this purpose. It is found that the corner frequency varies from 1 to 25 Hz and stress drops vary from 0.01 to 14 MPa for earthquakes of both the clusters (Mahato and Shashidhar, 2022).

Site response and source parameters of RTS earthquakes using borehole seismic data:

A linear scaling between seismic moment (M_o, in N-m) and stress drop ($\Delta\sigma$ in MPa) estimates is obtained for the Koyna earthquakes as: $\log_{10}\Delta\sigma = 0.62\log_{10} M_o - 8.03$. The maximum σ of 34.2 MPa is modeled at 0.1 km depth for an event of Mw 4.09, while the largest apparent stress (σ_a) of 43.3 MPa is modeled at 4 km for an event of Mw 3.16. The hypocentral depth plot of ($\Delta\sigma$ and σ_a reveals a seismogenic zone between 2.2 and 5.6 km depth, where most of the earthquakes (with large $\Delta\sigma$ and σ_a) have occurred. This could be attributed to the large stress/stain (associated with brittle, competent rocks) and high pore-fluid pressure (water saturated zone at hypocentral depths) beneath the Koyna seismic zone. The results suggest that most of the small Koyna events (Mw 2.9–4.2) satisfy the frictional overshoot stress-drop rupture model while only a few events follow the partial stress-drop rupture model. The reservoir-triggered Koyna earthquakes are associated with smaller stress drops in comparison with the rift-associated earthquakes in Kachchh, Gujarat and NSL (Mandal et al., 2021a).

8. Environmental Seismology and Earthquake Precursory Studies

8.1 Environmental Seismology

Cook et al. (2021) used seismic data from 76 broadband stations in Uttarakhand Himalaya to detect and evaluate the scope of early warning systems for mass wasting and floods in the Himalayan region. On 2021-02-07, Uttarakhand region of India experienced severe landslides and trolled over 200 lives. The signals of the events were observed up to 100 km from the disaster site and demonstrate the potential for these far-away monitoring stations to be useful for early warning. The records of the event at two of stations are shown in Fig.9. This discovery suggests a different way to monitor such remote Himalayan regions for mass wasting hazards.

WIHG studied this disaster using seismological data, satellite imagery and numerical modelling and estimated that $27 \times 10^3\ m^3$ of rock and glacier-ice collapsed from the steep north face of the Ronti Peak (Shugar et al., 2021; Tiwari A., et al., 2022). The main rock-fall followed by a noteworthy sequence of small events recorded by nearby seismic stations. The main event appears to have been initiated by precursory signals for nearly 2:30 h. The seismic data of three nearby stations within 50 km distance also distinguished debris flow and hitting obstacles from other seismic sources. The proximal high-quality seismic data allowed estimation of debris-flow speed and reconstruction of the complete chronological sequence, from the initiation of the nucleation phase to the occurrence of the rock-fall.

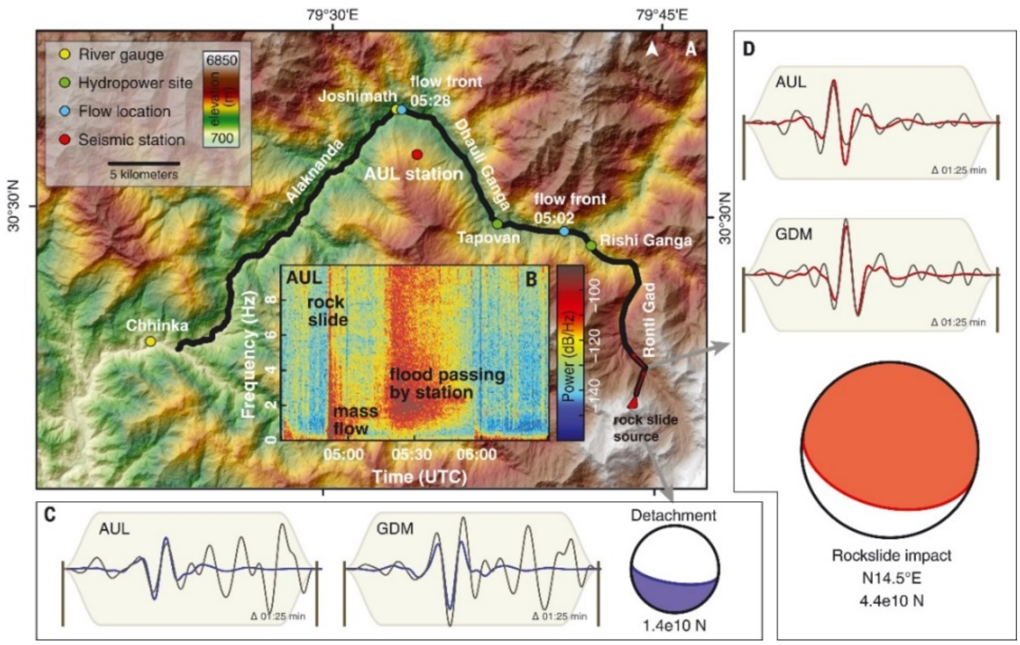

Figure 9. (A) Shaded relief map of 2021-02-07 slide event showing key geographic and instrument visual constraints of flow location; (B) Spectrogram at AUL station; (C&D) Lower hemisphere projections of single force focal sphere for the stations AUL and GDM. (From Cook et al., 2021) (*From Science, 374(6563), Kristen L. Cook, Rajesh Rekapalli, Michael Dietze, Marco Pilz,et al., Detection and potential early warning of catastrophic flowevents with regional seismic networks, 87-92. Reprinted with permission from AAAS.*)

8.2 Earthquake Precursory Studies

Vijaya Kumar et al. (2020) recognized pre- and co-seismic signatures in MT data for the Mw 4.6 earthquake that occurred on 2007-11-24 in the Koyna-Warna region. Wavelet analysis of the MT time series data shows significant enhancement at 3–6 Hz frequency band in the scalogram during the earthquake in comparison with pre- and post-time. The spectral polarization ratio technique was implemented on these events to identify the precursory signatures. A few days before the earthquake, a significant anomaly was identified for most of the earthquakes using this technique. Akilan et al. (2021) studied changes in the zenith total delay (ZTD) and total electron content (TEC) associated with the 2015 Nepal earthquake (Mw 7.8). They analyzed the ZTD derived from GPS data received at HYDE, LCK3 International GNSS Service (IGS) stations and MSUN operated by CSIR-NGRI. The decrease in ZTD and TEC suggests hydration in the atmosphere by the joining of ions in the atmosphere during earthquakes. Almost the same results regarding the changes in ZTD and TEC were obtained for another large event (the 1999 Chamoli earthquake of Mw 6.8) in the Himalayan region, although they differ slightly in intensity depending on the observation distance.

Probabilistic analysis was performed on the seismic data of 100 years (1918–2018) for forecast of probable future earthquakes above Mw $\geq$ 5.0 in NE India (20°–30°N and 86°–98°E) and its vicinity to ascertain mean occurrence period E(t) for earthquakes of Mw $\geq$ 5 (Chetia et al., 2019a). Here, Kolmogorov–Smirnov statistics constrained by Weibull distribution has been utilized to achieve the best fit on the dataset. E(t) is found to be $\sim$ 74 days with 50% probability. Similarly, cumulative probability function indicates a time of 140 days with 80% probability, while 400–500 days of recurrence time period is embedded with 90–100% probability for an earthquake of Mw $\geq$ 5.0 to recur following the occurrence of the last earthquake.

Mechanical deformations from within the earthquake preparation zones are believed to cause seismo-electromagnetic (SEM) emission in ultra-low frequency (ULF) band, i.e. between 0.001 and 10 Hz. The 3-component ULF induction coil magnetometer data from Multi-parametric Geophysical Observatory (MPGO), Tezpur were used to study SEM emissions employing both polarization ratio analysis and fractal analysis during the campaign period of Apr.20 – Sep.3, 2019 (Dey et al., 2021). The findings show candidate SEM emissions, in the form of enhancements in SZ/SH, associated with all the seven credible events, even as nine enhancements could not be attributed to immediately adjacent credible events.

WIHG operates an MPGO at Ghuttu (Tehri, Uttarakhand) for earthquake precursory studies. Inert gas (soil Radon) and magnetic field changes before the occurrence of small-to-moderate magnitude earthquakes provide evidence for short-term (months-to-days, hours) earthquake precursors. However, this remote site in the Higher-Himalaya, away from human generated noise, indicates that there are different background natural noises to make the data very complex. There is a very high hydrological effect in the gravity and radon emanation (Shukla et al., 2020; Chauhan et al., 2021). After removing the background noises, anomalous changes are reported in case of 19-20 moderate magnitude local earthquakes. Earlier, this observatory has also reported precursory changes during the Mw 7.8 Nepal earthquake of 2015.

ISR has established three MPGOs in Gujarat for precursory studies. Soil radon (Rn-222) data of the Badargadh station were used to identify precursory signal of two earthquakes of M3.7 and M4.2 which occurred on March 26, 2011, and May 17, 2011, respectively through advanced processing of the time series (Sahoo et al., 2020, 2021). The ultra-low frequency geomagnetic variations were observed before the Dholavira earthquake (M 5.1) of 2012-06-20 in the Kachchh region (Joshi and Rao., 2021).

The apparent resistivity imaging at MPGO, Tezpur, operated by CSIR-NEIST, was carried out since 2016-08-31 for fixed interval time of 3 days to investigate precursory signatures prior to earthquake events. Anomalies in apparent resistivity prior to earthquake events are observed. These are not influenced by the rainfall activity in the region during the investigation period. Weibull distribution technique with observed apparent resistivity data is adopted to look for and revalidate the observations. The Weibull parameters, i.e. K and m, are estimated to be 0.26 and 1.04, respectively. No precise relation between magnitude and earthquake precursory time is found. Weibull probability distribution indicates that the probability of an earthquake occurrence exceeds the measure up to 80% (9 days) after the precursory signal is observed (Chetia et al., 2020). Similarly, temporal variability of the soil radon emanations measured at the MPGO was scrutinized using singular spectrum analysis (SSA) (Chetia et al., 2019b). The study concludes that SSA eliminates diurnal and semidiurnal components from time series of soil radon emanation for better correlation of soil radon emanation with earthquakes.

Mukherjee et al. (2021) have proposed a novel approach for Earthquake Early Warning (EEW) System Design using deep learning Techniques. The method converts a seismic signal into audio signals and then uses popular speech recognition techniques. Both Convolutional Neural Network (CNN) and a Long Short-Term Memory (LSTM) network have been trained.

8.3 Ionospheric Seismology

Ionospheric seismology refers to the study of events of earthquakes and tsunamis through co-seismic ionospheric waves produced by the dynamic coupling between the Earth's surface and the atmosphere. The ionosphere is a highly dynamic ionized region of the Earth's upper atmosphere extending from $\sim$ 60 km to $\sim$ 1000 km. The origin of any perturbations in the ionospheric electron density can be traced to various sources either from above (e.g. solar, geomagnetic, etc.) or below (e.g. lower atmospheric, earthquakes, tsunamis, volcano eruptions, etc.) the ionosphere. In particular, short-period acoustic waves and long-period gravity waves emitted by earthquakes and tsunamis propagate upward in the region of exponentially decreasing atmospheric neutral density, and thus, their amplitude increases with atmospheric heights. On arrival at ionospheric heights, the waves redistribute ionospheric electron density and produce electron density perturbations known as co-seismic/co-tsunami ionospheric perturbations, respectively. Recently, it has been suggested that ionospheric signals produced by earthquakes and tsunamis can be inverted to infer the seismic source characteristics of large earthquakes and to envisage the propagation time and amplitudes of tsunami waves. It seems possible, but there are difficulties in terms of non-tectonic forcing mechanisms that act upon the ionospheric perturbation evolution at ionospheric altitudes (Bagiya et al., 2019).

A simple and direct 3D model is developed to estimate the combined effects of nontectonic forcing mechanisms of i) orientation between the geomagnetic field and tectonically induced atmospheric wave perturbations, ii) orientation between the GNSS satellite line of sight (LOS) geometry and coseismic atmospheric wave perturbations, and iii) ambient electron density gradients on the manifestations of Global Positioning System (GPS) – Total Electron Content (TEC) measured near field co-seismic ionospheric perturbations. This model can compute the nontectonic effects at various ionospheric altitudes depending on the propagation characteristics of seismo-acoustic rays (Fig.10). Further, this model is tested on earthquakes occurring at different latitudes. It is presumed that this model would induce and enhance a proper perception among the researchers about the seismic source characteristics derived based on the corresponding ionospheric manifestations (Bagiya et al., 2019).

Further, GPS-TEC observations provide adequate information on the spatial and temporal characteristics of earthquake induced ionospheric perturbations. However, one of the major limitations of this technique is the lack of altitude information of the recorded ionospheric perturbations. GPS derived TEC is an integrated quantity; hence it is difficult to relate the detection of ionospheric perturbations in TEC to a precise altitude. Using the modelled propagation of acoustic rays in space and time and their interaction with satellite-station line of sight (LOS) geometry, a novel method has been developed to infer the detection altitude of ionospheric perturbations observed through GPS-TEC. This modest method has been further upgraded to identify the distinct seismic sources that evolved along an extended rupture varying simultaneously in space and time akin to the seismic rupture of the Mw 9.0 2011-03-11 Tohoku-Oki earthquake (Bagiya et al., 2020).

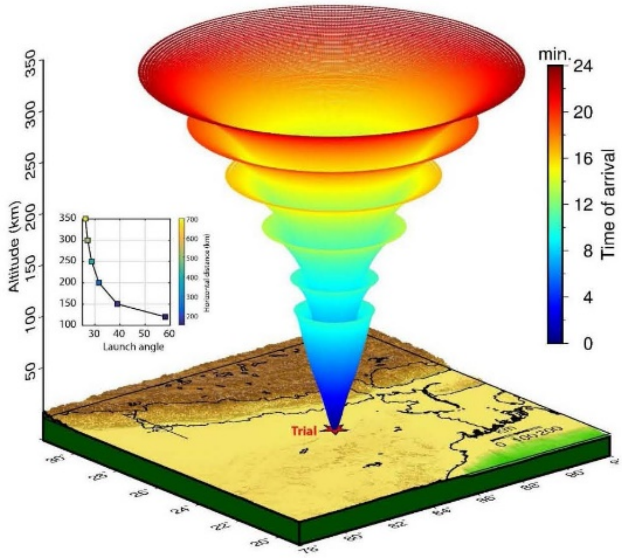

Figure 10. Propagation of seismo-acoustic waves in 3D space with time from the Trial seismic source assumed at 25°N 85°E. The propagation of six rays modeled at six different launch angles is shown. The first ray is launched at an angle of ∼58° that is the threshold angle at 120 km altitude. The rays with launch angles higher than this refract downward while those lower than this propagate further upward. Similarly, the second ray is launched at an angle of ∼38.8° that is the threshold propagation angle at 150 km altitude and so on. The inset shows the variation of the threshold angle and maximum horizontal distance along with the atmospheric altitudes. (From Bagiya et al., 2019) (*Courtesy IIG*)

In addition to the transient perturbations, prolonged ionospheric oscillations following large earthquakes (Mw > 8.0) have also been found to provide seismic source information from the ionosphere. Such ionospheric oscillations related to the earth-atmospheric resonance frequencies of ∼ 3.7 and ∼ 4.4 mHz following the 2012-04-11 Sumatra doublet (Fig.11) and 2011-03-11 Tohoku-Oki earthquakes were scrutinized (Nayak et al., 2021, 2022). The Earth's background free oscillations at ∼ 3.7 and ∼ 4.4 mHz resonantly couple with the atmospheric acoustic modes and thus energy cross-talk between the earth-atmosphere system is maximum at these frequencies. Our studies emphasized that resonant ionospheric signatures during the Sumatra doublet event were related to the seismic source. Therefore, resonant co-seismic ionospheric signatures could provide additional information on the low frequency features of seismic ruptures.

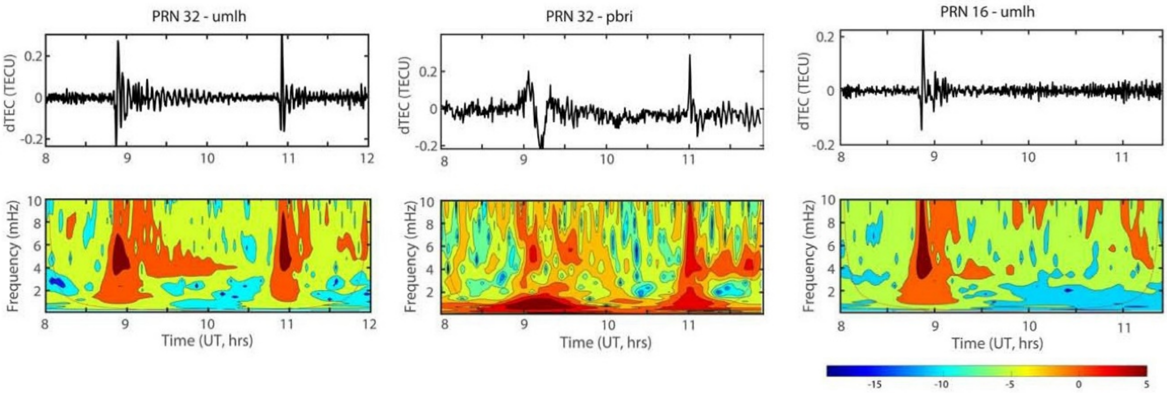

Figure 11. Power spectral analysis of Pseudo Random Number (PRN) 32 detrended TEC (dTEC) time series from umlh and pbri and of PRN 16 dTEC time series from umlh during 2012-04-11 Sumatra doublet earthquake. Resonant ionospheric signatures centered at $\sim$ 4 mHz could be noticed. (From Nayak et al., 2021) (*Courtesy IIG*)

Rapidly moving objects excite short-period waves, and slow objects excite long-period waves. This has been confirmed for atmospheric waves excited by vertical crustal movements associated with large earthquakes. We compared atmospheric wave amplitudes excited by ordinary earthquakes and by "tsunami" earthquakes, characterized by slow fault movements. It has been found that the 2010 Mentawai earthquake, a typical tsunami earthquake, excited abnormally large internal gravity waves from ionospheric observations. This is the first slow earthquake signature found in space (Heki et al., 2022).

In another initiative, the Sumatra 2004 tsunami induced ionospheric signatures, which were detected simultaneously in GPS-TEC $\sim$ 90 minutes before the arrival of actual tsunami over the Indian east coast, were successfully explained. This work offers an alternative tool to monitor the offshore signatures that travel ahead of tsunami in the ionosphere could potentially be an important early warning tool for the tsunami over coastal regions. These findings, with a bearing on mitigation of hazards in coastal regions, are likely to impact tsunami forecast related research in a significant manner.

9. Paleoseismology

The E-W trending reverse Dauki Fault (DF) in NE India has played a major role in the regional deformation of the adjoining areas and was believed to be active during the Late Quaternary time. Previous paleo-seismological studies conducted on the eastern and western part of the DF, Bangladesh, revealed that the fault ruptured in AD 849-920 and AD 1548 respectively. However, there were no studies on the DF from the southern side of the Shillong Plateau (SP), India. IIG has reported soft sediment deformation structures (SSDS) from five trenches in and around the DF zone, SP. Close to the Dauki village, five trenches in the eastern part of the DF show micro-faulting, sand dykes, disturbed strata, and water escape structures. The detailed investigation of SSDS indicates that the origin of deformation is seismically triggered. The ^{14}C AMS (Accelerator Mass Spectrometry) dating of deformation structures generated by earthquakes suggests that three seismic events occurred between 130 and 920 yr BP, 5415 to 9140 yr BP, and at about 4285 yr BP. This study confirms that DF is indeed active, at least, since the mid-Holocene (Lakshmi and Gawali, 2022).

The major seismic source in the Kachchh basin, i.e. the Kachchh Mainland Fault (KMF), was studied using various geological investigations during 2019 and 2022. After thorough scrutiny of high-resolution satellite imageries and field investigations, several trenches were dug across prospective sites along the KMF for detailed paleo-seismic study. Based on these investigations, it was concluded that the KMF illustrates an oblique strike-slip fault in the western and central segments. A total of six paleo-seismic events have been identified during the period from 890 – 1980 years BP (Kothyari et al., 2021), out of which five were in the Holocene whereas one was in Late Pleistocene. The slip rate shows variability from lesser values in the western flank (0.08 – 0.04 mm/yr) to progressively increasing values (0.22 – 0.36 mm/yr) towards the eastern flank.

10. Seismological Networks

10.1 National Network

The National Center for Seismology (NCS) under the Ministry of Earth Sciences (MoES), Government of India, is the nodal agency for monitoring and reporting earthquake activity in the country. It has got a network of more than 150 broadband seismological stations spread across the country. The details of this national network are available on https://seismo.gov.in/. The web portal of NCS also reports earthquake activity in the region (https://riseq.seismo.gov.in/riseq/earthquake).

10.2 Regional Networks

CSIR-NGRI has been operating 174 broadband seismometers and 41 strong motion accelerometers in different parts of the country in network and profile modes (Fig.12). In recent years, Uttarakhand Himalaya has been a focus of seismological studies. A setup of 76 three-component broadband stations (in network and profile modes) and 19 strong motion stations have been operating in this region since 2017 (Srinagesh et al., 2019). This network provides high-quality digital waveforms of thousands of local, regional, and teleseismic earthquakes. The data from this network have been used to pursue seismological studies, including research in environmental seismology, especially after the 2021-02-07 glacial burst and flood event in Uttarakhand.

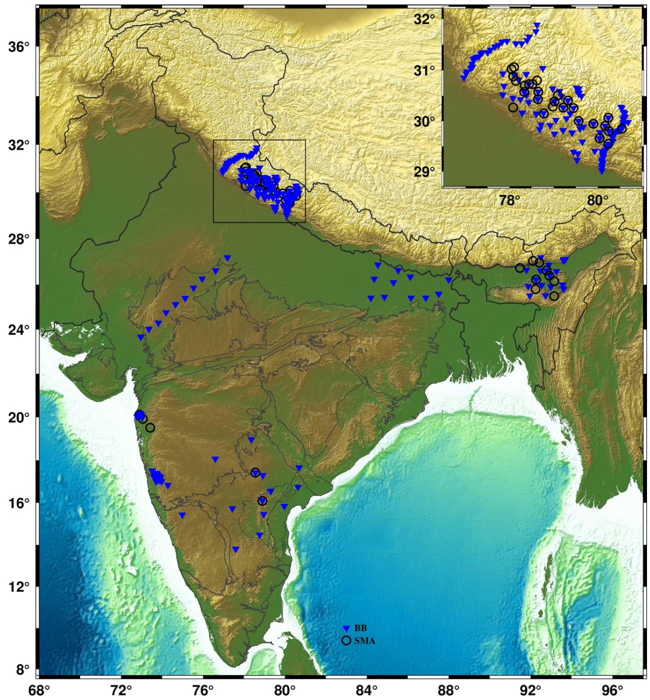

Figure 12. The BBS and SMA stations operated by CSIR-NGRI in different regions of India. Inset shows the coverage in the Uttarakhand Himalaya. (*Courtesy Dr. M. Ravi Kumar, Seismological Observatory, CSIR-NGRI*)

WIHG is operating seismological networks in the NW and NE sectors of the Himalaya and adjoining parts for seismogenesis and subsurface structure investigations (Fig.13). The NW Himalaya network includes 72 broadband seismographs and 25 accelerographs and covers Jammu & Kashmir, Ladakh, Himachal Pradesh, Uttarakhand, Punjab, and Haryana. A network of 8 broadband seismographs is being operated in the Siang valley of Arunachal Pradesh in NE Himalaya. The institute also has state-of-the-art Multi-Parametric Geophysical Observatory at Ghuttu, Garhwal Himalaya.

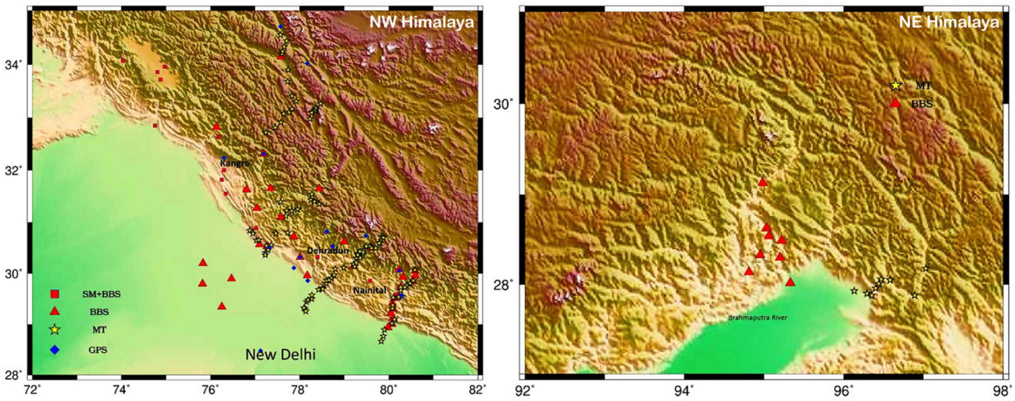

Figure 13. Geophysical Instrumentation network (permanent and temporary) operated by WIHG in the Himalaya and adjoining regions. Abbreviations: BBS - Broad Band Seismograph; SMS – Strong motion System; MT – Magnetotelluric; GPS – Global Positioning System; MCT – Main Central Thrust; MBT – Main Boundary Thrust; HFT – Himalayan Frontal Thrust. (*Courtesy WIHG*)

CSIR-4PI has established a regional broadband seismic and GNSS network in Kashmir Himalaya to assess earthquake hazard and risk in NW Himalaya with emphasis on Jammu & Kashmir, and Ladakh regions. This network started in 2013 with 8 stations in phase 1 and 7 stations were added in phase 2. Recently, 7 more stations are added in phase 3 (Fig.14). This network of collocated broadband seismic and GNSS stations enabled CSIR-4PI to initiate integrated broad seismic and GNSS studies for the first time in Kashmir valley. The network is running with 120 s broadband sensors and, in addition, CSIR-4PI is also equipped with 12 units of 5 s period seismometers useful for micro-tremor array measurements to image the subsurface geological mapping in terms of shear wave velocity. Mir et al. (2022) performed noise analysis of this seismic network for the period of 2014 – 2020.

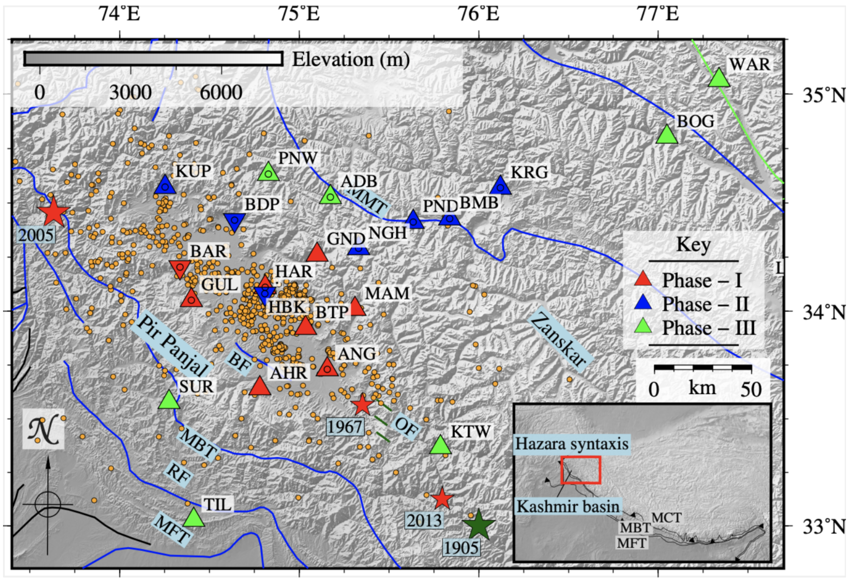

Figure 14. The location of broadband seismological and GNSS stations in Kashmir Himalaya operated by CSIR-4PI. (*Courtesy CSIR-4PI*)

A seismological network (Jammu and Kashmir Seismological Network [JAKSNET]) of 24 broadband three-component seismograph systems was installed in 2013 across Jammu and Kashmir (J&K), under joint collaborative efforts between Indian Institute of Science Education and Research (IISER)-Kolkata, Shri Mata Vaishno Devi

University, Katra (J&K), and University of Cambridge, United Kingdom (Sharma S., et al., 2020).

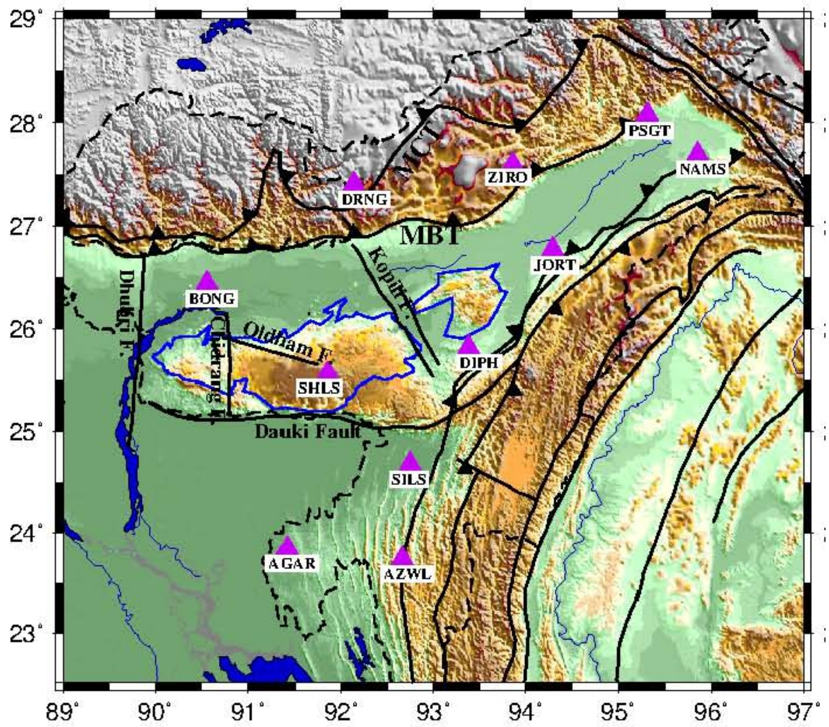

Figure 15. Regional network of 11 broadband seismological stations in NE India operated by Indian Institute of Geomagnetism. (*Courtesy IIG*)

A regional network of 11 broadband seismological stations has been established and operated by IIG in NE India (Fig.15) to study the geometry and continuity of crust and upper mantle discontinuities beneath the region, seismic ambient noise tomography focusing primarily on crustal and uppermost mantle structures, and crustal attenuation characteristics of high frequency body waves.

Strong motion accelerographs (SMA) have been installed and operated by CSIR-NEIST at different places in and around the Shillong Plateau and Mikir Hills. The acceleration time histories obtained from these accelerographs are filtered and processed for baseline corrections on a regular basis. These are then used as inputs for the estimation of several ground motion parameters including PGA, PGV and PGD, and Response spectra. A total of 234 earthquake events (M $\geq$ 3.5) have been recorded by these SMA stations during Sep.2016 to Sep.2021.

The Gujarat State Seismic Network (GSNet) under the aegis of the ISR, Gandhinagar, is operational since July 2006 (Fig.16). Presently, the network consists of 54 broadband seismograph stations (BBS) spread out in the state and neighboring areas. The data from almost 45 BBS are transmitted to the Institute through VSAT, where the earthquake activity is monitored in near real time (24x7).The network has a detectability of M 1.5 in the Kachchh region and M 2.0 in the other areas of Gujarat. Based on earthquake data of the Gujarat region, ISR developed a calibrated local magnitude scale (M_L) for Kachchh and Saurashtra regions. ISR has also procured 10 compact broadband sensors with 4G connectivity. In addition, 54 strong motion accelerographs are also deployed by ISR. It has also established three MPGOs in Kachchh for earthquake precursory studies.

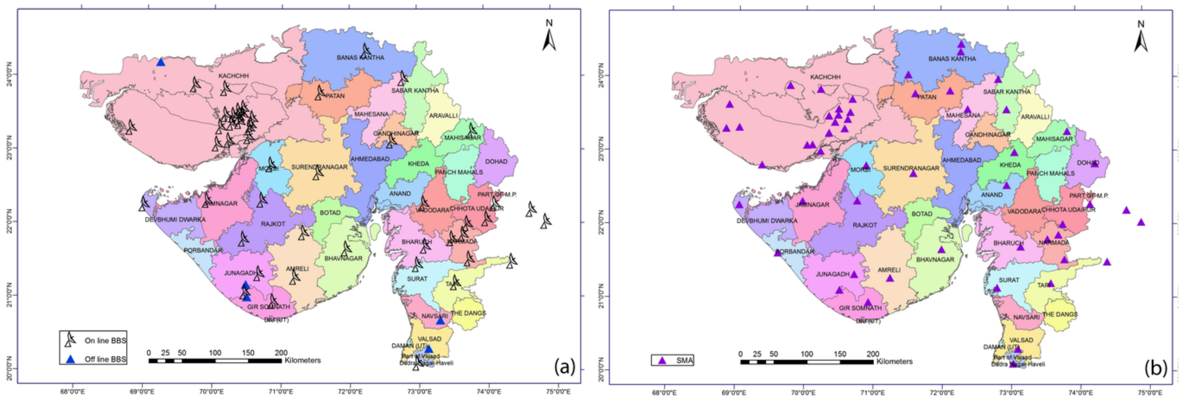

Figure 16. GSNet [(a) Broadband seismometers, (b) SMA] network operated by Institute of Seismological Research in Gujarat. (Source: `https://isr.gujarat.gov.in/maps`; accessed on 2023-01-31)

IIT-Kharagpur is operating a seismic network in the Sikkim Himalaya since 2019 (Fig.17). The network was deployed as an attempt to understand the seismic structure, lithospheric deformation, and seismicity of the Indian plate in Sikkim Himalaya (Uthaman et al., 2021, 2022).

11. Societal Projects

Monitoring of dams is an ongoing activity to keep a watch on the health of these dams. CSIR-NGRI has been involved in monitoring of many dams in different regions of the country, e.g. Srisailam dam (Andhra Pradesh), Bhatsa and Dhamni dams (Maharashtra), Kalpsar dam (Gujarat), Gandhisagar dam (Madhya Pradesh) to name a few. Estimation of seismic hazard for the cultural heritage sites like Shree Ram Mandir in Uttar Paradesh, and Somnath and Dwarka in Gujarat are among the most highlighted hazard based studies conducted by CSIR-NGRI.

11.1 Developing an Earthquake Resilient Society in the Vicinity of Himalaya

Among the seismically active continental regions, the Himalayan region is very significant with large human population in the immediate vicinity. The Himalayan region experienced four great earthquakes of M $\sim$ 8 within a short span of 55 years from 1897 to 1952. The region has not experienced an earthquake of similar magnitude since 1952. Developing an earthquake resilient society through the process of developing earthquake scenarios, as to what would be the impact if one of the past earthquakes repeats today, is an extremely useful approach and sharing this information with all concerned, doing the needful to educate and enrich the concerned government departments, and making the public a shareholder, helps. The 1905 Kangra earthquake of M $\sim$ 8 had claimed $\sim$ 20,000 human lives in addition to causing widespread damage. A scenario was built by the National Disaster Management Authority (NDMA), Government of India, as to what would be the consequences if such an earthquake occurred today? It was discovered that $\sim$ 0.9 million human lives would be lost in the states of Punjab, Haryana, Himachal Pradesh, and the Union Territory of Chandigarh if this earthquake occurred in the middle of the night. A year-long phase of training and educating at various levels to develop an earthquake resilient society in the states of Punjab, Haryana, Himachal Pradesh, and the Union Territory of Chandigarh during 2012-2013 culminated in a mega mock drill on the 13 February 2013. It demonstrated what all had been achieved and what was missing. Encouraged by the success a similar exercise was carried out for the repeat of the 1897 Shillong earthquake for 8 northeast Indian states during 2013-2014 culminating in mega mock drills on 10 and 13 March 2014 (Gupta, 2020; Goff et al., 2020; Gupta and Sabnis, 2021).

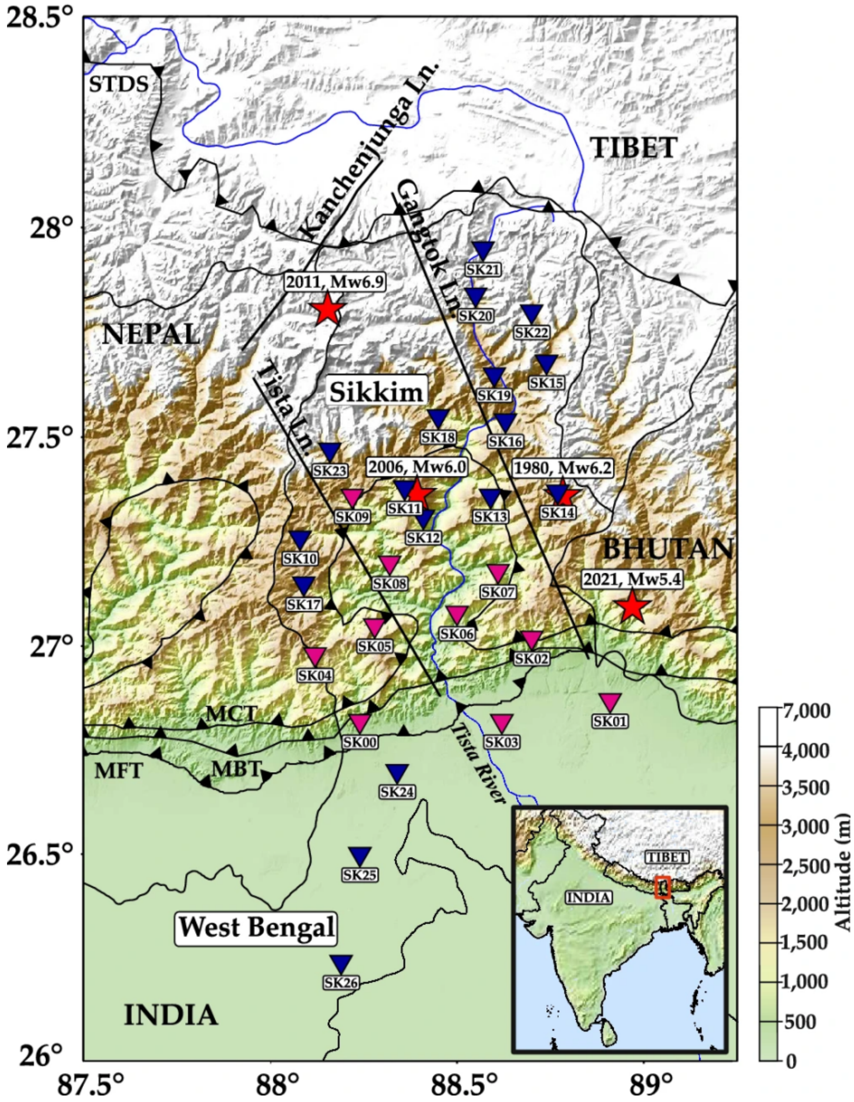

Figure 17. Seismological network operated by IIT-Kharagpur in the Sikkim Himalaya and adjoining Bengal basin. Stations with the sensor installed on pier are represented with pink inverted triangles and stations with the sensor buried are represented in blue inverted triangles. (From Uthaman et al., 2022) (*Courtesy Dr. Chandrani Singh, IIT-Kharagpur*)

12. Education and Outreach Programs

CSIR-NGRI along with various national agencies is involved in outreach activities to sensitize the general public to build a seismic resilient society. Gupta H.K., et al. (2020) opined that scenario-based research is important for disaster preparedness of the country, involving historical data of earthquakes superimposed on the current data pertaining to infrastructure, population, etc., for a Seismic Zone V. Such exercises carried out in NE India successfully raised awareness among the general public, and more importantly, among the various responders, streamlined the techniques and procedures of a diverse set of agencies – from administrative, to technical, including disaster response forces, fire-fighters, hospitals, etc. (Fig.18). All the concerned agencies successfully performed the mega mock exercises. This underscores that if the mitigation and preparedness measures are adequate, the impact of any great earthquake can be contained.

CSIR-NGRI is conducting various outreach activities in seismology by inviting students to the Institute, conducting webinars for students and general public, distributing booklets in different languages, and visiting different schools in different parts of the country to spread awareness about earthquakes, earthquake risks and precautions. In the last three years, CSIR-NGRI has reached around 20,000 students and general public through these outreach activities. CSIR-NGRI has also conducted 6 training courses (online and offline) in seismology during 2019-2022. These courses were attended by nearly 250 participants. Fig.19 shows participation of school children in one such event.

Figure 18. Mock-drill exercise at military hospital, Shillong, Meghalaya. (*Courtesy Dr. M. Ravi Kumar, CSIR-NGRI*)

Figure 19. Visit of students to CSIR-NGRI for an awareness program on seismology. (*Courtesy Dr. Sandeep K. Gupta, CSIR-NGRI*)

Figure 20. Demonstration during earthquake education awareness program on 30 Nov.2022 by WIHG in the Kendriya Vidyalaya, Raipur, Dehradun. (*Courtesy WIHG*)

Since 2017, WIHG is regularly conducting an outreach program titled "*Education and awareness program for earthquake preparedness and hazard mitigation: Uttarakhand*". In this program, the Institute's scientists visit various schools, organizations and villages to deliver lectures on safety and prevention measures to be taken before, during and after an earthquake (Fig.20). To make the lecture more effective an earthquake recording system is also demonstrated exhibiting real-time recording by the seismograph.

13. Other Significant Contributions

Joint Scientific Assembly of IAGA and IASPEI:

A major international scientific event related to the IUGG during this period has been organization of the Joint Scientific Assembly of IAGA and IASPEI in India during 21-27 August 2021 (JSA-2021). The Assembly was hosted virtually by CSIR-NGRI and INSA (the National Adhering body of IUGG) with support from other Earth science institutes. The virtual conference was attended by 828 participants from 53 countries, over 500 from IAGA and about 300 from IASPEI. A total of 778 abstracts were submitted under 53 symposia, which included 8 joint symposia, 1 Diamond Jubilee symposium commemorating 60^{th} anniversary of CSIR-NGRI, 27 IAGA symposia and 17 IASPEI symposia, including one from the Asian Seismological Commission. There were 3 joint plenary talks. The JSA-2021 was preceded by IAGA and IASPEI Schools for early carrier scientists and a GIFT Workshop for teachers.

Encyclopedia of Solid Earth Geophysics (ESEG) 2^{nd} Edition:

The second edition of ESEG was compiled and published in 2021 with 257 articles spread over 1950 pages in two volumes (https://link.springer.com/referencework/10.1007/978-3-030-58631-7). Almost 100 of the 257 articles are seismology related (edited by Gupta H.K., 2021e).

Diamond Jubilee of CSIR-National Geophysical Research Institute:

To commemorate the Diamond Jubilee of the creation of the CSIR-National Geophysical Research Institute, Hyderabad, India, the Geological Society of India published a special issue with 9 seismology related papers (edited by Tiwari and Gupta, 2021).

Silver Jubilee of the Asian Seismological Commission:

The Asian Seismological Commission (ASC), established in 1996, completed 25 years in 2021. A special volume of the Journal of the Geological Society of India was published to commemorate the Silver Jubilee of the Asian Seismological Commission, with 18 articles dealing with various aspects of Seismology in Asia (edited by Gupta H.K., et al., 2021).

Acknowledgement

I am thankful to Prof. Archana Bhattacharyya, Chairperson, INSA IUGG-IGU National Committee, India, for entrusting the responsibility of preparing this chapter on IASPEI Activities in India to me for the INSA National Report. I approached several Institutes and individuals engaged in seismological research in India seeking inputs for this chapter. The response has been overwhelming. I gratefully acknowledge the inputs received from the following researchers: Prof. Harsh Gupta, NASI Senior Scientist, CSIR-NGRI, Hyderabad, Dr. Prakash Kumar, Director, CSIR-NGRI, Hyderabad, Dr. M. Ravi Kumar (CSIR-NGRI), Dr. Prantik Mandal (CSIR-NGRI), Dr. Sandeep Gupta (CSIR-NGRI), Dr. G. Pavankumar (CSIR-NGRI), Dr. K Sain, Director, WIHG, Dehradun, Dr. Naresh Kumar (WIHG), Dr. D. Hazarika (WIHG), Prof. A.P. Dimri, Director, IIG, Mumbai, Dr. Sridevi Jade, Head, CSIR-4PI, Bengaluru, Dr. Sumer Chopra, Officiating Director General, ISR, Gandhinagar, Dr. Saurabh Baruah (CSIR-NEIST, Jorhat), Prof. Sagarika Mukhopadhyay (IIT-Roorkee), Prof. Dinesh Kumar (Kurukshetra University), Dr. Chandrani Singh (IIT-Kharagpur), and Dr. Arun Singh (IIT-Kharagpur). I gratefully acknowledge Prof. Harsh Gupta, Dr. M. Ravi Kumar, and Dr. Sandeep Gupta for reviewing this chapter and providing their valuable suggestions. The chapter has been compiled under the project MLP6404-28(AM) of CSIR-NGRI.

Acronyms used in the Chapter

ASC : Asian Seismological Commission

CSIR : Council of Scientific and Industrial Research

CSIR-4PI : CSIR-Fourth Paradigm Institute

CSIR-NEIST : CSIR-North East Institute of Science and Technology

CSIR-NGRI : CSIR-National Geophysical Research Institute

DST : Department of Science and Technology, Ministry of Science & Technology, Government of India

IAGA : International Association of Geomagnetism and Aeronomy

IASPEI : International Association of Seismology and Physics of the Earth's Interior

IGU : International Geographical Union

IIG : Indian Institute of Geomagnetism

IISER : Indian Institutes of Science Education and Research

IIT : Indian Institute of Technology

INSA : Indian National Science Academy

IUGG : International Union of Geodesy and Geophysics

MoES : Ministry of Earth Sciences, Government of India

NCS : National Center for Seismology

NDMA : National Disaster Management Authority

WIHG : Wadia Institute of Himalayan Geology

ADFB : Aravalli-Delhi Fold Belt

AMS : Accelerator Mass Spectrometry

APM : Absolute Plate Motion

BBS : Broad Band Seismograph

CB : Cuddapah Basin

CCB : Chiplakot Crystalline Belt

CCP : Common Conversion Point

CGGT : Chotanagpur Granitic Gneissic Terrain

CMB : Core Mantle Boundary

CNN : Convolutional Neural Network

DF : Dauki Fault

DSZ : Delhi Seismic Zone

DVP : Deccan Volcanic Province

EDC : Eastern Dharwar Craton

EDRI : Earthquake Disaster Risk Index

EEW : Earthquake Early Warning

EIC : Eastern Indian Craton

ESEG : Encyclopedia of Solid Earth Geophysics

FPA : Fast Polarization Azimuth

FPD : Fast Polarization Direction

GNSS : Global Navigation Satellite System

GMP : Ground Motion Parameter

GPS : Global Positioning System

HVSR : Horizontal to Vertical Spectral Ratio

IOGL : Indian Ocean Geoid Low

KMF : Kachchh Mainland Fault

LKZ : Ladakh – Karakoran Zone

LLSVP : Large Low Shear Velocity Province

LOS : Line of Sight

LPC : Lohit Plutonic Complex

LVZ : Low Velocity Zone

MBT : Main Boundary Thrust

MCT : Main Central Thrust

MCTZ : Main Central Thrust zone

MFT : Main Frontal Thrust

MHT : Main Himalayan Thrust

MPGO : Multi-parametric Geophysical Observatory

MTZ : Mantle Transition Zone

PASSCAL : Portable Array Seismic Studies of the Continental Lithosphere

PGA : Peak Ground Acceleration

PGD : Peak Ground Displacement

PGV : Peak Ground Velocity

RF : Receiver Function

RTS : Reservoir-Triggered Seismicity

SAR : Synthetic Aperture Radar

SEM : Seismo-electromagnetic

SGT : Southern Granulite Terrain

SMA : Strong Motion Accelerograph

SOC : Singhbhum-Odisha-Craton

SP : Shillong Plateau

SSA : Singular Spectrum Analysis

STD :South Tibetan Detachment

SWF : South Wagad Fault

TEC : Total Electron Content

ULF : Ultra-low Frequency

WDC : Western Dharwar Craton

WGE :Western Ghat Escarpment

ZTD : Zenith Total Delay

Bibliography

References cited in the Chapter

Akilan, A., Padhy, S., Dimri, V.P., Schuh, H., Abdul Azeez, K.K. (2021) Co-seismic and Post-seismic Changes in ZTD and TEC of the 2015 Nepal Earthquake. Pure Appl. Geophys., 178: 3339–3354. https://doi.org/10.1007/s00024-021-02830-y

Anbazhagan, P., Mog, K., Rao, K.S.N., Prabhu, N.S., Agarwal, A., et al. (2019) Reconnaissance report on geotechnical effects and structural damage caused by the 3 January 2017 Tripura earthquake, India. Nat. Hazards, 98: 425-450.

Arjun, V.H., Gupta, S., Tiwari, V.M. (2022) Lithospheric Structure of Dharwar Craton from joint analysis of Gravity, Topography and Teleseismic Travel-Time Residuals, J. Asian Earth Sci., 239, 105397, https://doi.org/10.1016/j.jseaes.2022.105397

Bagiya, M.S., Sunil, A.S., Rolland, L., Nayak, S., Ponraj, M., et al. (2019) Mapping the Impact of Non-Tectonic Forcing mechanisms on GNSS measured Coseismic Ionospheric Perturbations. Sci. Rep., 9, 18640, https://doi.org/10.1038/s41598-019-54354-0

Bagiya, M.S., Thomas, D., Astafyeva, E., Bletery, Q., Lognonné, P., et al. (2020) The Ionospheric view of the 2011 Tohoku-Oki earthquake seismic source: the first 60 seconds of the rupture. Sci. Rep., 10, 5232, https://doi.org/10.1038/s41598-020-61749-x.

Baruah, S., Boruah, G.K., Sharma, S., Hoque, W.A., Chetia, T., et al. (2020) Seismic vulnerability assessment of earthquake-prone mega-city Shillong, India using geophysical mapping and remote sensing. Georisk: Assessment and Management of Risk for Engineered Systems and Geohazards, 14:2, 112-127, DOI: 10.1080/17499518.2019.1598560

Baruah, S., Sharma, A., Dey, C., Saikia, S., Boruah, G.K., et al. (2021) Correlation between crustal anisotropy and seismogenic stress field beneath Shillong–Mikir Plateau and its vicinity in North East India. Geomatics, Nat. Hazards Risk, 12(1): 2070-2086. https://doi.org/10.1080/19475705.2021.1947902

Biswal, S., Kumar, S., Roy, S.K., Kumar, M.R., Mohanty, W.K., et al. (2020) Upper Mantle Anisotropy beneath the Western Segment, NW Indian Himalaya, Using Shear Wave Splitting. Lithosphere, 1: 1-9. https://doi.org/10.2113/2020/8856812

Biswas, R., Singh, C. (2019) Lateral variation of crustal attenuation properties from southern Tibet to eastern Nepal Himalaya. Geophys. J. Int., 217: 257-270.

Biswas, R., Singh, C. (2020a) Attenuation of high frequency body waves in the crust of western Tibet. Phys. Earth Planet. Inter., 298, 106323.

Biswas, R., Singh, C. (2020b) An investigation of regional variations of coda wave attenuation in western Tibet. J. Seismol., 24(6): 1235-1254.

Biswas, R., Singh, C. (2020c) Seismic attenuation structure across the Karakoram fault in western Tibet. Geophys. J. Int., 223(2): 1418-1431.

Boruah, G.K., Baruah, S., Sharma, S., Barua, A.G., Baruah, S. (2022) Estimation of site-specific amplification factors and expected peak ground motion at Shillong city, Meghalaya: A deterministic approach. J. Earth Syst. Sci., 131(2), 69.

Chanu, N.M., Kumar, N., Kumar, A., Mukhopadhyay, S., Babu, V.G. (2022) Along-strike variation in the shear wave crustal structure of the NE Himalaya and Indo-Burmese arc: Evidence based on surface wave dispersion analysis. Geol. J., 57: 5161-5175. https://doi.org/10.1002/gj.4465

Chaudhary, P., Roy, K.S., Kamra, C., Chopra, S. (2022) Development of empirical relationship between the observed and the estimated ground acceleration values of small to moderate earthquakes in the northwest (Gujarat) and northeast (NE) regions of India. Geomatics, Nat. Hazards, Risk, 13(1): 364-389. https://doi.org/10.1080/19475705.2022.2028906

Chauhan, V., Kumar, N., Shukla, V., Verma, S.K. (2021) Multiple Linear regression analysis to estimate hydrological effects in Soil Rn-222 at Ghuttu, Garhwal Himalaya: A prerequisite to identify earthquake precursors. Curr. Sci., 120(12): 1905-1911.

Chetia, T., Baruah, S., Dey, C., Sharma, S., Baruah, S. (2019a) Probabilistic analysis of seismic data for earthquake forecast in North East India and its vicinity. Curr.Sci., 117(7): 1167-1173.

Chetia, T., Baruah, S., Dey, C., Sharma, S., Baruah, S. (2019b) Singular spectrum and principal component analysis of soil radon (Rn-222) emanation for better detection and correlation of seismic induced anomalies, Nonlinear Process. Geophys.: Discussions. https://doi.org/10.5194/npg-2019-37

Chetia, T., Baruah, S., Baruah, S., Dey, C., Sharma, S. (2020) Weibull distribution analysis of precursory time due apparent resistivity anomaly prior to earthquakes in the vicinity of multi-parametric geophysical observatory, Tezpur, India. Geomatics, Nat. Hazards Risk 11(1): 1093-1114. https://doi.org/10.1080/19475705.2020.1775714

Cook, K.L., Rekapalli, R., Dietze, M., Pilz, M., Cesca, S., et al. (2021) Detection and potential early warning of catastrophic flow events with regional seismic networks. Science, 374: 87-92.

Coudurier-Curveur, A., Tapponnier, P., Okal, E., Van der Woerd, J., Kali, E., et al. (2020) A composite rupture model for the great 1950 Assam earthquake across the cusp of the East Himalayan Syntaxis. Earth Planet. Sci. Lett., 531, 115928.

Das, R., Rai, S.S. (2019) Redefining Dharwar Craton-Southern Granulite Terrain boundary in south India from new seismological constraints. Precambrian Res., 332, 105394. https://doi.org/10.1016/j.precamres.2019.105394

Das, R., Mukhopadhyay, S. (2020) Regional variation of coda wave attenuation in Northeast India: An understanding of the physical state of the medium. Phys. Earth. Planet Inter., 299: 1-13. https://doi.org/10.1016/j.pepi.2019.106404

Dey, C., Baruah, S., Rawat, G., Chetia, T., Baruah, S., et al. (2021) Appraisal of contemporaneous application of polarization ratio and fractal analysis for studying possible seismo-electromagnetic emissions during an intense phase of seismicity in and around Assam Valley and the Eastern Himalayas, India. Phys. Earth Planet. Inter., 318, 106759.

Dubey, A.K., Singh, A., Kumar, M.R., Jana, N., Sarkar, S., et al. (2022) Tomographic imaging of the plate geometry beneath the Arunachal Himalaya and Burmese subduction zones. Geophys. Res. Lett., 49, e2022GL098331.

Elliott, J.R., de Michele, M., Gupta, H.K. (2020) Earth observation for crustal tectonics and earthquake hazards. Surv. Geophys., 41: 1355-1389. https://doi.org/10.1007/s10712-020-09608-2

Goff, J., Gupta, H.K., Glade, T. (2020) Editorial at the occasion of the 100th volume of natural hazards. Nat. Hazards, 100(1): 1-2.

Gogoi, A., Baruah, S., Sharma, S. (2023) Regression analysis on ground motion parameters for the earthquakes (Mw[?] 4.0) in NE India with special emphasis on 3 Jan 2016 M6. 7, Tamenglong earthquake. Phys. Chem. Earth, Parts A/B/C 129, 103316

Grujic, D., Hetenyi, G., Cattin, R., Baruah, S., Benoit, A., et al. (2018) Stress transfer and connectivity between the Bhutan Himalaya and the Shillong Plateau. Tectonophysics, 744: 322-332.

Gupta, H.K. (2020) Recent earthquakes in Delhi and developing an earthquake resilient society. J. Geol. Soc. India, 96: 1-4.

Gupta, H.K. (2021a) Understanding anthropogenic earthquakes. Curr. Sci., 120(9): 1415-1416.

Gupta, H.K. (2021b) Koyna, India, an ideal site for near field earthquake observations. J. Geol. Soc. India, 97(10): 1144-1151.

Gupta, H.K. (2021c) Studies of artificial water reservoir triggered earthquakes at Koyna, India: A Summary. J. Geol. Soc. India, 97(12): 1556-1564.

Gupta, H.K. (2021d) Artificial water reservoir-triggered seismicity (RTS): Most prominent anthropogenic seismicity. Surv. Geophys., https://doi.org./10.1007/s10712-021-09675-z

Gupta, H.K. (2021e) Encyclopedia of Solid Earth Geophysics, 2nd Edition, Vol.I & II, Springer ISBN: ISBN 978-3-030-58631-7 (Editor-in-Chief). https://link.springer.com/referencework/10.1007/978-3-030-58631-7

Gupta, H.K. (2022a) Three different types of earthquake sequences in the Deccan Volcanic Province of India. Geosystems and Geoenvironment. https://doi.org/10.1016/j.geogeo.2022.100035

Gupta, H.K. (2022b) Koyna, India: A very prominent site of artificial water reservoir-triggered seismicity. J. Earth Syst. Sci., https://doi.org/10.1007/s12040-021-01780-2

Gupta, H.K., Sabnis, K.A. (2021) Developing an earthquake resilient society in the vicinity of Himalaya. J. Geol. Soc. India, 97(12): 1593-1602.

Gupta, H.K., Rekapalli, R. (2022) A short note on the Aftershock Duration of Strong to Major Himalayan Earthquakes. J. Geol. Soc. India. https://doi.org/10.1007/s12594-022-xxxx-x

Gupta, H.K., Kanchan, A., Duarah, R., Saxena, R.S., Baruah, S. (2020). Himalayan Earthquakes and Developing an Earthquake Resilient Society, J. Geol. Soc. India, 96:433-446, https://doi.org/10.1007/s12594-022-1955-8

Gupta, H.K., Zhongliang, W., Banerjee, P., Li, L. (2021) 25 Years of Asian Seismological Commission. J. Geol. Soc. India, 97(12): 1475-1602.

Gupta, S., Kumar, S. (2022) Lithosphere thickness variation across the Deccan Volcanic Province-Eastern Dharwar Craton, South India: Insight into evolution of the Deccan Volcanic Province. J. Earth Syst. Sci., 131, 10. https://doi.org/10.1007/s12040-021-01748-2

Gupta, S., Mahesh, P., Kanna, N., Sivaram, K., Paul, A. (2022) 3-D seismic velocity structure of the Kumaun–Garhwal (Central) Himalaya: insight into the Main Himalayan Thrust and earthquake occurrence, Geophys. J. Int., 229(1):138–149. https://doi.org/10.1093/gji/ggab449

Gupta, S.V., Parvez, I.A., Ankit, Khan, P.K., Chandra, R. (2020) Site Effects Investigation in Srinagar City of Kashmir Basin Using Microtremor and Its Inversion, J. Earthq. Eng., DOI: 10.1080/13632469.2020.1816232

Gupta, S.V., Parvez I A and Khan P K (2022) Imaging sub-surface geological complexity (2D/3D) beneath Greater Srinagar region of Kashmir Basin, Northwest Himalaya. Near Surf. Geophys., 20(1): 94-114. DOI:10.1002/nsg.12186

Hajra, S., Hazarika, D., Bankhwal, M., Kundu, A., Kumar, N. (2019) Average crustal thickness and Poisson's ratio beneath the Kali River Valley, Kumaon Himalaya. J. Asian Earth Sci., 173: 176-188.

Hajra, S., Hazarika, D., Kumar, N., Pal, S.K., Roy, P.N.S. (2021) Seismotectonics and stress perspective of the Kumaon Himalaya: A geophysical evidence of a Lesser Himalayan duplex. Tectonophysics, 806: 1-17, 228801.

Hajra, S., Hazarika, D., Shukla, V., Kundu, A., Pant, C.C. (2022a) Stress dissipation and seismic potential in the central seismic gap of the north-west Himalaya. J. Asian Earth Sci., 239, 105432. https://doi.org/10.1016/j.jseaes.2022.105432

Hajra, S., Hazarika, D., Mondal, S., Pal, S.K., Roy, P.N.S. (2022b) Deformation of the upper crust in the Kumaon Himalaya analyzed from seismic anisotropy and gravity lineament studies. Phys. Earth Planet. Inter. 322, 106827.

Hazarika, D., Hajra, S., Kundu, A., Bankhwal, M., Kumar, N., et al. (2021) Imaging the Moho and Main Himalayan Thrust beneath the Kumaon Himalaya: Constraints from receiver function analysis. Geophys. J. Int., 224: 858–870.

Hazarika, D., Kundu, A., Ghosh, P. (2022) Seismotectonic scenario of the indenting northeast corner of the Indian plate in the Tidding-Tuting Suture Zone of the Eastern Himalayan Syntaxis. Tectonophysics, 824, 229197, https://doi.org/10.1016/j.tecto.2021.229197

Hebert, H., Occhipinti, G., Schindele, F., Gailler, A., Pinel-Puyssegur, B., et al. (2020) Contributions of Space Missions to Better Tsunami Science: Observations, Models and Warning. Surv. Geophys., 41: 1535-1581. https://doi.org/10.1007/s10712-020-09616-2

Heki, K., Bagiya, M.S., Takasaka, Y. (2022) Slow fault slip signatures in coseismic ionospheric disturbances. Geophys. Res. Lett., 49, e2022GL101064. https://doi.org/10.1029/2022GL101064

Illa, B., Reshma, K.S., Kumar, P., Srinagesh, D., Haldar, C., et al. (2021a) Pn tomography and anisotropic study of the Indian shield and the adjacent regions. Tectonophysics, 813, 228932.

Illa, B., Kumar, P., Reshma, K.S., Srinu, U., Srinagesh, D. (2021b) Sn wave tomography of the uppermost mantle beneath the Indian shield and its adjacent regions. Phys. Earth Planet. Inter., 319, 106785.

Jaiswal, N., Singh, C., Sarkar, S., Tiwari, A.K., Jana, N. (2022) Pg attenuation tomography beneath western Tibet. J. Seismol., pp.1-13.

Jana, N., Singh, A., Tiwari, A.K., Singh, C., Biswas, R. (2019) Mantle deformation patterns and signatures of rift, beneath Eastern Ghats Mobile Belt. Phys. Earth Planet. Inter., 289: 20-33.

Jana, N., Singh, A., Tiwari, A.K., Eken, T., Singh, A., et al. (2021) Seismic anisotropy and mantle deformation beneath Eastern Ghats Mobile Belt using direct-S waves. Precambrian Res., 360, 106215.

Jana, N., Singh, C., Singh, A., Eken, T., Dubey, A.K., et al. (2022) Lithospheric architecture below the Eastern Ghats Mobile Belt and adjoining Archean cratons: Imprints of India-Antarctica collision tectonics. Gondwana Res., 111: 209-222.

Joshi, S., Rao, K.M. (2021) Ultra-low frequency geomagnetic variations before Dholavira earthquake (M 5.1) on 20th June 2012 in Kachchh region, Gujarat, India. Geotectonics, 55: 633–645. doi: 10.1134/S0016852121040142

Kamra, C., Chopra, S., Yadav, R.B.S., Joshi, V. (2020) Characterization of major fault systems in the Kachchh Intraplate Region, Gujarat, India, by focal mechanism and source parameters. Seismol. Res. Lett., 91(6): 3496-3517.

Kamra, C., Chopra, S., Yadav, R.B.S. (2021) Joint inversion for stress and fault orientations using focal mechanisms of earthquakes in the Saurashtra horst, a part of the stable continental region of India, and source parameter estimation. J. Seismol., 25(4): 1141-1159. https:// doi.org/10.1007/s10950-021-10016-1

Kanna, N., Gupta, S. (2020) Crustal seismic structure beneath the Garhwal Himalaya using regional and teleseismic waveform modelling. Geophys. J. Int., 222: 2040-2052.

Kanna, N., Gupta, S. (2021) Seismic crustal shear velocity structure across NW Himalaya and Ladakh-Karakoram using receiver function modelling: Evidence of the Main Himalayan Thrust. Phys. Earth Planet Inter., 311, 106642. https://doi.org/10.1016/j.pepi.2020.106642

Kothyari, G.C., Kandregula, R.S., Kotlia, B.S., Lakhote, A., Swamy, K.V., et al. (2021) Palaeoseismic investigations along the Kachchh Mainland Fault: a comprehensive review and new insights of the past earthquakes in the Kachchh basin, Western India. Quat. Int., 599: 184-209.

Kumar, A., Kumar, N., Mukhopadhyay, S., Klemperer, S.L. (2021) Tomographic image of shear wave structure of NE India based on analysis of Rayleigh wave data. Front. Earth Sci., 9: 179-196, 680361. https://doi.org/10.3389/feart.2021.680361

Kumar, N., Yadav, D.N. (2019) Coda Q estimation for Kinnaur region and surrounding part of NW Himalaya. J. Seismol., 23(2): 271-285.

Kumar, N., Aoudia, A., Guidarelli, M., Babu, V.G., Hazarika, D., et al. (2019) Delineation of lithosphere structure and characterization of the Moho geometry under the Himalaya-Karakoram-Tibet collision zone using surface wave tomography. Geol. Soc. Spec. Pub., SP481, 19-40. http://doi.org/10.1144/SP481-2017-172

Kumar, N., Kumar, K., Gautam, Mishra, M., Kumar, S., Kumar, P. (2021b) Upper mantle anisotropy from shear wave splitting of teleseismic earthquakes in the Kumaun-Garhwal and adjoining area of NW Himalaya. J. Asian Earth Sci., 5: 1-9, 100054.

Kumar, P., Devi, S., Monika, Srivastava, A., Sandeep, et al. (2019) Site response study based on H/V method using S-wave: A case study in the Kumaon Himalaya, India. Himal. Geol., 40(2): 213-219.

Kumar, P., Monika, Sandeep, Kumar, S., Kumari, R., Kumar, D., et al. (2021) Characterization of shear wave attenuation and site effects in the Garhwal Himalaya, India from inversion of strong motion records. J Earth Syst. Sci., 130:1-19.

Kumar, S., Sharma, N. (2019) The seismicity of central and north-east Himalayan region. Contrib. Geophys. Geod., 49(3): 265-281. https://doi.org/10.2478/congeo-2019-0014

Kumar, S., Gupta, S., Kanna, N., Sivaram, K. (2020) Crustal structure across the Deccan Volcanic Province and Eastern Dharwar Craton in south Indian shield using receiver function modelling. Phys. Earth Plant. Inter., 306, 106543.

Kumari, R., Kumar, P., Kumar, N., Sandeep (2020) Role of site effect for the evaluation of attenuation characteristics of P, S and coda waves in Kinnaur region, NW Himalaya. J. Earth Syst. Sci., 129: 1-18.

Kumari, R., Kumar, P., Kumar, N., Sandeep (2021) Implications of site effects and attenuation properties for estimation of earthquake source characteristic in Kinnuar Himalaya, India. Pure Appl. Geophys., 178: 4345-4366.

Kumar, V., Rai, S.S., Hawkins, R., Bodin, T. (2022) Seismic imaging of crust beneath the western Tibet-Pamir and western Himalaya using ambient noise and earthquake data. J. Geophys. Res. Solid Earth, 127, e2021JB022574. https://doi.org/10.1029/2021JB022574

Kumar, V.P., Gupta, S., Borah, K., Prakasam, K.S., Rai, S.S. (2022) Seismic anisotropy beneath the Kumaun–Garhwal Himalaya using core-refracted shear wave phases. Geophys. J. Int., 229(3): 1978-1989.

Kundu, A., Hazarika, D., Hajra, S., Singh, A.K., Ghosh, P. (2020) Crustal Thickness and Poisson's Ratio variations in the northeast India–Asia collision zone: Insight into the Tuting-Tidding Suture zone, Eastern Himalaya. J. Asian Earth Sci, 188, 104099. https://doi.org/10.1016/j.jseaes.2019.10409

Lakshmi, B.V., Gawali, P.B. (2022). Soft sediment deformation features in Dauki Fault region: Evidence of paleoeqrthquakes, Shillong Plateau, NE India. Environ. Earth Sci., 81.

Madhusudhan, S., Gupta,S., Kann, N., Sivaram, K., Sudesh Kumar (2022) Seismic characteristic of underthrusting Indian lithosphere beneath the eastern Kumaun Himalaya using regional earthquake waveform analysis, J. Asian Earth Sci., 237, 105356. https://doi.org/10.1016/j.jseaes.2022.105356

Mahato, C.R., Shashidhar, D. (2022) Stress drop variations of triggered earthquakes at Koyna-Warna, western India: A case study. J. Earth Syst. Sci. 131(2): 1-10. https://doi.org/10.1007/s11069-021-05096-8

Mahesh P., A. Sateesh, C. Kamra, S. Kumar, S. Chopra, et al. (2020) Earthquake swarms in Palghar district, Maharashtra, Deccan Volcanic province. Curr. Sci., 118(5): 701.

Mandal, P. (2019a) Passive source seismic imaging of the crust and upper mantle underlying the Archean Singhbhum Craton, Eastern India. J. Asian Earth. Sci., 176: 300-314.

Mandal, P. (2019b) A possible origin of intraplate earthquakes in the Kachchh rift zone, India, since the 2001 Mw7.7 Bhuj earthquake. J. Asian Earth Sci., 170: 56-72.

Mandal, P. (2019c) Shear-wave splitting in the Rajasthan craton, India. J. Asian Earth Sci., 173: 1-10.

Mandal, P. (2020) Strong ground motions from two moderate size (Mw5.5) Kachchh intraplate earthquakes, Gujarat, India. Nat. Hazards, 103: 2441–2458. https://doi.org/10.1007/s11069-020-04092-8

Mandal, P. (2020a) Three-dimensional seismic velocity imaging of the Kachchh rift zone, Gujarat, India: Implications toward the crustal mafic pluton induced intraplate seismicity. J. Asian Earth Sci., 192, 104226.

Mandal, P. (2021) Shear-wave splitting observations: Implications toward the variable anisotropic structure of the upper mantle below the Kachchh rift zone, Gujarat, India. Phys. Earth Planet. Inter., 310, 106618.

Mandal, P. (2021a) Seismic velocity images of a crystallized crustal magma-conduit (related to the Deccan plume) below the seismically active Kachchh rift zone, Gujarat, India. Nat. Hazards. https://doi.org/10.1007/s11069-021-05051-7

Mandal, P. (2022a) Evidence of secular variation in Archean crust formation in the Eastern Indian Shield. Sci. Rep., 12, 14040. https://doi.org/10.1038/s41598-022-18372-9

Mandal, P. (2022b) Seismic velocity images of a crystallized crustal magma-conduit (related to the Deccan plume) below the seismically active Kachchh rift zone, Gujarat, India .Nat. Hazards, 111: 239-260.

Mandal, P., Asano, K. (2019) Three-dimensional ground motion modelling in the Kachchh rift zone, Gujarat, India. Phys. Earth Planet. Inter., 297. https://doi.org/10.1016/j.pepi.2019.106322

Mandal, P., Kumar, P., Sreenivas, B., Babu, EVSSK, Bhaskar Rao, Y.J. (2021) Variations in crustal and lithospheric structure across the Eastern Indian Shield from Passive Seismic source imaging: Implications to changes in the tectonic regimes and crustal accretion through the Precambrian, Precambrian Res., 360, 106207, 1-19.

Mandal, P., Satayanarayana, H.V.S., Shashidhar, D., Arti Devi, Srinagesh D. (2021a) Simultaneous estimation of site response and source parameters of reservoir-triggered earthquakes using data from the borehole seismic network in the Koyna–Warna seismic zone, Maharashtra, India. Nat. Hazards, 111: 1335 -1354. https://doi.org/10.1007/s11069-021-05096-8

Mandal, P., Srinagesh, D., Suresh, G, et al. (2021b) Characterization of earthquake hazard at the Palghar and Pulichintala swarm activity regions (India) through three-dimensional modelling of b-value and fractal (correlation) dimensions. Nat. Hazards,108: 1183–1196. https://doi.org/10.1007/s11069-021-04726-5

Mandal, P., Srinivas, D., Suresh, G., Srinagesh, D. (2021c) Modelling of crustal composition and Moho depths and their Implications toward seismogenesis in the Kumaon–Garhwal Himalaya. Sci. Rep., 11, 14067. https://doi.org/10.1038/s41598-021-93469-1

Mandal, P., Kumar, S., Gupta, S., Prasad, B.N.V., Saidixit, M. (2022) Delineation of detailed crustal seismic velocity structure and Moho depths in the Hyderabad region, eastern Dharwar craton, India. Nat. Hazards, 114: 2219-2241. https://doi.org/10.1007/s11069-022-05469-7

Mandal, P., Saha, S., Kumar, S., et al. (2022a) Modelling of Moment Tensors and Source Parameters of the 25 July 2021 Rare Lower Crustal Hyderabad (India) Earthquake of Mw 3.9. Pure Appl. Geophys, 179: 993–1010. https://doi.org/10.1007/s00024-022-02973-6

Mandal, P., Srinagesh, D., Vijayaraghavan, R., Suresh, G., Naresh, B., et al. (2022b) Seismic velocity imaging of the Kumaon–Garhwal Himalaya, India. Nat. Hazards, 111: 2241-2260. https://doi.org/10.1007/s11069-021-05135-4

Mandal, P., Srinivas, D., Vengala, P., Srinagesh, D., Suresh, G., Naresh, B. (2022c) Delineation of crustal and lithospheric structure below the 2019 Palghar swarm activity region, Maharashtra, India. Nat. Hazards, 114: 205-235. https://doi.org/10.1007/s11069-022-05387-8

Manglik, A., Gupta, S., Tiwari, V.M. (2021) Geophysical studies for the crust and upper mantle structure of the Himalaya: Contributions of CSIR-NGRI. J. Geol. Soc. India, 97: 1190-1199. https://doi.org/10.1007/s12594-021-1848-2

Manglik, A., Suresh, M., Nagarjuna, D., Pavankumar, G. Demudu Babu, M., et al. (2022) Subsurface Expressions of the Aravalli-Delhi Fold Belt in the Western Ganga Basin by Magnetotellurics. J. Geol. Soc. India, 98(12): 1721-1727. https://doi.org/10.1007/s12594-022-2242-4

Medved, I., Koulakov, I., Mukhopadhyay, S., Jakovlev, A. (2022) Lithosphere Structure in the Collision Zone of the NW Himalayas Revealed by a Local Earthquake Tomography. J. Geodyn., 152: 1-11, https://doi.org/10.1016/j.jog.2022.101922

Mir, R.R., and Parvez I A (2020) Ground motion modelling in NW Himalaya using stochastic finite-fault method, Nat. Hazards (10.1007/s11069-020-04068-8)

Mir, R.R., Parvez, I.A., Gaur, V.K. (2021) Shear wave velocity structure beneath North-Western Himalaya and adjoining areas. Preprint at EarthArxiv, https://doi.org/10.31223/X5DK68

Mir, R.R., Parvez I A, Laske, G., Gaur, V.K. (2022) Sensor orientation and noise analysis of the Kashmir-Zanskar seismic network: an appraisal from 2014-2020, J. Seismol., 1-18, DOI:10.1007/s10950-022-10090-z

Mohanty, D.D., Singh, A. (2022) Shear wave birefringence and current configuration of active tectonics of Shillong plateau: an appraisal of Indian plate motion and regional structures. Int. J. Earth Sci., 111(1): 269-286.

Monika, Kumar, P., Sandeep, Kumar, S., Joshi, A., Devi, S. (2020) Spatial variability studies of attenuation characteristics of $Q\alpha$ and $Q\beta$ in Kumaon and Garhwal region of NW Himalaya. Nat. Hazards, 103: 1219-1237

Mukherjee, T., Singh, C., Biswas, P.K. (2021) A Novel Approach for Earthquake Early Warning System Design using Deep Learning Techniques. arXiv preprint arXiv:2101.06517.

Mullick, N., Rai, S.S., Saha, G. (2022) Lithospheric structure of the South India Precambrian terrains from surface wave tomography. J. Geophys. Res. Solid Earth, 127, e2022JB024244. https://doi.org/10.1029/2022JB024244

Nagamani, D., Sivaram K., Purnachandra Rao, N., Satyanarayana, H.V.S. (2020) Ambient noise and earthquake HVSR modelling for site characterization in southern mainland, Gujarat, J. Earth Syst. Sci., 129(1): 1-14.

Nagar, M., Pavankumar, G., Mahesh, P., Nikam, R., Nagarjuna, D., et al. (2021) Magnetotelluric evidence for trapped fluids beneath the seismogenic zone of the Mw6.0 Anjar earthquake, Kachchh intraplate region, northwest India. Tectonophysics, 228969. https://doi.org/10.1016/j.tecto.2021.228969

Nanajee, U., Roy, S.K., Kumar, M.R. (2022) Spatial variation of crustal anisotropy in the Arunachal Himalaya inferred from splitting of local S waveforms. J. Asian Earth Sci., 234, 105278. https://doi.org/10.1016/j.jseaes.2022.105278

Nayak, S., Bagiya, M.S., Maurya, S., Hazarika, N.K., Kumar, A.S.S., et al. (2021) Terrestrial resonant oscillations during the 11 April 2012 Sumatra doublet earthquake. J. Geophys. Res. Space Phys., 126, e2021JA029169. https://doi.org/10.1029/2021JA029169

Nayak, S., Bagiya, M.S., Sunil, A.S. (2022) Spatial manifestation of resonant ionospheric signatures during the 11 March 2011 Tohoku-Oki earthquake. Adv. Space Res., 69: 3000–3007. https://doi.org/10.1016/j.asr.2022.01.027

O'Kane, A., Copley, A., Mitra, S., Wimpenny, S. (2022) The geometry of active shortening in the northwest Himalayas and the implications for seismic hazard. Geophys. J. Int., 231: 2009-2033. https://doi.org/10.1093/gji/ggac303

Parija, M.P. (2021) Earthquake Swarm and Quiescence Precursory to the NE Himalaya 2011 Sikkim Earthquake (M 6.9) , J. Geol. Soc. India, 98: 178-180.

Paul, A., Hazarika, D. (2022) Occurrences of low-stress drop earthquakes in the eastern Ladakh-Karakoram zone and their tectonic implications. J. Asian Earth Sci.:X, 7 (2022) 100080, https://doi.org/10.1016/j.jaesx.2022.100080

Paul, A., Hazarika, D., Wadhawan M, Kumar, N. (2021) Upper mantle anisotropy in the northwest Himalaya and Ladakh-Karakoram zone based on SKS splitting analysis. J. Geodyn., 144, 101817.

Paul, H., Ravi Kumar, M. (2022) Strong influence of tomographic models on geoid prediction: Case studies from Indian Ocean and Ross Sea geoids. Tectonophysics, 836, 229429.

Paul, H., Pandey, A., Ravi Kumar, M., Kumar, S. (2021) Investigation of crustal thickness and uppermost mantle velocity beneath Gujarat, western India, utilizing Moho reflected P phases. Phys. Earth Planet. Inter., 310, 106619.

Pavankumar, G., Manglik, A. (2021) Complex tectonic setting and deep crustal seismicity of the Sikkim Himalaya: An electrical resistivity perspective. Phys. Chem. Earth, Parts A/B/C, 124(2). https://doi.org/10.1016/j.pce.2021.103077

Pavankumar, G., Chakravarthi, N.N., Demudu Babu, M., Manglik, A. (2020) Magnetotelluric study of an intraplate seismic zone in the Palghar region of the Deccan Volcanic Province, India. J. Earth Syst. Sci.,129(1):1-16. https://doi.org/10.1007/s12040-020-01398-w

Pavankumar, G., Manglik, A., Demudu Babu, M., Chakravarthi, N.N. (2021) Magnetotelluric evidence for the presence of a deep electrical conductor in the vicinity of the Delhi Seismic Zone, India. J. Earth Syst. Sci., 130(2): 1-16. https://doi.org/10.1007/s12040-021-01565-7

Parvin, S.S., Naresh, B., Raghavan, R.V., et al. (2021) Source Parameters of Shallow Microtremors Induced by Seasonal Groundwater Recharge in Hyderabad, Southern Peninsular India. J. Geol. Soc. India, 97: 1073–1079. https://doi.org/10.1007/s12594-021-1822-z

Rao, B.P., Ravi Kumar, M. (2022a) Evolution of the Western Ghats: Constraints from receiver function imaging and harmonic decomposition. Tectonophysics, 838, 229472.

Rao, B.P., Ravi Kumar, M. (2022b) Lowermost mantle (D" layer) structure beneath the Indian Ocean: Insights from modeling of ScS-S and PcP-P residuals. J. Asian Earth Sci., 225, 105038.

Rao, B.P., Ravi Kumar, M., Saikia, D. (2020) Seismic Evidence for a Hot Mantle Transition Zone Beneath the Indian Ocean Geoid Low. Geochemistry, Geophysics, Geosystems, 21, e2020GC009079.

Ravi Kumar, M., Padma Rao, B., Mahesh, P., Venkatesh, V. (2022) Scattered wave imaging of the Main Himalayan Thrust and mid-crustal ramp beneath the Arunachal Himalaya and its relation to seismicity. J. Asian Earth Sci., 236, 105335.

Rekapalli, R., Gupta, H.K. (2021) Characterization of injection-induced seismicity at north central Oklahoma, USA (Short Communication). J. Seismol., 25: 327-337. https://doi.org/10.1007/s10950-020-09978-5

Reshma, K.S., Illa, B., Kumar, P., Srinagesh, D. (2022) Lg Q in the Indian Shield. Pure Appl. Geophys., 179: 149-168.

Roy, S.K., Kumar, M.R., Srinagesh, D. (2021a) Mantle deformation beneath India inferred from shear wave splitting. J. Geol. Soc. India, 97: 1200-1206. doi: 10.1007/s12594-021-1849-1

Roy, S.K., Srinagesh, D., Suresh, G., Srinivas, D. (2021b) Seismicity and Disparate deformation of the crust and upper mantle beneath the Doda-Kisthwar region, NW Himalaya. Phys. Earth Planet. Inter., 310, 106635. https://doi.org/10.1016/j.pepi.2020.10663.

Saha, G., Rai, S.S., Prakasam, K.S., Gaur, V.K. (2021) Distinct lithospheres in the Bay of Bengal inferred from ambient noise and earthquake tomography. Tectonophysics, 809, 228855. https://doi.org/10.1016/j.tecto.2021.228

Sahoo S.K., K.M. Rao, C. Barman, U. Lakshmi, G. (2020) Identification of earthquake precursors in soil radon-222 data of Kutch, Gujarat, India using empirical mode decomposition based Hilbert Huang Transform. J. Environ.Radioact., 222, 106353. Doi.org/10.1016/j.jenvrad.2020.106353

Sahoo S.K., M. Katlamudi, U. Lakshmi G. (2021) Observation of ULF electromagnetic emissions before the M 7.8 New Zealand earthquake of November 13, 2016. Geodyn. Tectonophys., 12 (4), 891–901. Doi: 10.5800/GT-2021-12-4-0561

Saikia, U., Kumar, V.P., Rai, S.S. (2019) Complex upper mantle deformation beneath the Dharwar craton inferred from high density splitting measurements: Distinct lateral variation from west to east. Tectonophysics, 755: 10-20.

Saikia, D., Ravi Kumar, M., Singh, A. (2020) Palaeoslab and plume signatures in the mantle transition zone beneath Eastern Himalaya and adjoining regions. Geophys. J. Int., 221: 468-477.

Sandeep, Joshi, A., Sah, S.K., Kumar, P., Lal, S., et al. (2019a) Modeling of 2011 Indo Nepal Earthquake and Scenario Earthquakes in the Kumaon Region and Comparative Attenuation Study Using PGA Distribution with the Garhwal Region. Pure Appl. Geophys., 176(11): 4687- 4700.

Sandeep, Joshi, A., Sah, S.K., Kumar, P., Lal, S., et al. (2019b) Modelling of strong motion generation areas for a great earthquake in central seismic gap region of Himalayas using the modified semi-empirical approach. J. Earth Syst. Sci., 128:100, 1-12.

Sandeep, Joshi, A., Devi, S., Kumar, P., Sah, S.K., et al. (2019c) Strong motion generation area modeling of the 2008 Iwate earthquake, Japan using modified semi-empirical technique. J. Earth Syst. Sci., 128:202, 1-16

Sandeep, A. Joshi, P. Kumari, Kumar, P., Sah, S.K., et al. (2020) Strong ground motion simulation techniques—a review in world context. Arab. J. Geosci., 13(673), 1-12.

Sandeep, S. Devi, Kumar, P., Monika, Kumar, R. (2022) Strong Motion Modelling of the 1999 Izmit Earthquake Using Site Effect in a Semi-Empirical Technique: A More Realistic Approach. Pure Appl. Geophys., 179: 483-497.

Sarkar, S., Jaiswal, N., Singh, C., Dubey, A.K., Singh, A. (2021) Source spectral studies using Lg wave in western Tibet. J. Seismol., 25(2): 625-638.

Sateesh A., Mahesh, P., Singh, A.P., Kumar, S., Chopra, S., et al. (2019) Are earthquake swarms in South Gujarat, northwestern Deccan Volcanic Province of India monsoon induced? Environ. Earth Sci., 78, 381. https://doi.org/10.1007/s12665-019-8382-1

Sharma, A., Vashisth, D., Naresh, B., et al. (2021) An ML scale for Eastern Dharwar Craton and adjoining regions. J. Seismol., 25: 1251–1263. https://doi.org/10.1007/s10950-021-10028-x

Sharma, J., Kumar, M.R., Roy, S.K., Pal, S.K., Roy, P.N.S. (2021) Low-Velocity Zones and Negative Radial Anisotropy Beneath the Plume Perturbed Northwestern Deccan Volcanic Province. J. Geophys. Res. Solid Earth, 126(2), e2020JB020295.

Sharma, N., Srinagesh, D., Suresh, G., Srinivas, D. (2021) Stochastic simulation of strong ground motions From Two M > 5 Uttarakhand Earthquakes. Front. Earth Sci., 9, 599535. doi: 10.3389/feart.2021.599535

Sharma, S., Sarma, J.N., Baruah, S. (2018) Dynamics of Mikir hills plateau and its vicinity: inferences on Kopili and Bomdila Faults in Northeastern India through seismotectonics, gravity and magnetic anomalies. Ann. Geophys., 61(3), SE338-SE338.

Sharma, S., Mitra, S., Sharma, S., Priestley, K., Wanchoo, S.L., et al. (2020) A Report on Broadband Seismological Experiment in the Jammu and Kashmir Himalaya (JAKSNET). Seismol. Res. Lett., 91: 1915–1926, doi: 10.1785/0220190389

Shashidhar, D., Mallika, K., Mahato, C., et al. (2019a) A Catalogue of Earthquakes in the Koyna-Warna Region, Western India (2005–2017). J. Geol. Soc. India, 93: 7–24 . https://doi.org/10.1007/s12594-019-1115-y

Shashidhar, D., Mallika, K., Gahalaut, K., Mahato, C.R., Satyanarayana, H.V.S. (2019b) A New Earthquake Sequence at Koyna–Warna, India, and Its Implication for Migration of the Reservoir Triggered Seismicity. Bull. Seismol. Soc. Am., 109(2): 827-831.

Shashidhar, D., Rodriguez, I.V., Mallika, K., Kühn, D., Wilks, M., et al. (2020) Relative locations of an earthquake sequence recorded 1 during June 2017 on the Koyna-Warna borehole seismic network of western India. Bull. Seismol. Soc. Am., 110(6): 3130-3138. https://doi.org/10.1785/012020068

Shukla, N., Hazarika, D., Kundu, A., Mukhopadhyay, S. (2022) Spatial variations of crustal thickness and Poisson's ratio in the northeastern region of India based on receiver function analysis. Geol. J., https://doi.org/10.1002/gj.4469

Shukla, V., Chauhan, V., Kumar, N., Hazarika, D. (2020) Assessment of Rn-222 continuous time series for the identification of anomalous changes during moderate earthquakes of the Garhwal Himalaya. Appl.Radiat. Isot., 166, 109327, 1-10.

Shugar, D.H., Jacquemart, M., Shean, D., Bhushan, S., Upadhyay, K., et al. (2021) A massive rock and ice avalanche caused the 2021 disaster at Chamoli, Indian Himalaya. Science, 373(6552): 300-306. https://doi.org/10.1126/science.abh4455

Singh, A., Singh, C. (2019) Seismic imaging of the deep crustal structure beneath Eastern Ghats Mobile Belt (India): Crustal growth in the context of assembly of Rodinia and Gondwana supercontinents. Precambrian Res., 331, 105343.

Singh, A., Saikia, D., Ravi Kumar, M. (2021) Seismic Imaging of the Crust beneath Arunachal Himalaya. J. Geophys. Res. Solid Earth, 126, e2020JB020616.

Singh, B., Mandal, P. (2020) Upper mantle seismic anisotropy beneath the Kachchh rift zone, Gujarat, India, from shear wave splitting analysis. J. Earth Syst. Sci., 129(1): 1-11.

Singh, C., Biswas, R., Jaiswal, N., Ravi Kumar, M. (2019a) Spatial variations of coda wave attenuation in Andaman–Nicobar subduction zone. Geophys. J. Int., 217(3): 1515-1523.

Singh, C., Jaiswal, N., Mukhopadhyay, S. (2019b) PgQ model for Nepal Himalaya. Phys. Earth Planet. Inter., 286: 13-20. doi.org/10.1016/j.pepi.2018.10.009

Singh, S.K., Srinagesh, D., Pérez-Campos, X., Srinivas, D., Suresh, G., et al. (2020). Seismic wave amplification in the central Indo-Gangetic Plains, India, estimated from the ratio of soft to hard site source spectrum. J. Seismol., 24: 679–692. https://doi.org/10.1007/s10950-020-09931-6

Sivaram, K. (2021) Simulation of Strong Ground Motion in the National Capital Region, India, from a Future 8.5 Magnitude Earthquake Using Two-Step Empirical Green's Function Method. Bull. Seismol. Soc. Am., 111(6): 3374–3386. doi: https://doi.org/10.1785/0120200239

Sivaram, K., Gupta, S. (2022) Frequency-dependent attenuation characteristics of coda and body waves in the Kumaun Himalaya: Implications for regional geology and seismic hazards. Pure Appl. Geophys., https://doi.org/10.1007/s00024-022-02963-8.

Sivaram, K., Kumar, V.P., Gupta, S., Prasad, B.N.V., Kumar, S. (2022) Upper mantle seismic anisotropy beneath the Deccan Volcanic Province and the adjacent Eastern Dharwar Craton in south Indian shield from shear wave splitting analysis. Phys. Earth Planet. Inter., 322, 106829.

Sribin, C., Rao, B.P., Kumar, M.R., Tomson, J.K. (2021) Mantle deformation beneath the Western Ghats, India: Insights from core-refracted shear wave splitting analysis. J. Asian Earth Sci., 218, 104848.

Srijayanthi G., Chatterjee, R.S., Kamra, C., Chauhan, M., Chopra, S., et al. (2022) Seismological and InSAR based investigations to characterise earthquake swarms in Jamnagar, Gujarat, India–An active intraplate region. J. Asian Earth Sci.: X, 8, pp.100118.

Srinu, U., Kumar, P., Haldar, C., Kumar, S. Ravi Kumar, M., et al. (2021) X-discontinuity beneath the Indian shield—evidence for remnant Tethyan Oceanic lithosphere in the mantle. J. Geophys. Res. Solid Earth, 126, e2021JB021890.

Srinagesh, D., Mandal, P., Vijaya Raghavan, R., Gupta, S., Suresh, G., et al. (2019) Digital seismic network: to map Himalayan orogen and seismic hazard, Curr. Sci., 116(4): 518-519.

Srinagesh, D., Singh, D.K., Vikas, G., Naresh, B., Roy, S., et al. (2020) An appraisal of recent earthquake activity in Palghar region, Maharashtra, India, Curr. Sci., 118(10): 1592-1596. doi: 10.18520/cs/v118/i10/1592-1598

Srinagesh, D., Sunil kumar, T.C., Naresh, B., Vitthal, S., Singh, D.K., et al. (2021) A study of Palnadu earthquake sequence in the Cuddapah basin and its tectonic implications. J. Earth Syst. Sci., 130, 52. https://doi.org/10.1007/s12040-021-01552-y

Surve, G., Kanaujia, J., Sharma, N. (2021) Probabilistic seismic hazard assessment studies for Mumbai region. Nat. Hazards 107: 575–600. https://doi.org/10.1007/s11069-021-04596-x

Tiwari, A., Sain, K., Kumar, A., Tiwari, J., Paul, A., et al. (2022) Potential seismic precursors and surficial dynamics of a deadly Himalayan disaster: an early warning approach. Sci. Rep., 12(1): 1-13.

Tiwari, A.K., Singh, A., Saikia, D., Singh, C., Eken, T. (2022a) Crustal anisotropy beneath southeastern Tibet inferred from directional dependence of receiver functions. Phys. Earth Planet. Inter., 331, 106912.

Tiwari, A.K., Singh, C., Sandvol, E., Mukhopadhyay, S., Singh, A., et al. (2022b) Sn attenuation tomography of southeastern Tibet: new constraints on lithospheric mantle deformation. Geophys. J Int., 228(2): 1038-1053.

Tiwari, V.M., Gupta, H.K. (2021) 60 Years of CSIR-National Geophysical Research Institute. J. Geol. Soc. India, 97(10): 1113-1324.

Uthaman, M., Singh, A., Singh, C., Dubey, A., Kumar, G. (2021) Discerning structure and seismic hazards in the Sikkim Himalayas. Eos, 102.

Uthaman, M., Singh, C., Singh, A., Jana, N., Dubey, A.K., et al. (2022) Spatial and temporal variation of the ambient noise environment of the Sikkim Himalaya. Sci. Rep., 12(1): 1-13.

Vashishtha, M., Karukola, B., Mukhopadhyay, S. (2022) Effect of Source Rupture Process on Surface Wave Group Velocity: An Example Using 2015 Nepal Earthquake Data. Pure Appl. Geophys. https://doi.org/10.1007/s00024-022-03008-w

Vijaya Kumar, P.V., Rawat, V.S., Patro, P.K., Gupta, A.K., Narendra Babu (2020) Assessment and recognition of pre- and co-seismic electromagnetic signatures from magnetotelluric data: a case study from Koyna–Warna seismoactive region, India. Acta Geophys., 69: 1–15. https://doi.org/10.1007/s11600-020-00510-4

Wadhawan, M., Rana, N., Gahalaut, V., et al. (2021) Monsoonal rainfall induced shallow earthquake Swarm in the Amravati district of the central India. J. Earth Syst. Sci., 130,29. https://doi.org/10.1007/s12040-020-01511-z

Other publications during 2019-2022

Bhatia, M., Rekapalli, R., Kumar, M., Agrawal, M. (2022) Microseism source distribution inferred from noise recordings at the Gujarat Seismic Network, India. J. Earth Syst. Sci., 131, 23. doi: 10.1007/s12040-021-01779-9

Bhukta, K., Khan, P.K., Mandal, P. (2020) Estimation of source parameters of local earthquakes based on inversion of waveform data. Curr. Sci., 119: 1159-1168.

Bhukta, K., Paul, A., Khan, P.K. (2022) SKS and SKKS splitting measurements beneath the Northwest Himalaya. Pure Appl. Geophys. https://doi.org/10.1007/s00024-021-02935-4

Biswas, K., Mandal, P., Khan, P.K. (2019) Estimation of coda Q for the eastern Indian craton. J. Earth Syst. Sci., 128: 1-16.

Chaudhury, J., Mitra, S., Sarkar, T. (2021) Hales Discontinuity in the Southern Indian Continental Lithosphere: Seismological and Petrological Models. J. Geophys. Res. Solid Earth, 126, e2020JB020564. https://doi.org/10.1029/2020JB020564

Chaudhary, P., Chopra, S., Kamra, C., Das, A. (2019) New Insight into the Recent Earthquake Activity in North Cambay Basin, Western India: Seismological and Geodetic Perspectives. Bull. Seismol. Soc. Am., 109(6): 2240-2251.

Chetia, T., Baruah, S. (2022) Multi-Parametric Geophysical Observatory for Earthquake Precursory Research in Assam Valley, Eastern Himalaya (India): Seismotectonic Features of Kopili and Bomdila Faults. Geotectonics, 56(2): 212-227.

Chetia, T., Baruah, S., Dey, C., Baruah, S., Sharma, S. (2022) Seismic induced soil gas radon anomalies observed at multiparametric geophysical observatory, Tezpur (Eastern Himalaya), India: an appraisal of probable model for earthquake forecasting based on peak of radon anomalies. Nat. Hazards, 111(3): 3071-3098.

Das, A., Prizomwala, S.P., Solanki, T., Chauhan, G., Thakkar, M.G., et al. (2019) Relative assessment of tectonic activity along the seismically active Katrol Hill Fault, Kachchh, western India. J. Geol. Soc. India, 94(2): 179-187.

Devi, S., Kumar, S., Monika, P. (2021) Strong-Motion Simulation of the 1988 Indo-Burma and Scenario Earthquakes in NE India by Integrating Site Effects in a Semi-Empirical Technique. Pure Appl. Geophys., 178: 2839–2854.

Devi, S., Kumar, S., Monika, P., Joshi, A. (2022) Modelling of 2016 Kumamoto earthquake by integrating site effect in semi-empirical technique. Nat. Hazards, 111: 1931-1950.

Dey, C., Baruah, S., Abdelwahed, M.F., Saikia, S., Molia, N., et al. (2022) The 28 April 2021 Kopili Fault Earthquake (Mw 6.1) in Assam Valley of North East India: Seismotectonic Appraisal. Pure Appl. Geophys. https://doi.org/10.1007/s00024-022-03072-2

Dey, S., Powali, D., Chaudhury, J., Ghosh, M., Mandal, R., et al. (2019) 28 August 2018 (Mw 4.5) Bengal Basin earthquake highlights active basement fault beneath the sediments. Curr. Sci., 116(10): 1633-1636.

Dutta, A., Biswas, R., Singh, C., Kumar, M.R., Jana, N., et al. (2021) Depth-wise attenuation mechanism of seismic waves in the Andaman region. Soil Dyn. Earthq. Eng., 151, 107000

Dwivedi, V.K., Dubey, R.K., Pancholi, V., Rout, M.M., Singh, P., et al. (2020) Multi criteria study for seismic hazard assessment of UNESCO world heritage Ahmedabad City, Gujarat, Western India. Bull. Eng. Geol. Environ., 79(4): 1721-1733.

Gorshkov, A.I., Hasan, H., Mandal, P., Novikova, O. (2022) Identifying potential earthquake sources in the continental environments. Surv. Geophys., 43: 529-559. https://doi.org/10.1007/s10712-021-09683-z

Gupta, A.K., Mandal, P. (2020) Delineation of average 1-D shear velocity structure below north India, by surface wave dispersion study. J. Geol. Soc. India, 96: 58-64.

Gupta, V., Paul, A., Kumar, S., Dash, B. (2021b) Spatial distribution of landslides vis-a-vis epicentral distribution of earthquakes in the vicinity of the Main Central Thrust zone, Uttarakhand Himalaya, India. Curr. Sci., 120(12): 1927-1932.

Haldar, C., Sain, K., Kumar, S. (2022b) Seismic imaging of intra-crustal low-velocity layer beneath the Kishtwar region, North-West Himalaya, India using receiver function technique. Himal. Geol., 43(1A): 1-11.

Haldar, C., Kumar, P., Pandey, O.P., Sain, K., Kumar, S. (2022a) Lower crustal intraplate seismicity in Kachchh region (Gujarat, India) triggered by crustal magmatic infusion: Evidence from shear wave velocity contrast across the Moho. Geosystems and Geoenvironment, 1, 100073.

Hazarika, D., Kayal, J.R. (2022) Recent felt earthquakes (Mw 5.0–5.9) in Mizoram of north-east India region: Seismotectonics and precursor appraisal. Geol. J., 57(2): 877-885. doi.org /10.1002/ gj.4290.

Jaiswal, N., Singh, C., Singh, A. (2020) Crustal structure of western Tibet revealed by Lg attenuation tomography. Tectonophysics, 775, 228245.

Joshi, V., Chopra, S., Kumar, S. (2020) A local magnitude scale ML for the Saurashtra horst: An active intraplate region, Gujarat, India. J. Earth Syst. Sci., 129(1): 1-9.

Kanaujia, J., Mitra, S., Gupta, S.C., Sharma, M.L. (2019) Crustal anisotropy from shear-wave splitting of local earthquakes in the Garhwal Lesser Himalaya. Geophys. J. Int., 219(3): 2013-2033. doi: 10.1093/gji/ggz404

Kayal, J.R., Baruah, S., Hazarika, D., Das, A. (2022) Recent large and strong earthquakes in the eastern Himalayas: An appraisal on seismotectonic model. Geol. J., doi:10.1002/gj.4576.

Kumar, S., Gupta, V., Kumar, P., Sundriyal, Y.P. (2021a) Coseismic landslide hazard assessment for the future scenario earthquakes in the Kumaun Himalaya, India. Bull. Eng. Geol. Environ., 80: 5219–5235.

Kumar, S., Kumar, R.C., Roy, K.S., Chopra, S. (2021b) Seismic Monitoring in Gujarat, India, during 2020 Coronavirus Lockdown and Lessons Learned. Seismol. Res. Lett., 92(2A): 849–858.

Kumar, V., Rai, S.S. (2019) Complex seismic image of the Main Himalayan Thrust in Garhwal and implication for earthquake hazard. J. Earth Syst. Sci., 131, 79. https://doi.org/10.1007/s12040-022-0

Kumar, V., Chopra, S., Choudhury, P., Kumar, D. (2020) Estimation of near surface attenuation parameter kappa (ϰ) in Northwest and Northeast Himalaya region, Soil Dyn. Earthq. Eng, 136, 106237.

Kundu, A., Hazarika, D. (2022) Estimation of source parameters and scaling relations for local earthquakes of Lohit Valley in Arunachal Himalaya, Northeast India. Geol. J., DOI: 10.1002/gj.4423.

Kundu, A., Hazarika, D., Yadav, D.K., Ghosh, P. (2022). Crustal thickness and Poisson's ratio variations in the Siang Window and adjoining areas of the Eastern Himalayan Syntaxis. J. Asian Earth Sci., 231, 105225. https://doi.org/10.1016/j.jseaes.2022.105225.

Lakshmi, B.V. (2021) Seismically induced soft sediment deformation structures in and around Chamoli, Garhwal Himalaya, India. J. Earth Environ. Sci. Res., 3(2): 1-4.

Mandal, P. (2020) Relocations and local earthquake tomography: Implications toward the mafic pluton induced crustal seismicity in Kachchh, Gujarat, India, for last 18 years. J. Asian Earth Sci., 190: 1-9, 104196.

Mandal, P. (2021a) Structure of the seismically active Kachchh region. J. Geol. Soc. India, 10: 1163-1168.

Mandal, P. (2021b) Lessons Learned from the Occurrences of Major Devastating Mw[?]7.5 Earthquakes in the Asian Countries during the last 25 years. J. Geol. Soc. India, 97: 1494-1497.

Mandal, P. (2022) Peak Ground Acceleration prediction using Artificial Neural Networks for Kachchh, Gujarat, India. Nat. Hazards, 114; 3043–3059. https://doi.org/10.1007/s11069-022-05504-7

Mandal, P., Srinagesh, D., Suresh, G., Naresh, B., Singh, D.K., et al. (2022) Three-dimensional b-value and fractal dimension mapping of the Uttrakhand Himalayan region, J. Geol. Soc. India, 98: 1365-1379.

Minocha, S., and Parvez, I A. (2020) Self-Organized Fractal Seismicity and b-Value of Aftershocks of the 2015 Gorkha Earthquake, Nepal. Int. J. Geosci., 11: 562-579. doi: 10.4236/ijg.2020.118030

Mitra, S., Wanchoo, S.K., Priestley, K. (2022) Seismic coda-wave attenuation tomography of the Jammu and Kashmir Himalaya. J. Geophys. Res. Solid Earth, 127, e2022JB024917. https://doi.org/10.1029/2022JB024917

Mittal, H., Sharma, B., Sandhu, M., Kumar, D. (2021) Spatial distribution of high-frequency spectral decay factor kappa (ϰ) for Delhi, India. Acta Geophysica, https://doi.org/10.1007/s11600-021-00674-7

Mohan K., Dugar, S., Pancholi, V., Dwivedi, V., Chopra S., et al. (2021) Micro-seismic hazard assessment of Ahmedabad city, Gujarat (Western India) through near-surface characterization/soil modeling. Bull. Earthq. Eng., 19: 623–656.

Naresh B., Mandal, P., Solomon Raju, P., Vijaya Raghavan, R., Suresh, G., et al. (2020). Magnitude estimation of regional earthquakes in India and its adjoining region. J. Earth. Syst. Sci., 129: 112. https://doi.org/10.1007/s12040-020-1374-4.

Nekrasova, A.K., Kossobokov, V.G., Parvez, I., Tao, X. (2020) Unified Scaling Law for Earthquakes as Applied to Assessment of Seismic Hazard and Associate Risks. Izvestiya, Phys. Solid Earth, 56: 83-94, DOI:10.1134/S1069351320010097

Pancholi, V., Bhatt, N.Y., Dwivedi, V.K., Choudhury, P., Chopra, S. (2020) Geotechnical Investigation for Estimation of Liquefaction Hazard for the Capital City of Gujarat State, Western India. Geotech. Geol. Eng., 38: 6551-6570. https://doi.org/10.1007/s10706-020-01454-8.

Pandey, P., Chauhan, P., Bhatt, C.M., Thakur, P.K, Kannaujia, S., et al. (2021) Cause and process mechanism of rockslide triggered flood event in Rishiganga and Dhauliganga River Valleys, Chamoli, Uttarakhand, India using satellite remote sensing and in situ observations. J. Indian Soc. Remote Sens., 49(5): 1011-1024. https://doi.org/10.1007/s12524-021-01360-3.

Pandey, S., Yuan, X., Debayle, E., Geissler, W.H., Heit, B. (2022) Plume-lithosphere interaction beneath south-western Africa -Insights from multi-mode Rayleigh wave tomography. Tectonophysics, 842, 229587.

Parshad, R., Kumar, P., Snehmani, Srivastva, P.K. (2019) Seismically induced snow avalanches at Nubra–Shyok region of Western Himalaya, India. Nat. Hazards, 99: 843-855.

Parvez, I.A. (2021) Application of neo-deterministic seismic hazard assessment to India. In: Panza, G., Kossobokov, V., De Vivo, B., Laor, E. (Eds) Earthquakes and Sustainable Infrastructure: neo-deterministic (NDSHA) approach guarantees prevention rather than cure. Imprint: Elsevier. Paperback ISBN: 9780128235034), pp. 525-541.

Paul, A., Hazarika, D. (2022) Seismic anisotropy for understanding the dynamics of crust and upper mantle: A case study in the northwest Himalaya and eastern Ladakh-Karakoram zone. In: Recent Developments in Using Seismic Waves as a Probe for Subsurface Investigations: Theory and Practices, Taylor & Francis Group, https://doi.org/10.1201/9781003177692, pp. 42

Paul, A., Tiwari, A., Upadhyay, R. (2019) Central Seismic Gap and Probable zone of large earthquake in North West Himalaya. Himal. Geol., 40 (2): 199-212.

Paul H., Kumar, M.R., Kumar, S. (2021) Evidence for reactivation of new faults and seismicity migration away from the causative fault of the 2001 MW 7.7 Bhuj earthquake, western India. Geophys. J. Int., 226 (3): 1800-1813.

Pavan Kumar, V., Gupta, S., Borah, K., Prakasam, K.S., Rai, S.S. (2022) Seismic anisotropy beneath the Kumaun-Garhwal Himalaya using core-refracted shear wave phases, Geophys. J. Int., 229(3): 1978–1989, https://doi.org/10.1093/gji/ggac043

Powali, D., Sharma, S., Mandal, R., Mitra, S. (2020) A reappraisal of the 2005 Kashmir (Mw 7.6) earthquake and its aftershocks: Seismotectonics of NW Himalaya. Tectonophysics, 789, 228501. https://doi.org/10.1016/j.tecto.2020.228501

Priestley, K., Ho, T., Mitra, S. (2019) The crust structure of the Himalaya: a synthesis. In: Treloar, P.J., Searle, M.P. (eds) Himalayan Tectonics: A Modern Synthesis. Geol. Soc. Spec. Pub., 483, 483–516. https://doi.org/10.1144/SP483-2018-127

Rawat, G., Luirei, K. (2022) Deep crustal resistivity structure of the Lohit Valley in the Eastern Himalayan Syntaxial region, Geol. J., 57: 4920-4928. doi:10.1002/gj.4422.

Roy, K.S., Sharma, J., Kumar, S., Kumar, M.R. (2021) Effect of coronavirus lockdowns on the ambient seismic noise levels in Gujarat, northwest India. Sci. Rep., 11, 7148. https://doi.org/10.1038/s41598-021-86557-9

Saha, G., Rai, S.S., Shalivahan (2019) Occurrence of diamond in peninsular India and its relationship with deep Earth seismic properties. J. Earth Syst. Sci. 128, 43. https://doi.org/10.1007/s12040-019-1088-7

Saha, G.K., Prakasam, K.S., Rai, S.S. (2020) Diversity in the peninsular Indian lithosphere revealed from ambient noise and earthquake tomography; Phys. Earth Planet. Inter. 306, 106523.

Sairam, B., Singh, A.P., Patel, V., Chopra, S., Kumar, M.R. (2019) VS30 mapping and site characterization in the seismically active intraplate region of Western India: implications for risk mitigation. Near Surf. Geophys., 17(5): 533-546.

Sandhu, K., Kumar, D. (2019) The 2011 Sikkim earthquake (MW 6.9) of the Himalaya: Estimates of earthquake source parameters and representability of attenuation characteristics, J. Asian Earth Sci., 169: 237-243.

Sandhu, M., Sharma, B., Mittal, H., Yadav R.B.S., Kumar, D., et al. (2020) Simulation of strong ground motion due to active Sohna fault in Delhi, National Capital Region (NCR) of India: an implication for imminent plausible seismic hazard. Nat. Hazards, 104: 2389-2408.

Sangwan, P., Kumar, D. (2020) Estimation of Coda Q for Northeast India using nonlinear regression. J. Earth Syst. Sci., 129, 229. https://doi.org/10.1007/s12040-020-01483-0

Sharma, A., Kumar, D., Paul, A. (2020) Estimation of site response functions for the Kumaun Garhwal region of Himalaya, India. J. Seismol., 24: 655-678. https://doi.org/10.1007/s10950-020-09920-9

Sharma, A., Yadav, R., Kumar, D., Paul, A., Teotia, S.S. (2021) Estimation of site response functions for the central seismic gap of Himalaya, India. Nat. Hazards, 109: 1899-1933. https://doi.org/10.1007/s11069-021-04903-6.

Shastri, A., Kumar, S. (2021) Estimation of Coda-Q for Mainland Gujarat region of Western Deccan Volcanic Province, India. J. Earth Syst. Sci., 130 (4), doi.org/10.1007/s12040-021-01731-x.

Shastri, A., Kumar, S. (2022) Source parameters and scaling relations for small earthquakes in mainland Gujarat region of Western Deccan Volcanic Province, India. Geomatics, Nat. Hazards Risk, 13 (1): 2925-2948.

Shreyasvi, C., Venkataramana, K., Chopra, S., Rout, M.M. (2019) Probabilistic seismic hazard assessment of Mangalore and its adjoining regions, a part of Indian Peninsular: an intraplate region. Pure Appl. Geophys., 176(6): 2263-2297.

Singh A.P., Koulakov, I., Kumar, M.R., Kumar, S., Kayal, J.R. (2019) Seismic velocity structure and intraplate seismicity beneath the Deccan Volcanic Province of western India. Phys. Earth Planet. Inter., 287: 21-36.

Singh, A.P., Sairam, B., Pancholi, V., Chopra, S., Kumar, M.R. (2020) Delineation of thickness of intrabasaltic rocks beneath the Deccan Volcanic province of western India through micro tremor analysis. Soil dyn. Earthq. Eng., 138, 106348. http://dx.doi.org/10.1016/j.soildyn.2020.106348.

Singh, K.D., Mohan, K., Chopra, S. (2021) Magnetotelluric investigation in the swarm prone intraplate Talala region of Saurashtra, Gujarat, western India. J. Appl. Geophys., 192: 104381. https://doi.org/10.1016/j.jappgeo.2021.104381

Singh, R., Sharma, S., Mitra, S., Khan, P.K. (2019) Mapping of coda-wave attenuation and its frequency dependency over eastern Indian Shield. Pure Appl. Geophys., 176(12): 5291-5313. https://doi.org/10.1007/s00024-019-02284-3

Singh, R., Paul, A., Shalini, Joshi, P., Kumar, S., et al. (2020) Reverse migratory behaviour of the earthquakes aftershock sequences along Himalayan Seismic Belt, Northwest Himalaya. Quat. Int., 585: 163-170

Singh, S., Devbrat, B.P., Sinha, A., Rao, K.M., Guha, A., et al. (2020) Ultra-Low Frequency (ULF) Magnetic Field Emissions Associated With Some Major Earthquakes Occurred In Indian Subcontinent. Atmos. Sol. Terr. Phys, 211, 105469. doi:10.1016/j.jastp.2020.105469

Sunil, A.S., Bagiya, M.S., Bletery, Q., Ramesh, D.S. (2021) Association of ionospheric signatures to various tectonic parameters during moderate to large magnitude earthquakes: Case study. J. Geophys. Res. Space Phys., 126, e2020JA028709. https://doi.org/10.1029/2020JA028709

Thomas, D., Bagiya, M.S., Hazarika, N.K., Ramesh, D.S. (2022) On the Rayleigh wave induced ionospheric perturbations during the Mw 9.0 11 March 2011 Tohoku-Oki earthquake. J. Geophys. Res. Space Phys., 127, e2021JA029250. https://doi.org/10.1029/2021JA029250

Tiwari, A., Paul, A., Singh, R., Upadhyay, R. (2021) Potential seismogenic asperities in the Garhwal-Kumaun region, NW Himalaya: Seismotectonic implications. Nat. Hazards, 107: 73–95.

Vorobieva, I., Gorshkov, A.I., Mandal, P. (2021) Modelling the seismic potential of the Indo-Burman megathrust. Sci. Rep., 11:21200. https://doi.org/10.1038/s41598021-00586-y

Wadhwan, M., Hazarika, D., Paul, A., Kumar, N., Gupta, V., et al. (2022a) Seismic anisotropy and crustal deformation in the Satluj valley and adjoining region of northwest Himalaya revealed by the splitting analysis of Moho converted Ps phases. J. Asian Earth Sci., 238, 105377. https://doi.org/10.1016/j.jseaes.2022.105377

Wadhawan, M., Hazarika, D., Saikia, S. (2022b) Application of teleseismic receiver function in investigation of crustal thickness and Poisson's ratio. In: Recent Developments in Using Seismic Waves as a Probe for Subsurface Investigations: Theory and Practices, Taylor & Francis Group, https://doi.org/10.1201/9781003177692, pp. 32

Yadav, D.K., Hazariak, D., Kumar, N., Singh, A.K. (2021) Microseismicity study in the Siang valley of Arunachal Himalaya: Tectonic Implication of the 2019 Mw 5.9 Mechuka Earthquake. Himal. Geol., 42(2): 290-298.

Yadav, D.N., Kumar, N., Babu, G.B., Kumari, R., Pal, S.K. (2022) Crustal velocity structure and seismotectonics of the Kinnaur region of northwest Himalaya: New constraints based on recent micro-earthquake data. J. Asian Earth Sci., 224: 1-16, 105005.